



**permafrost**  
cci

**CCI+ PHASE 2**  
**PERMAFROST**

**D5.1 CLIMATE ASSESSMENT REPORT (CAR)**

**VERSION 5.0**

**15 NOVEMBER 2025**

**PREPARED BY**

**b·geos**

*GAMMA REMOTE SENSING*



**UNI  
FR**

UNIVERSITÉ DE FRIBOURG  
UNIVERSITÄT FREIBURG



ALMA MATER STUDIORUM  
UNIVERSITÀ DI BOLOGNA

**West University of Timisoara TERRASIGNA™**

**NORCE**



**UiO • University of Oslo**

## Document status sheet

Issue	Date	Details	Authors
1.0	30.10.2019	first version, year 1	I. Nitze, G. Grosse, H. Matthes, M. Wieczorek, A. Bartsch, B. Heim
2.0	30.09.2020	second version: update of service case status and dissemination activities representing year 2	I. Nitze, G. Grosse, H. Matthes, M. Wieczorek, A. Bartsch, B. Heim
2.1	16.10.2020	Inclusion of IPA (represented through Isabelle Gärtner-Roer) evaluation	A. Bartsch
3.0	30.09.2021	update of service case status and dissemination activities representing year 3	I. Nitze, H. Matthes, M. Wieczorek, S. Lisovksi, B. Heim, A. Bartsch
3.1	19.01.2022	Update (name of cci dataset) in Table 1	A. Bartsch
4.0	17.05.2024	update of service case status and dissemination activities representing year 4 (CCI phase II); inclusion of rock glacier monitoring	I. Nitze, G. Grosse, H. Matthes, M. Wieczorek, B. Heim, A. Bartsch, L. Rouyet, T. Echelard, L. Schmid, C. Pellet, R. Delaloye, F. Sirbu, A. Omacu, V. Poncos, F. Brardinoni, A. Kääb, T. Strozzi, N. Jones
5.0	15.11.2025	Inclusion of 5 new service cases and update of dissemination activities, validation summary and operationalization plan	A. Bartsch, T. Strozzi, L. Rouyet, H. Matthes, B. Heim, M. Wieczorek, I. Nitze

## Author team

Guido Grosse, Ingmar Nitze, Birgit Heim, Mareike Wieczorek, Heidrun Matthes, AWI  
Line Rouyet, Thomas Echelard, Lea Schmid, Cécile Pellet, Reynald Delaloye, UNIFR  
Flavius Sirbu, Alexandru Onaca, WUT

Valentin Poncos, Terrasigna

Francesco Brardinoni, University of Bologna

Line Rouyet, NORCE

Sebastian Westermann, Andreas M. Kääb, UiO

Tazio Strozzi and Nina Jones, GAMMA

Annett Bartsch, BGEOS

## ESA Technical Officer

Frank Martin Seifert

EUROPEAN SPACE AGENCY CONTRACT REPORT

The work described in this report was done under ESA contract. Responsibility for the contents resides in the authors or organizations that prepared it.

## TABLE OF CONTENTS

Executive summary .....	5
1 Introduction .....	7
1.1 Purpose of the document .....	7
1.2 Structure of the document .....	7
1.3 Applicable documents .....	7
1.4 Reference Documents .....	8
1.5 Bibliography .....	9
1.6 Acronyms .....	10
1.7 Glossary .....	10
2 Products generated by Permafrost_cci .....	13
3 Assessment of products and other feedback .....	15
3.1 Introduction and rationale .....	15
3.2 Use Case Study 1 - Climate Observations: Linking pan-Arctic glacier mass balance and permafrost thaw through atmospheric circulation patterns .....	16
3.3 Use Case Study 2 - ALT, PFR and ground temperature trends: comparison to landcover trends .....	19
3.4 Use Case Study 3 - Permafrost trends: affected Arctic Infrastructure .....	27
3.5 Use Case Study 4 - Permafrost trends: affected Arctic Coastal Infrastructure .....	32
3.6 Use Case Study 5 - Permafrost variations: understanding Arctic change through identification similarities with sea ice .....	36
3.7 Use Case Study 6 – Analysis of Permafrost_cci Rock Glacier Inventories (RoGI) .....	40
3.8 Use Case Study 7 – Global compilation of Rock Glacier Velocity (RGV) .....	44
3.9 Further documented use .....	46
3.9 Permafrost_cci utility based on evaluation results for GRD, ALT and EXT .....	49
3.10 Assessment of utility of Rock Glacier Inventory (RoGI) Products .....	61
4 Progress in regard to user requirements .....	65
4.1 Algorithm selection .....	65
4.2 Product specification .....	65
4.3 Plan for operationalization of PE, GT and ALT .....	69
5 Publications and outreach .....	70
5.1 Peer-reviewed scientific articles .....	70

5.2	News Stories.....	76
5.3	User workshops.....	77
5.4	Outreach activities.....	82
5.5	Presentations at scientific conferences (Phase II) .....	83
5.7	Student teaching and courses .....	89
6	References.....	91
6.1	Bibliography.....	91
6.2	Acronyms .....	95

## Executive summary

This document presents the Climate Assessment Report (CAR) version 5 of the European Space Agency (ESA) Climate Change Initiative (CCI) Permafrost project (Permafrost\_cci). CCI is ESA's global monitoring program whose main objective is to provide Earth Observation (EO)-based Essential Climate Variable (ECV) timeseries to the climate modelling and climate user communities. At the start of the project, there was no consistent global Earth Observation-based mapping of the parameters permafrost temperature and active layer thickness as called for within the GCOS strategy. Permafrost\_cci for the first time provides such information for different epochs and meets the requirements for the production of a climate data record. Permafrost\_cci was part of phase I of CCI+ (2018–2021) and has been selected for phase II (2022–2025) with the production of ECVs for permafrost, set by the Global Climate Observing System (GCOS)/World Meteorological Organisation (WMO). The CAR describes the scientific assessments of the produced variables for the ECV permafrost: i) permafrost temperature expressed as Ground Temperature per Depth (GTD) [°C] ii) Active Layer Thickness (ALT) [cm], iii) permafrost extent expressed as Permafrost Fraction (PFR) [%] derived from GTD at 2 m depth, iv) Rock Glacier Inventory (RoGI) and, v) and Rock Glacier Velocity (RGV). The CAR also summarizes the Use Cases of the Permafrost\_cci products and current activities within Permafrost\_cci with regard to user requirements defined by the climate modelling user community.

Use case #1 combines GRACE/GRACE-FO glacier mass balance and ESA CCI Permafrost active-layer thickness data. Coherent interannual variability are revealed across the Arctic. Shared signals between glacier mass loss and permafrost thaw are driven primarily by large-scale atmospheric circulation modes (Greenland Blocking Index, North Atlantic Oscillation), explaining  $\approx 75\%$  of the common variability.

Use case #2 compares Landsat-derived trends separated between fire and non-fire affected areas. Particularly increasing variance within burned areas, with locally strong increase in ALT, may result in triggering further permafrost disturbances. However, more detailed analysis will be conducted to verify/falsify this hypothesis.

Use case #3 covers a joint study with H2020 Nunataryuk which had a focus on infrastructure across the Arctic. Almost 97% of all mapped objects showed a positive trend in ground temperature and 93% for ALT (CRDPv2). 55% of the identified human impacted area will be shifting to above 0 °C ground temperature at two meter depth by 2050 if current permafrost warming trends continue at the pace of the last two decades.

Use case #4 presents a first panarctic satellite-based record of coastal settlements affected by multiple risks among others considering Permafrost\_cci records (CRDPv3). By 2100, 77% of coastal infrastructure will see ground temperature at 2 m shift from negative to positive, based on 2000–2019 trend.

Within use case #5 a first pan-arctic satellite-based record of similarities between permafrost (CRDPv3) and sea ice variations was developed. A high proportion of significant correlation was found in many regions, with values over 80% for Svalbard and the Laptev Sea adjacent land area. In the case of MAGT,

high significant correlations were found for more distant sea ice basins than for the NDVI derivatives, indicating influences of large-scale atmospheric circulation patterns.

Based on results of the PVIR, Permafrost\_cci GTD and PFR products for the Northern hemisphere are considered to be most reliable in the permafrost temperature range with GTD < 1°C as well as PFR <14% is reliable as non-permafrost.

Recommendations from the user workshops held at the European Permafrost Conference EUCOP 2023 in Puigcerda, Spain, including the WMO GTN-P general assembly meeting, included an increased temporal as well as vertical resolution of the CryoGrid products, specifically to facilitate climate modelling applications requiring these resolutions.

Use case #6 evaluates the value of using spaceborne Interferometric Synthetic Aperture Radar (InSAR) primarily based on Sentinel-1 SAR images, to assign a kinematic attribute to the inventoried landforms and improve the assessment of rock glacier activity. The results show the value of InSAR for the systematic documentation of the rock glacier creep rate at the regional scale. The use case also highlighted several limitations in the Rock Glacier Inventory (RoGI) procedure applied in Permafrost\_cci Phase 1. The conclusions contributed to update the workflow for RoGI production in Permafrost\_cci Phase 2.

Use case #7 provides an overview of RGV products at the global scale based on compilation of available in-situ and remote sensing data. The number of time series included is growing at each annual update of the State of the Climate (Bulletin of the American Meteorological Society), but the number of investigated sites remain limited, which show the need to develop systematic remote sensing approach for monitoring the newest ECV quantity for permafrost. The preliminary assessment of the Permafrost\_cci RGV products show that the InSAR-RGV result from the iteration 1 Permafrost\_cci Phase 2 are promising. We propose an easily transferable method to automate the production of RGV by averaging unwrapped Sentinel-1 interferograms. The developed method appears to be suitable to produce consistent InSAR-RGV, which are comparable to GNSS-RGV interannual trends, although we need to include more years of data to confirm this primary conclusion.

## 1 Introduction

### 1.1 Purpose of the document

This document is the Climate Assessment Report (CAR) version 5 (update of [RD-1]) of the ESA CCI+ project Permafrost\_cci providing the user requirements of climate science and climate services for Permafrost\_cci ECV products, the Climate Research Data Packages (CRDP) of the Permafrost\_cci project. Besides the required WMO/GCOS Permafrost ECVs i) permafrost temperature, and ii) active layer thickness, Permafrost\_cci provides iii) permafrost extent (permafrost fraction within a pixel), as an additional variable derived from permafrost temperature: the areal fraction within the grid cell that fulfils the definition for the existence of permafrost (ground temperature  $<0$  °C for two consecutive years), iv) Rock Glacier Inventory (RoGI) and, v) and Rock Glacier Velocity (RGV).

The generation of the Permafrost\_cci CRDP i) Ground Temperature per Depth (GTD) per year, Active Layer Thickness (ALT) per year, and Permafrost FRaction (PFR) per year time series relies on the ground thermal model Permafrost\_cci CryoGrid, that is forced by EO time series of Land Surface Temperature (LST) and considering Snow Water Equivalent (SWE) with boundary conditions of EO-derived Land Cover [RD-3].

The Permafrost\_cci CRDPv4 released in 2025, is an update of CRDPv3 and includes three time series covering the Northern Hemisphere north of 30° N and Antarctica:

- simulated EO-forced **mean annual Ground Temperature per Depth (GTD) in five discrete depths** (0 m, 1 m, 2 m, 5 m, 10 m) from 1997 to 2023
- simulated EO-forced **annual Active Layer Thickness (ALT)** from 1997 to 2023
- **annual Permafrost FRaction (PFR)** derived from GTD from 1997 to 2023

Rock glacier products include:

- **Rock Glacier Inventories (RoGI)**, documenting the distribution and morpho-kinematic characteristics of rock glaciers in selected regions.
- **Rock Glacier Velocity (RGV)**, as time series of annualised surface velocity values expressed in m/y and measured/computed on a rock glacier or a part of it.

### 1.2 Structure of the document

The CAR is organized in 6 chapters. Chapter 1 provides the introduction and the overview on Permafrost\_cci including applicable documents and the community glossary for Permafrost. Chapter 2 summarized the products of Permafrost\_cci. Chapter 3 and its subsections describe the use cases and assessment. Further progress is documented in Chapter 4, what also includes plans for operationalization. Chapter 5 lists publications and outreach, Chapter 6 the references.

### 1.3 Applicable documents

[AD-1] GEO/CEOS Quality Assurance framework for Earth Observation (QA4EO) protocols 3-4

[AD-2] ESA 2017: Climate Change Initiative Extension (CCI+) Phase 1 – New Essential Climate Variables – Statement of Work. ESA-CCI-PRGM-EOPS-SW-17-0032

[AD-3] ESA Climate Change Initiative. CCI Project Guidelines. EOP-DTEX-EOPS-SW-10-0002

[AD-4] ECV 9 Permafrost: Assessment report on available methodological standards and guides, 1 Nov 2009, GTOS-62

[AD-5] Requirements for monitoring of permafrost in polar regions - A community white paper in response to the WMO Polar Space Task Group (PSTG), Version 4, 2014-10-09. Austrian Polar Research Institute, Vienna, Austria, 20 pp.

[AD-6] ESA. 2022. Climate Change Initiative Extension (CCI+) Phase 2 – New Essential Climate Variables – Statement of Work. ESA-EOP-SC-AMT-2021-27.

[AD-7] GCOS. 2022. The 2022 GCOS Implementation Plan. GCOS – 244 / GOOS – 272. Global Observing Climate System (GCOS). World Meteorological Organization (WMO).

[AD-8] GCOS. 2022. The 2022 GCOS ECVs Requirements. GCOS – 245. Global Climate Observing System (GCOS). World Meteorological Organization (WMO).

[AD-9] GTN-P. 2021. Strategy and Implementation Plan 2021–2024 for the Global Terrestrial Network for Permafrost (GTN-P). Authors: Streletskiy, D., Noetzli, J., Smith, S.L., Vieira, G., Schoeneich, P., Hrbacek, F., Irrgang, A.M.

#### 1.4 Reference Documents

[RD-1] Nitze, I., Grosse, G., Heim, B., Wieczorek, M., Matthes, H., Bartsch, A., Strozzi, T. (2019): ESA CCI+ Climate Assessment Report, v1.0

[RD-2] Nitze, I., Grosse, G., Heim, B., Wieczorek, M., Matthes, H., Bartsch, A., Strozzi, T. (2020): ESA CCI+ Climate Assessment Report, v2.0

[RD-3] Nitze, I., Grosse, G., Heim, B., Wieczorek, M., Matthes, H., S. Lisovski Bartsch, A., Strozzi, T. (2021): ESA CCI+ Climate Assessment Report, v3.0

[RD-4] van Everdingen, Robert, ed. 1998 revised May 2005. Multi-language glossary of permafrost and related ground-ice terms. Boulder, CO: National Snow and Ice Data Center/World Data Center for Glaciology. (<http://nsidc.org/fgdc/glossary/>; accessed 23.09.2009)

[RD-5] Bartsch, A., Westermann, Strozzi, T., Wiesmann, A., Kroisleitner, C., 2019: ESA CCI+ Permafrost Product Specifications Document, v1.0

[RD-6] Bartsch, A., Westermann, Strozzi, T., Wiesmann, A., Kroisleitner, C., 2021: ESA CCI+ Permafrost Product Specifications Document, v2.0

[RD-7] Rouyet, L., Pellet, C., Schmid, L., Echelard, T., Delaloye, R., Brardinoni, F., Sirbu, F., Onaca, A., Poncos, V., Kääb, A., Strozzi, T., Bartsch, A. 2024. ESA CCI+ Permafrost Phase 2 – CCN4 Mountain Permafrost: Rock Glacier Inventories (RoGI) and Rock glacier Velocity (RGV) Products. D1.1 User Requirement Document (URD), v2.0. European Space Agency.

[RD-8] Rouyet, L., Schmid, L., Pellet, C., Echelard, T., Delaloye, R., Brardinoni, F., Sirbu, F., Onaca, A., Poncos, V., Kääb, A., Strozzi, T., Bernhard, P., Bartsch, A. 2024. ESA CCI+ Permafrost Phase 2 – CCN4 Mountain Permafrost: Rock Glacier Inventories (RoGI) and Rock glacier Velocity (RGV) Products. D1.2 Product Specification Document (PSD), v2.0. European Space Agency.

[RD-9] RGIK. 2023. Guidelines for inventorying rock glaciers: baseline and practical concepts (version 1.0). Rock glacier inventories and kinematics, 25 pp. <https://doi.org/10.51363/unifr.srr.2023.002>.

[RD-10] RGIK. 2023. InSAR-based kinematic attribute in rock glacier inventories. Practical InSAR guidelines (version 4.0). [Rock glacier inventories and kinematics](#), 33 pp, [www.rgik.org](http://www.rgik.org).

[RD-11] Rouyet, L., Pellet, C., Echelard, T., Schmid, L., Delaloye, R., Brardinoni, F., Sirbu, F., Onaca, A., Poncos, V., Brardinoni, F., Wendt, L., Lauknes, T. R., Kääb, A., Strozzi, T., Bernhard, P., Bartsch, A. 2025. ESA CCI+ Permafrost Phase 2 – CCN4 Mountain Permafrost: Rock Glacier Inventories (RoGI) and Rock glacier Velocity (RGV) Products. D3.2 Climate Research Data Package (CRDP), v2.0. European Space Agency.

[RD-12] Rouyet, L., Pellet, C., Echelard, T., Schmid, L., Delaloye, R., Brardinoni, F., Sirbu, F., Onaca, A., Poncos, V., Brardinoni, F., Wendt, L., Lauknes, T. R., Kääb, A., Strozzi, T., Bernhard, P., Bartsch, A. 2025. ESA CCI+ Permafrost Phase 2 – CCN4 Mountain Permafrost: Rock Glacier Inventories (RoGI) and Rock glacier Velocity (RGV) Products. D4.1 Product Validation and Intercomparison Report (PVIR), v2.0. European Space Agency.

[RD-13] Rouyet, L., Pellet, C., Echelard, T., Schmid, L., Delaloye, R., Brardinoni, F., Sirbu, F., Onaca, A., Poncos, V., Brardinoni, F., Wendt, L., Lauknes, T. R., Kääb, A., Strozzi, T., Bernhard, P., Bartsch, A. 2025. ESA CCI+ Permafrost Phase 2 – CCN4 Mountain Permafrost: Rock Glacier Inventories (RoGI) and Rock glacier Velocity (RGV) Products. D4.2 Product User Guide (PUG), v2.0. European Space Agency.

[RD-14] Rouyet, L., Pellet, C., Schmid, L., Echelard, T., Delaloye, R., Brardinoni, F., Sirbu, F., Onaca, A., Poncos, V., Wendt, L., Lauknes, T. R., Kääb, A., Strozzi, T., Bernhard, P., Bartsch, A. 2024. ESA CCI+ Permafrost Phase I – CCN1 & CCN2 Mountain Permafrost: Rock Glacier Kinematics as New Associated Parameter of ECV Permafrost. D2.2 Algorithm Theoretical Basis Document (ATBD), v2.0. European Space Agency.

[RD-15] RGIK 2023. Rock Glacier Velocity as an associated parameter of ECV Permafrost: baseline concepts (version 3.2). [IPA Action Group Rock glacier inventories and kinematics](#), 12 pp.

[RD-16] RGIK. 2023. Rock Glacier Velocity as an associated parameter of ECV Permafrost: practical concepts (version 1.2). [IPA Action Group Rock glacier inventories and kinematics](#), 17 pp.

[RD-17] Nitze, I., Grosse, G., Heim, B., Wieczorek, M., Matthes, H., S. Lisovski Bartsch, A., Strozzi, T. (2023): ESA CCI+ Climate Assessment Report, v4.0

## 1.5 Bibliography

A complete bibliographic list that supports arguments or statements made within the current document is provided in Section 6.1.

## 1.6 Acronyms

A list of acronyms is provided in section 6.2.

## 1.7 Glossary

The glossary below based on [RD-4] and [AD-2] provides a selection of terms relevant for the Climate Change Initiative. A comprehensive glossary is available as part of the Product Specifications Document [RD-4,5,8].

### active-layer thickness

The thickness of the ground layer that is subject to annual thawing and freezing above permafrost. The thickness of the active layer depends on factors such as the ambient air temperature, vegetation, drainage, soil or rock type and total water content, snowcover, and degree and orientation of slope. As a rule, the active layer is thin in the High Arctic (it can be less than 15 cm) and becomes thicker farther south (1 m or more). The thickness of the active layer can vary from year to year, primarily due to variations in the mean annual air temperature, distribution of soil moisture, and snowcover. The thickness of the active layer includes the uppermost part of the permafrost wherever either the salinity or clay content of the permafrost allows it to thaw and refreeze annually, even though the material remains cryotic ( $T < 0^{\circ}\text{C}$ ).

Use of the term "depth to permafrost" as a synonym for the thickness of the active layer is misleading, especially in areas where the active layer is separated from the permafrost by a residual thaw layer, that is, by a thawed or noncryotic ( $T > 0^{\circ}\text{C}$ ) layer of ground.

REFERENCES: Muller, 1943; Williams, 1965; van Everdingen, 1985

### continuous permafrost

Permafrost occurring everywhere beneath the exposed land surface throughout a geographic region with the exception of widely scattered sites, such as newly deposited unconsolidated sediments, where the climate has just begun to impose its influence on the thermal regime of the ground, causing the development of continuous permafrost. For practical purposes, the existence of small taliks within continuous permafrost has to be recognized. The term, therefore, generally refers to areas where more than 90 percent of the ground surface is underlain by permafrost.

REFERENCE: Brown, 1970.

### discontinuous permafrost

Permafrost occurring in some areas beneath the exposed land surface throughout a geographic region where other areas are free of permafrost. Discontinuous permafrost occurs between the continuous permafrost zone and the southern latitudinal limit of permafrost in lowlands. Depending on the scale of mapping, several subzones can often be distinguished, based on the percentage (or fraction) of the land surface underlain by permafrost, as shown in the following table.

Permafrost	English usage	Russian Usage
Extensive	65-90%	Massive Island
Intermediate	35-65%	Island

Sporadic	10-35%	Sporadic
Isolated Patches	0-10%	-

SYNONYMS: (not recommended) insular permafrost; island permafrost; scattered permafrost.

REFERENCES: Brown, 1970; Kudryavtsev, 1978; Heginbottom, 1984; Heginbottom and Radburn, 1992; Brown et al., 1997.

### **mean annual ground temperature (MAGT)**

Mean annual temperature of the ground at a particular depth. The mean annual temperature of the ground usually increases with depth below the surface. In some northern areas, however, it is not uncommon to find that the mean annual ground temperature decreases in the upper 50 to 100 metres below the ground surface as a result of past changes in surface and climate conditions. Below that depth, it will increase as a result of the geothermal heat flux from the interior of the earth. The mean annual ground temperature at the depth of zero annual amplitude is often used to assess the thermal regime of the ground at various locations.

### **permafrost**

Ground (soil or rock and included ice and organic material) that remains at or below 0 °C for at least two consecutive years. Permafrost is synonymous with perennially cryotic ground: it is defined on the basis of temperature. It is not necessarily frozen, because the freezing point of the included water may be depressed several degrees below 0°C; moisture in the form of water or ice may or may not be present. In other words, whereas all perennially frozen ground is permafrost, not all permafrost is perennially frozen. Permafrost should not be regarded as permanent, because natural or man-made changes in the climate or terrain may cause the temperature of the ground to rise above 0 °C. Permafrost includes perennial ground ice, but not glacier ice or icings, or bodies of surface water with temperatures perennially below 0 °C; it does include man-made perennially frozen ground around or below chilled pipe-lines, hockey arenas, etc.

Russian usage requires the continuous existence of temperatures below 0 °C for at least three years, and also the presence of at least some ice.

SYNONYMS: perennially frozen ground, perennially cryotic ground and (not recommended) biennially frozen ground, clima frost, cryic layer, permanently frozen ground.

REFERENCES: Muller, 1943; van Everdingen, 1976; Kudryavtsev, 1978.

### **Rock glacier (RoGI)**

Debris landforms generated by the former or current creep of frozen ground (permafrost), detectable in the landscape with the following morphologies: front, lateral margins and optionally ridge-and-furrows surface topography. Reference: RGIK. 2023. Guidelines for inventorying rock glaciers: baseline and practical concepts (version 1.0). IPA Action Group Rock Glacier Inventories and Kinematics, 25 pp. DOI: 10.51363/unifr.srr.2023.002.

### **Rock glacier velocity (RGV)**

Time series of annualised surface velocity values expressed in m/y and measured/computed on a rock glacier or a part of it. Reference: RGIK. 2023. Rock glacier velocity as an associated parameter of ECV Permafrost: Baseline concepts (version 3.2). IPA Action Group Rock Glacier Inventories and Kinematics, 12 pp.

## 2 Products generated by Permafrost\_cci

The **Permafrost\_cci baseline component** is establishing Earth Observation (EO) based products for the permafrost ECV spanning the period from 1997 to 2023. The required Permafrost ECVs by WMO/GCOS for Permafrost are [AD-2,3,4] i) **permafrost temperature** and ii) **active layer thickness**. Permafrost\_cci added iii) **permafrost extent** (permafrost fraction) as a mapped permafrost variable, which is the fraction within an area (pixel) for which the definition for the existence of permafrost (ground temperature  $< 0$  °C for two consecutive years) is fulfilled. The main focus of Permafrost\_cci lies on the ECV permafrost temperature, as its derivation also forms the base for the producing the active layer thickness and permafrost fraction variables.

Since ground temperature and seasonal thaw depth cannot be directly observed with space-borne sensors, a variety of satellite and reanalysis data are combined in a ground thermal model to infer these subsurface parameters. The algorithm uses remotely sensed data sets of Land Surface Temperature (MODIS LST/ ESA LST CCI) and landcover (ESA Landcover CCI) to drive the transient permafrost model CryoGrid-3 (CryoGrid-2 in Obu et al., 2019), which yields thaw depth and ground temperature at various depths, while ground temperature then forms the basis for deriving permafrost fraction for a specified location and time.

The Permafrost Climate Research Data Package (CRDP v3) Version 4.0 of the Climate Research Data Package [RD-3] consists of time series covering the years from 1997 and 2023 for

- i) Permafrost temperature expressed as Ground Temperature per Depth (GTD) [°C]
- ii) Active Layer Thickness (ALT) [m] (maximum annual active layer depth)
- iii) Permafrost extent expressed as Permafrost FRaction (PFR) [%] derived from GTD at 2 m depth.

The **Permafrost\_cci mountain permafrost component** focuses on the generation of two products: **Rock Glacier Inventory** (RoGI) and **Rock Glacier Velocity** (RGV) [AD-5]. The user relevance and rationale to define the product specifications have been described in the URD [RD-7] and PSD [RD-8].

In periglacial mountain environments, the permafrost occurrence is patchy and the preservation of permafrost is controlled by site-specific conditions, which require the development of dedicated products as a complement to GT and ALT measurements and permafrost models. Rock glaciers are the best visual expression of the creep of mountain permafrost and constitute an essential geomorphological heritage of the mountain periglacial landscape. Their dynamics is largely influenced by climatic factors. There are increasing evidence that the interannual variations of the rock glacier creep rates are influenced by changing permafrost temperature, making RGV a key parameter for the monitoring of the cryosphere in mountains.

The integration of RoGI and RGV products in Permafrost\_cci Phase 2 agrees with the objectives of the *Rock Glacier Inventories and Kinematics* (RGIK) community ([www.rgik.org](http://www.rgik.org)). RoGI is a valuable product to document past and present permafrost extent in mountains. It is a recommended first step to comprehensively characterise and select the landforms that can be used for RGV monitoring. The systematic generation of an international RGV database concurs with the recent GCOS and GTN-P decisions to add RGV as a new product of the ECV Permafrost to monitor changing mountain permafrost conditions [AD-6 to AD-8].

RoGI and RGV products form a unique validation dataset for climate models in mountain regions, where direct permafrost measurements are very scarce or even totally lacking. Using satellite remote sensing, generating systemic RoGI at the regional scale and documenting RGV interannual changes over many landforms become feasible. Within Permafrost\_cci, we mostly use Synthetic Aperture Radar Interferometry (InSAR) technology based on Sentinel-1 images that provide a global coverage, a large range of detection capability (mm–cm/yr to m/yr) and fine spatio-temporal resolutions (tens of m pixel size and 6–12 days of repeat-pass). InSAR can be complemented by SAR offset tracking technique and spaceborne/airborne optical photogrammetry.

### 3 Assessment of products and other feedback

#### 3.1 Introduction and rationale

Warming of the Cryosphere is already exceeding the global average temperature increase and models project further strong warming for these regions (IPCC 2021, IPCC, 2019; IPCC, 2013). Permafrost is an important component of the Cryosphere and defined as ground that remains frozen for at least two consecutive years (Van Everdingen, 1998). Ongoing permafrost warming (Romanovsky et al., 2010; Biskaborn et al., 2019) and near-surface thawing in permafrost regions, associated with rising air temperatures, are considered to reinforce warming of the atmosphere through the partial conversion of the large permafrost soil organic carbon pool into greenhouse gases, a process termed “permafrost carbon feedback” (Schuur et al., 2015). A further challenge for monitoring the impacts of permafrost thaw dynamics is represented by rapid thaw processes that may mobilize a significant amount of carbon over short time spans of years to decades (Turetsky et al., 2019). Worldwide monitoring of permafrost is therefore essential to understand and assess the feedbacks between climate change and permafrost thaw and their impact on the Earth’s climate system.

The recently published thorough analysis of global permafrost temperatures by the Global Terrestrial Network for Permafrost (GTN-P) and the International Permafrost Association (IPA) demonstrated that permafrost is warming at a global scale (Biskaborn et al., 2019). This study showed that during the reference decade (2007 to 2016) ground temperature near the depth of zero annual amplitude in the continuous permafrost zone increased by  $0.39 \pm 0.15$  °C. Over the same period, discontinuous permafrost warmed by  $0.20 \pm 0.10$  °C. Permafrost in mountains warmed by  $0.19 \pm 0.05$  °C and in Antarctica by  $0.37 \pm 0.10$  °C. Globally, permafrost temperature increased by  $0.29 \pm 0.12$  °C.

However, despite the great efforts by the GTN-P/IPA in managing qualified long-term permafrost observations at a global scale, the observation points are very scarce and clustered. For example, Biskaborn et al. (2015) pointed out that GTN-P permafrost boreholes and active layer measurement sites are clustered along transportation corridors in areas with developed infrastructure. They further demonstrated that the distribution of GTN-P sites is concentrated within zones where projected temperature rise is smaller while a much lower number of sites are located within Arctic areas where climate models project very large temperature increases.

There has been no globally consistent and spatially continuous mapping of the ECV parameters permafrost temperature and active layer thickness. IPA had therefore established a permafrost mapping focus group (action group ‘Overseeing the production of the next generation of IPA global permafrost mapping product and service’), which sought to assess different permafrost mapping initiatives for the compilation of a new global database for permafrost properties. Permafrost\_cci contributed to this IPA activity by providing satellite-driven permafrost datasets. The Permafrost\_cci products are further expected to aid understanding of permafrost dynamics by satellite-observed land surface changes across large regions, in particular disturbances along latitudinal gradients as well as degradation associated with permafrost coastal processes.

The following sections provide a first assessment of the CRDPv0 to CRDPv4 by the climate research group with respect to the so far identified applications.

Seven Use Case studies cover a broad range of applications demonstrating the value and impact of CCI+ Permafrost products for different aspects of climate research. A utility assessment based on the PVIR is provided in addition.

### 3.2 Use Case Study 1 - Climate Observations: Linking pan-Arctic glacier mass balance and permafrost thaw through atmospheric circulation patterns

Sasgen, I., Steinhoefel, G., Kasprzyk, C., Matthes, H., Westermann, S., Boike, J., Grosse, G. (2024). Atmosphere circulation patterns synchronize pan-Arctic glacier melt and permafrost thaw. *Commun Earth Environ* 5, 375. <https://doi.org/10.1038/s43247-024-01548-8>

#### **Key points:**

- Combined GRACE/GRACE-FO glacier mass balance and ESA CCI Permafrost active-layer thickness data reveal coherent interannual variability across the Arctic.
- Shared signals between glacier mass loss and permafrost thaw are driven primarily by large-scale atmospheric circulation modes (Greenland Blocking Index, North Atlantic Oscillation), explaining  $\approx 75\%$  of the common variability.
- The CCI Permafrost product provided a spatially consistent, pan-Arctic record of active-layer thickness, enabling detection of synchronous anomalies and their connection to circulation patterns.

#### *Service:*

- Earth Observation data integration
- Permafrost monitoring and process attribution
- Cryosphere–atmosphere coupling

#### *End user (s)*

- Cryosphere and climate researchers
- Earth System Model validation and benchmarking communities

#### *Intermediate user (s)*

- Research institutes and data-service providers combining satellite and in-situ data for pan-Arctic assessments

#### **Applications**

The Arctic cryosphere exhibits rapid and spatially complex responses to atmospheric variability. Understanding how short-term atmospheric circulation patterns modulate glacier melt and permafrost thaw complements long-term trend analyses and is critical for attribution of extremes and feedback processes. By jointly analysing GRACE/GRACE-FO gravimetry and ESA CCI Permafrost active-layer thickness data, *Sasgen et al. (2024)* identified synchronous anomalies in glacier mass and permafrost dynamics across regions opposite around the pole. These covariations reflect large-scale summer circulation modes and highlight the need to include dynamic atmospheric patterns in projections of future Arctic impacts.

#### *Essential Climate Variables*

- Cryosphere
  - Active Layer Thickness

### Models

- none

### Climate Data Records

Obu, J.; Westermann, S.; Barboux, C.; Bartsch, A.; Delaloye, R.; Grosse, G.; Heim, B.; Hugelius, G.; Irrgang, A.; Kääb, A.M.; Kroisleitner, C.; Matthes, H.; Nitze, I.; Pellet, C.; Seifert, F.M.; Strozzi, T.; Wegmüller, U.; Wieczorek, M.; Wiesmann, A. (2021): ESA Permafrost Climate Change Initiative (Permafrost\_cci): Permafrost active layer thickness for the Northern Hemisphere, v3.0. NERC EDS Centre for Environmental Data Analysis, 28 June 2021. doi:10.5285/67a3f8c8dc914ef99f7f08eb0d997e23.

<https://dx.doi.org/10.5285/67a3f8c8dc914ef99f7f08eb0d997e23>

### Agencies

- European Space Agency (ESA) Climate Change Initiative (CCI)
- National Aeronautics and Space Administration (NASA) – The GRACE (Gravity Recovery and Climate Experiment) and GRACE Follow-On missions

### Satellite observations

- MODIS Landsurface temperature
- GRACE / GRACE-FO satellite gravimetry

### Description

Permafrost and glaciers are key components of the Arctic cryosphere that respond sensitively to both long-term climatic trends and short-term atmospheric variability. Understanding how these systems covary under different circulation regimes is crucial for identifying the drivers of extreme melt and thaw events and for constraining feedbacks in the coupled climate system (Screen et al., 2018, Biskaborn et al., 2019). In this context, we combined satellite gravimetry, remote sensing, and in-situ observations to explore the large-scale synchrony of glacier mass loss and permafrost thaw across the Arctic (see Sasgen et al., 2024). We focus on the role of atmospheric circulation patterns—particularly the Greenland Blocking Index (GBI) and North Atlantic Oscillation (NAO)—in shaping pan-Arctic variability in glacier and permafrost dynamics beyond the gradual effects of long-term warming (Silva et al., 2022; Hanna et al., 2016; Delhasse et al., 2020).

Our analysis combines multiple observational systems to resolve the relationship between glacier mass balance and permafrost active-layer thickness across the circum-Arctic. GRACE and GRACE-FO satellite gravimetry data (Wouters et al., 2019, Rechtner et al., 2014) are used to estimate annual glacier-mass variations for eight glacier regions from 2002–2023, including Alaska, Arctic Canada, Svalbard, and the Russian Arctic. ESA’s CCI Permafrost v3 product provided annual active-layer-thickness estimates from 2003–2019. To evaluate and complement these remote-sensing estimates, field measurements from the Circumpolar Active Layer Monitoring (CALM) network (Nelson et al., 2021) are included for 13 long-term sites, selected for near-continuous coverage north of 60° N. All time series were detrended and standardized to isolate interannual variability, and a factor analysis was applied to identify common temporal modes of change between glacier and permafrost regions. The resulting principal component is defined as a pan-Arctic Impact Index, which is then correlated with atmospheric

reanalysis fields—geopotential height at 500 hPa and air temperature at 700 hPa—to identify dominant circulation drivers. All Arctic glacier systems exhibit significant mass loss during the period 2002–2023, with the largest annual rates in the Gulf of Alaska ( $-46.5 \pm 13.4 \text{ Gt yr}^{-1}$ ) and northern Arctic Canada ( $-29.9 \pm 5.6 \text{ Gt yr}^{-1}$ ). The CCI Permafrost ALT shows a consistent increase in active-layer thickness between 0.4 and 1.4 cm  $\text{yr}^{-1}$  across most permafrost regions, particularly in central and eastern Siberia.. At several CALM sites—such as Barrow, Franklin Bluff, Lake Akhmelo, and Zackenberg—the timing and amplitude of anomalies in the CCI data closely matched in-situ observations, confirming that the satellite-derived fields capture realistic interannual variations across diverse permafrost landscapes.

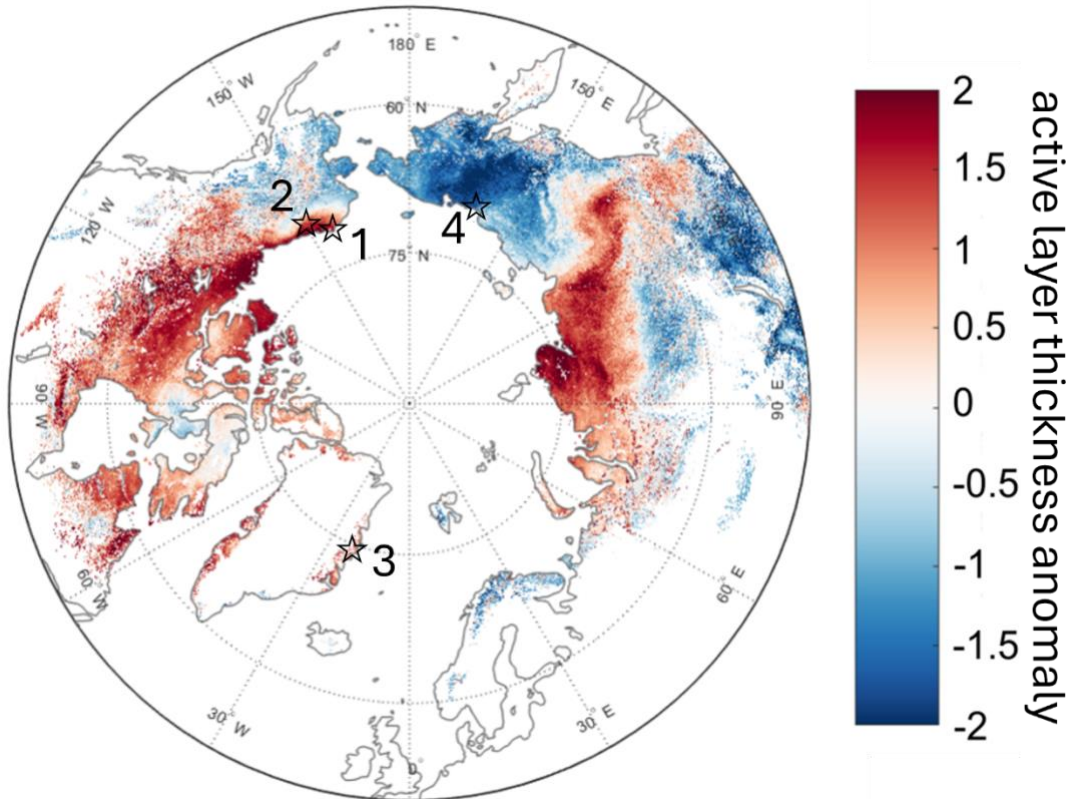


*Figure 1: Detrended standardized anomaly of active-layer thickness from ESA CCI Permafrost for 2012, with example CALM sites marked (1 – Utqiagvik (Barrow), 2 – Franklin Bluffs, 3 – Zackenberg, 4 – Lake Akhmelo)*

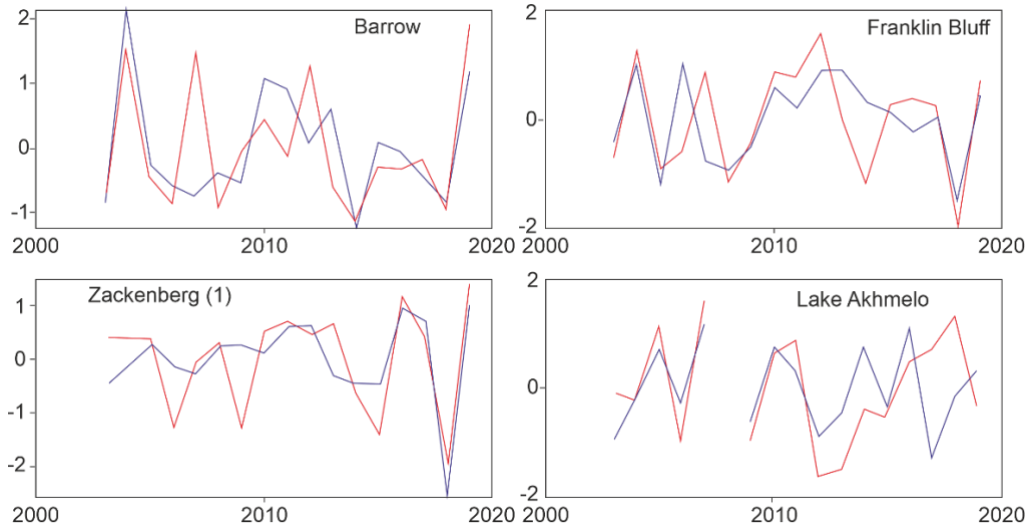


Figure 2: Comparison of standardized detrended active-layer-thickness anomalies from CALM observations (red) and ESA CCI Permafrost (blue) for selected sites.

By analysing detrended anomalies, we identify pronounced interannual covariations between glacier-mass changes and permafrost thaw anomalies in regions far apart—especially between northern Canada and central Siberia. These opposing yet synchronous variations reveal that Arctic glacier and permafrost systems respond coherently to hemispheric-scale atmospheric forcing rather than local thermal trends. The factor analysis demonstrates that the first principal component captures the majority of shared variability between the glacier and permafrost records. When the Arctic Impact Index defined for this analysis is compared with summer (JJA) atmospheric fields, it shows strong correlations with geopotential height anomalies indicative of the GBI–NAO composite circulation pattern. Approximately 75 % of the common variability in glacier mass balance and permafrost active-layer thickness is explained by these dominant atmospheric modes. The spatial pattern reflects negative pressure anomalies over Greenland and the Arctic Ocean, coupled with positive anomalies over Eurasia and North America—conditions that drive warmer, moister summers in Eurasia and cooler conditions in the Canadian Arctic. These findings highlight the need for climate models to represent dynamic atmospheric drivers of Arctic cryosphere change.

### 3.3 Use Case Study 2 - ALT, PFR and ground temperature trends: comparison to landcover trends

#### Key points:

- The HRPC (Hot Spot Regions of Permafrost Change) dataset, including lake changes and wildfires, was compared with The ESA CCI Ground Temperature dataset, and further auxiliary datasets of elevation, permafrost properties and thermokarst landscapes.
- State-of-the art explainable AI SHAP values were calculated to determine key environmental drivers of lake change over 600,000 lakes across the Arctic. in a second analysis the impact of wildfires was calculated for post-wildfire areas.
- The likelihood of lake drainage in permafrost regions is primarily influenced by the lake's origin and local lake morphologies, with the main factors varying across different regions. Notably,

peak drainage occurs in "warm" permafrost, characterized by a mean annual ground temperature ranging from -8 to -3 °C.

*Service:*

- Adaptation
- Planning

*End user (s)*

- Modellers
- Local communities
- Policy makers
- Government agencies
- Researchers

*Intermediate user (s)*

- Research institutes and academia

*Applications*

Permafrost is changing significantly due to the rapidly changing climate. Permafrost landscapes are changing rapidly with potentially strong impacts on local biogeochemical cycles but also implications on the global climate. Over the past years first pan-Arctic landscape disturbance maps and datasets have been created and published. These datasets can be used to better quantify environmental drivers of landscape change. With this information, it will become possible to project future landscape dynamics of a further warming arctic.

*Essential Climate Variables*

- Cryosphere
  - Permafrost ground temperature
  - Active Layer Thickness

*Climate Data Records*

ESA Permafrost Climate Change Initiative (Permafrost\_cci): Permafrost version 2 data products, Obu, J.; Westermann, S.; Barboux, C.; Bartsch, A.; Delaloye, R.; Grosse, G.; Heim, B.; Hugelius, G.; Irrgang, A.; Kääb, A.M.; Kroisleitner, C.; Matthes, H.; Nitze, I.; Pellet, C.; Seifert, F.M.; Strozzi, T.; Wegmüller, U.; Wieczorek, M.; Wiesmann, A. (2020): ESA Permafrost Climate Change Initiative (Permafrost\_cci): Permafrost version 2 data products. Centre for Environmental Data Analysis, 15.05.2024. <http://catalogue.ceda.ac.uk/uuid/1f88068e86304b0fbd34456115b6606f>

*Agencies*

- European Space Agency (ESA) Climate Change Initiative (CCI)

*Satellite observations*

- MODIS Landsurface temperature

*Description*

The Science use case 2 in Permafrost\_cci focuses on the cross-analysis of the existing ESA GlobPermafrost Hot Spot Regions of Permafrost Change (HRPC) product with output from the Permafrost\_cci transient permafrost model. The HRPC contains information on Landsat-based trends of landscape disturbances, which may trigger changes in the ground thermal regime or become enhanced by regional to local changes in ground thermal regime.

We hypothesize that climatic fluctuations directly impact permafrost properties and ground thermal regime as measured by active layer thickness (ALT) or permafrost/ground temperature. This in turn will likely impact the initiation and enhancement of permafrost region disturbances (PRD).

Based on this hypothesis we spatially compared the HRPC data products (Nitze et al., 2018 a,b) with the dynamic annual (1997-2018) ALT and PFR (permafrost probability) as well as static permafrost temperature Permafrost CCI+ data products (Obu et al, 2018) for all four core transects of the HRPC data analysis in western Siberia (T1), eastern Siberia (T2), Alaska (T3), and eastern Canada (T4).

Lake drainage - ground temperature relationship

A first cross-analysis between current Permafrost\_cci products and GlobPermafrost HRPC disturbance trends focused on the analysis of the spatial relationship between lake drainage and mean annual ground temperature. Lake changes were quantified using trends of multispectral indices of Landsat-time series data from 1999 through 2014 (Nitze et al., 2017, 2018). This includes net lake changes of each individual lake (<1ha) within the transects, as well as the gross increase and decrease (individual fractions of lake area gain and loss). Furthermore, we calculated lake shore change rates in cm per year for each individual lake ( $n > 600,000$ ).

Lakes in permafrost often exhibit a dynamic behaviour, where lakes often expand over time and ultimately drain once they reach a drainage gradient or permafrost destabilizes. Lake drainage can occur in different magnitudes, where lakes can drain completely or only partially.

Figure 2 shows the relation between net lake area loss of shrinking lakes (negative net lake change) from the HRPC lake change datasets (Nitze et al., 2018b) for all 4 analyzed continental scale permafrost transects. It reveals distinct clusters of lake area loss intensity and mean annual ground-temperature MAGT distributions. All sites show a bimodal distribution of lake area loss, but with different magnitude. The first cluster is typically located at <20 % lake area loss (net change), which is caused by subtle lake fluctuations, data uncertainty, partial lake drainage or a combination of these factors. Lakes with a lake area increase were kept from the analysis. This cluster is the most dominant in T4 (Eastern Canada), which is characterized by mostly stable lake areas across the transect region and thus the permafrost temperature gradient. The second cluster is typically close to 100%, which translates to complete lake drainage. This second cluster is more common in Transects T1-T3, which are more dominated by frozen ice-rich sediments rather than glacially-carved bedrock like T4. The relation of these drainage clusters to MAGT is diverse among the different transects. While T2 is characterized by cold MAGT of predominantly  $<-4^{\circ}\text{C}$ , complete lake drainage events clustered at around  $-6^{\circ}\text{C}$ . In T1

and T3, which have very strong lake dynamics (Nitze et al., 2018a), the complete drainage cluster is close to 0 °C, which may indicate the influence of landscape-scale permafrost degradation and widespread surface permafrost loss in the affected regions. However, regional conditions and differences should be considered and more detailed local to regional-scale analysis will reveal further links between ground temperature, other environmental factors, and the dynamics of permafrost region disturbances such as lake drainages.

#### Drivers of lake drainage

Furthermore, we quantified the impact of environmental variables, such as permafrost, climate, lake shape and geomorphology on lake drainage. We used the RandomForest Feature Importances and SHAP/shapley explainable AI methods (SHAP) based on Random Forest and XGBoost machine learning models. This allowed us to retrogressively model lake drainage and to determine the key drivers of lake drainage and stability for each of the ~600k individual lakes in the HRPC lake dataset.

In this use case the HRPC dataset served as the main data source. The CCI Permafrost Ground Temperature dataset v3 (Obu et al., 2019) served as one of the main auxiliary datasets among Climate (ERA5-Land, Copernicus Climate Change Service, 2019), thermokarst characteristics (Olefeldt et al., 2015), IPA permafrost properties (Brown et al., 1997) or geomorphology based on the MERIT DEM (Yamazaki et al., 2017)

Lake shape and local geomorphology are the most important predictors for lake drainage. These correlate very well with lake formation mechanisms and landscape location. Arctic lowland thermokarst lakes e.g., are much more affected by lake drainage than glacially formed lakes on the Canadian shield.

Permafrost and climate variables show a weaker impact on lake drainage. However, ground temperatures between -8 and -3°C show a stronger positive influence on lake drainage, implying a critical threshold of permafrost degradation in this temperature range. Generally, lakes in permafrost are more likely to drain than in thawed soils (>0°C).

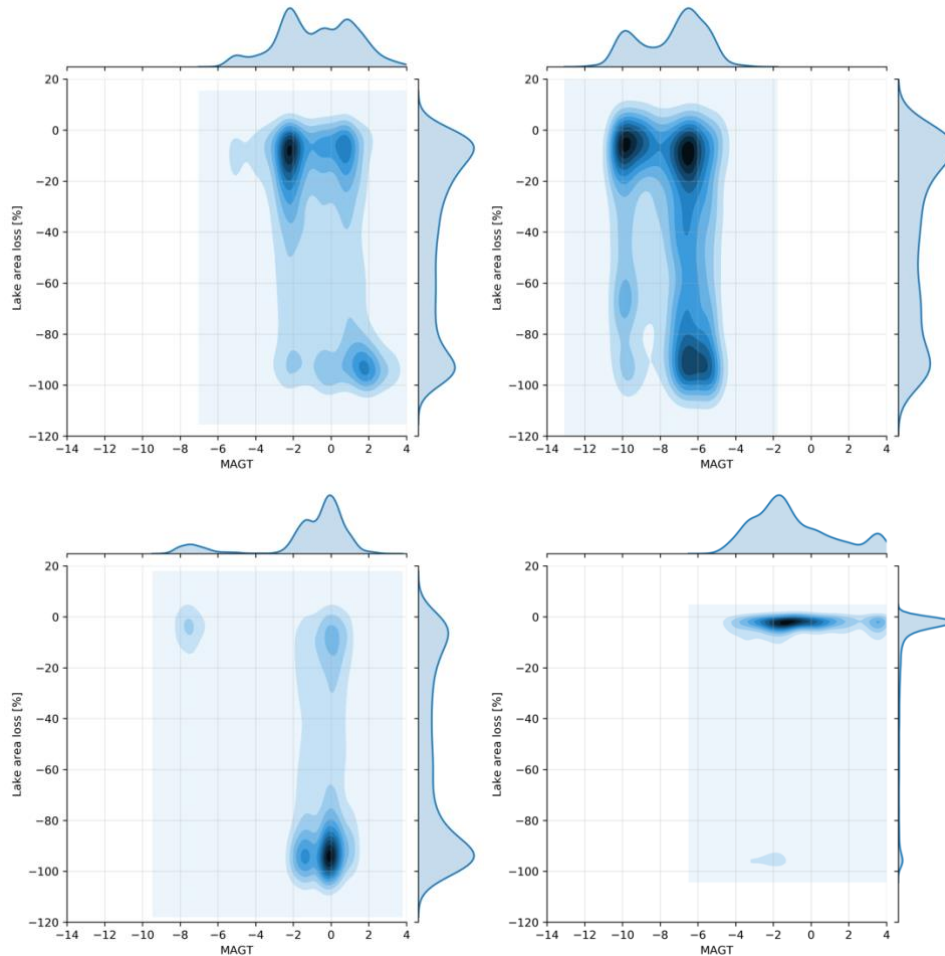


Figure 2: 2D density plots of lake area loss % (per lake) vs. MAGT. Darker colors represent a higher density and thus more lake drainage events. Upper left: T1 Western Siberia; upper right: T2 Eastern Siberia; lower left: T3 Alaska; lower right: T4 Eastern Canada.

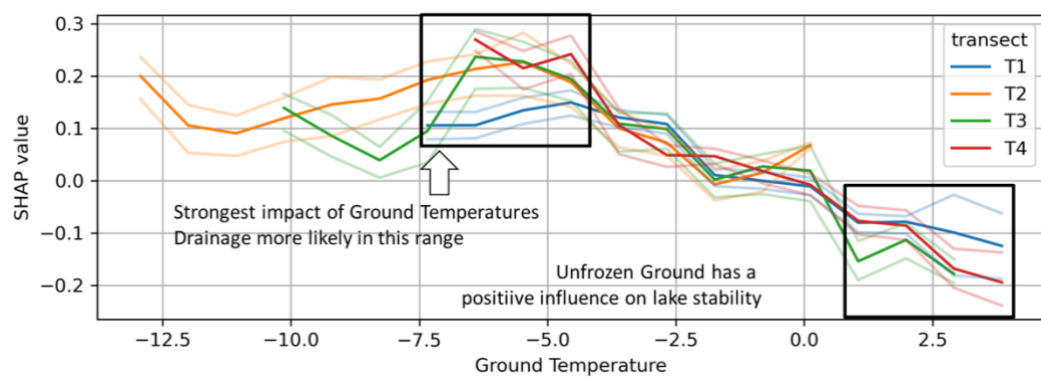


Figure 3: SHAP values (median+/-25th and 75th percentile) of ground temperatures for complete drainage (> 75% lake area loss). Ground temperatures contribute strongest to lake drainage from -8 to -3 °C. Positive SHAP values (y-axis) indicate a positive influence on lake drainage and vice versa.

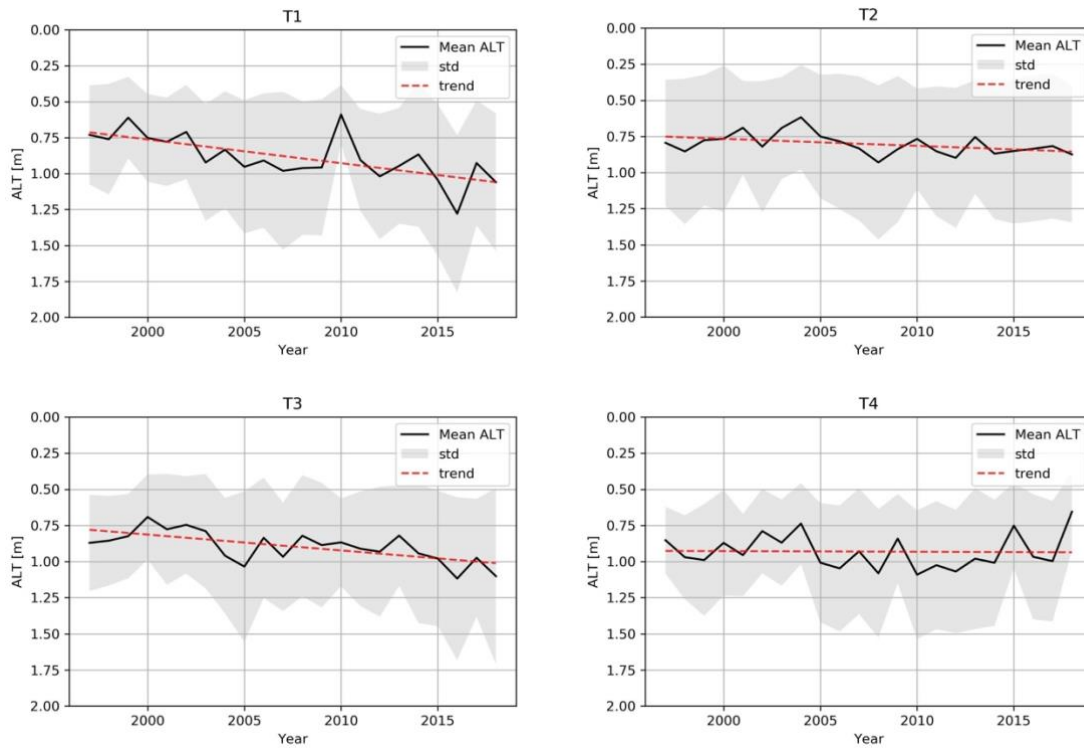


Figure 4: Comparison of Active Layer Thickness dynamics (in meter) in different HRPC Transects (T1: Western Siberia, T2: Eastern Siberia, T3: Alaska, T4: Eastern Canada) derived from annual ALT datasets (1997-2018).

#### Active layer thickness dynamics

The active layer trends show clear differences between the different transect regions (Figure 4). Transects T1 and T3 show the largest increase in mean ALT, which correlates with the observed lake drainage dynamics. Larger regions within both transects were particularly affected by lake drainage within the past two decades (Nitze et al., 2017, 2018, 2020). Transect T2 was much less affected by ALT deepening, while Transect T4 has a flat trend, although with strong annual fluctuation.

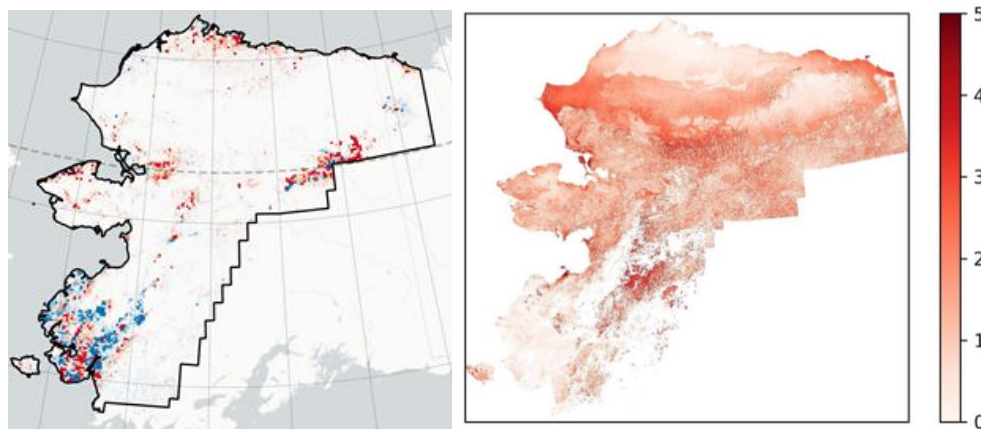


Figure 5: Spatial comparison of (left) Lake area change (1999-2014) from HRPC Datasets and (right) increase in Active Layer Thickness (ALT) trends in % from annual CCI ALT dataset in T3 Alaska.

### Wildfire - ALT interactions

Wildfires are a widespread disturbance in the boreal, mostly semi-arid continental permafrost regions such as Central Yakutia, interior Alaska or NW Canada. Two of these regions are located within the HRPC transects T2 and T3. We analyzed the ALT trajectories from 1999 until 2018 within burned areas, non-burned areas and individual fire scars. For this purpose, we calculated the mean and standard deviations of annual ALT within the burn scars. Furthermore, we applied a linear model to compare the change (slope) in mean ALT and its standard deviation for each region and burn status.

*Table 1: Change in mean and standard deviation of Active Layer Thickness in burned and non-burned areas across all 4 transects.*

Region	Fire		No Fire	
	Mean	Std	Mean	Std
T1	+40.10	+102.23	+49.11	+47.44
T2	+15.45	+21.66	+13.59	+10.11
T3	+30.05	+95.73	+29.74	+59.37
T4	+30.95	+56.63	+0.86	+34.33

### Individual Fires

On an individual burn scar level we can directly identify the impact of wildfires. Figure 6 shows the mean (line) and standard deviation (shading) of ALT for the Anaktuvuk River fire scar area from 1999 through 2018. The Anaktuvuk tundra fire in northern Alaska (Jones et al, 2009) burned around 1000 km<sup>2</sup> (100,000 ha) tundra, partially underlain by ice-rich permafrost, in late summer 2007. Before the large fire in 2007, the mean ALT fluctuated rather strongly (mean ALT 0.53-0.75), depending on annual weather conditions. However, The variance within the analysed site was very low which indicates a rather homogeneous ALT. After the intense tundra fire mean ALT increased to deeper depths (0.7-0.8 m). At the same time the variance of ALT increased markedly within the burned region.

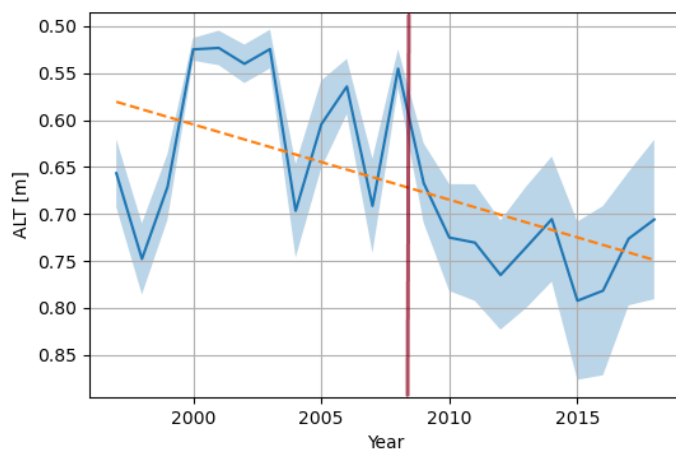


*Figure 6: Mean (line), standard deviation (shading) and trend of mean (orange dashed line) of modelled active layer thickness (ALT) within the Anaktuvuk firescar in northern Alaska. Burn date (2007) indicated with a red line.*

In all sites, ALT was larger for burned sites than for non-burned sites, which can be expected as wildfires predominantly occur in warmer, forested boreal sites. However, the trajectories of ALT exhibit a different behaviour. In all transects T1-T4, mean ALT increased within burned areas (+15-40%), but also in non-burned areas (+14-49%), except T4 (+1%), with similar magnitudes between burned and non-burned areas (Table 3). In comparison, variance of ALT increased in burned sites within all transects increased much stronger than in non-burned areas, even (almost) doubling in standard deviation.

Although the impact of wildfire on ALT seems to be much stronger in T4, the impact on ground stability may be much weaker than in the other regions, due to primarily underlying bedrock. We hypothesize a much stronger effect of increasing ALT in e.g. ice-rich permafrost in Alaska (T3) or eastern Siberia (T2). Particularly increasing variance within burned areas, with locally strong increase in ALT, may result in triggering further permafrost disturbances. However, more detailed analysis will be conducted to verify/falsify this hypothesis.

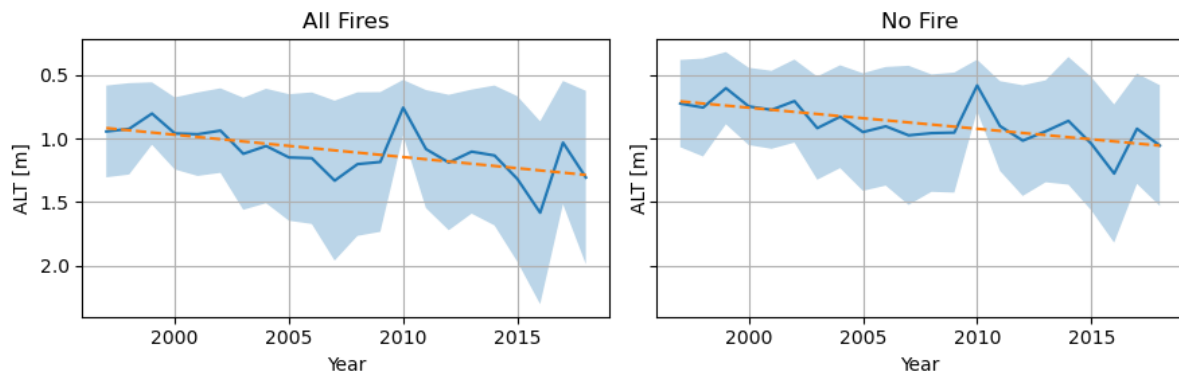


Figure 7: Mean (line), standard deviation (shading) and trend of mean (orange dashed line) of modelled active layer thickness (ALT) in burned and unburned regions in Transect T1 Western Siberia.

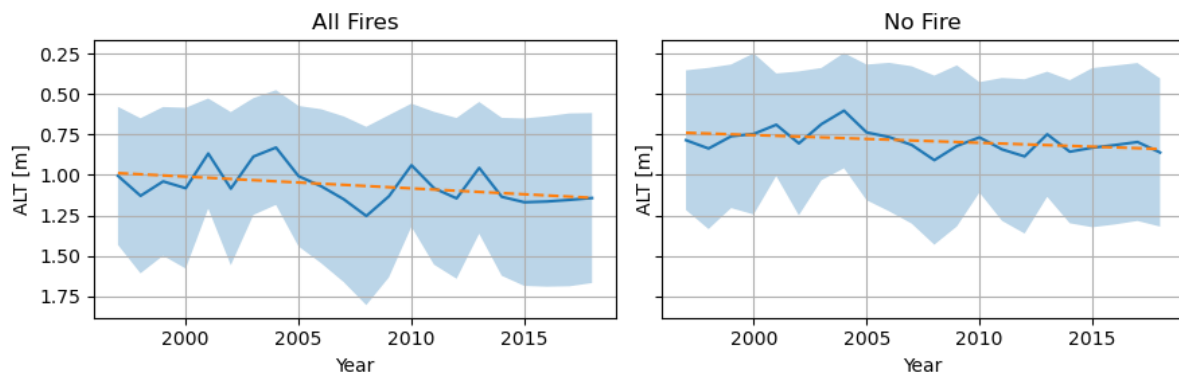


Figure 8: Mean (line), standard deviation (shading) and trend of mean (orange dashed line) of modelled active layer thickness (ALT) in burned and unburned regions in Transect T2 Eastern Siberia.

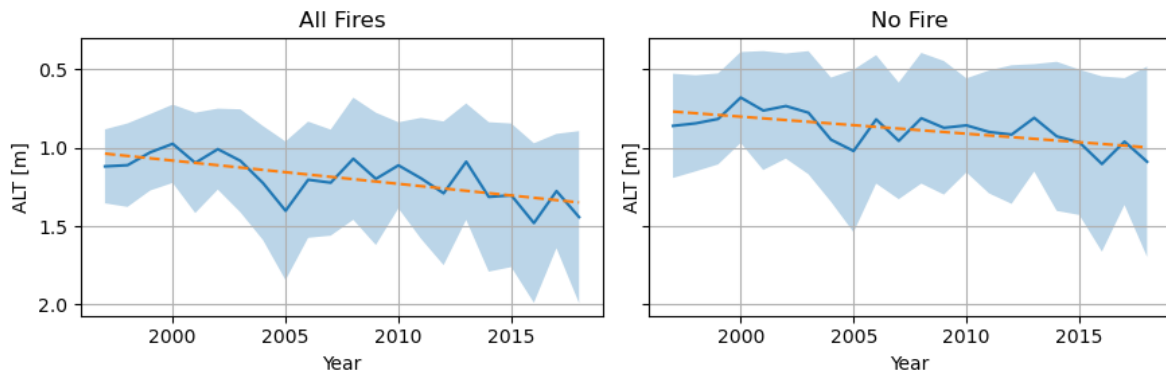


Figure 9: Mean (line), standard deviation (shading) and trend of mean (orange dashed line) of modelled active layer thickness (ALT) in burned and unburned regions in Transect T3 Alaska.

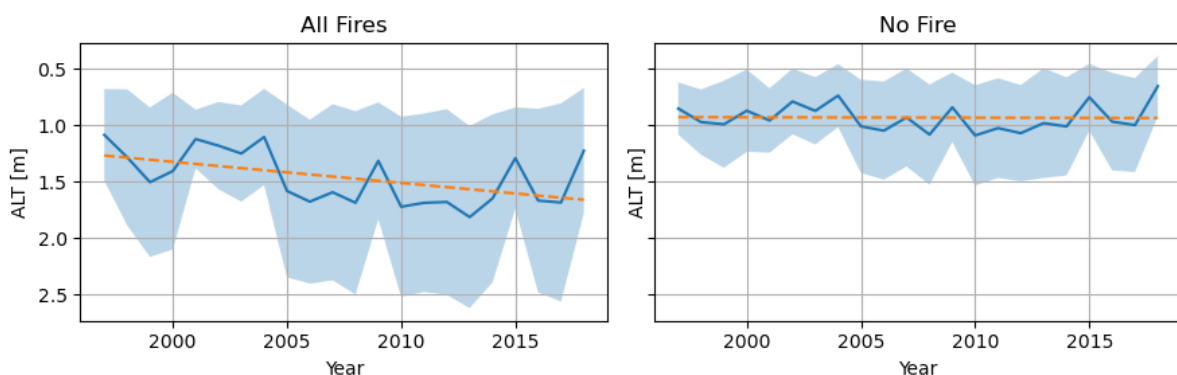


Figure 10: Mean (line), standard deviation (shading) and trend of mean (orange dashed line) of modelled active layer thickness (ALT) in burned and unburned regions in Transect T4 Eastern Canada.

### 3.4 Use Case Study 3 - Permafrost trends: affected Arctic Infrastructure

- Bartsch, A., Pointner, G., Nitze, I., Efimova, A., Jakober, D., Ley, S., Högström, E., Grosse, G., and Schweitzer, P. (2021): Expanding infrastructure and growing anthropogenic impacts along Arctic coasts, Environmental Research Letters, Volume 16, Number 11, <https://doi.org/10.1088/1748-9326/ac3176>.

#### Key points:

- A first panarctic satellite-based record of expanding infrastructure and anthropogenic impacts along all permafrost affected coasts was developed and combined with Permafrost\_cci records.
- Almost 97% of all mapped areas showed a positive trend in ground temperature and 93% for ALT.
- 55% of the identified human impacted area will be shifting to above 0 °C ground temperature at two meter depth by 2050 if current permafrost warming trends continue at the pace of the last two decades.

#### Service:

- Adaptation
- Disaster Risk reduction

*End user (s)*

- Local communities
- Policy makers
- Government agencies
- Researchers

*Intermediate user (s)*

- Research institutes and academia

*Applications*

Permafrost is permanently frozen ground. Warming of the Arctic results in widespread increase of ground temperatures and permafrost degradation is occurring in many regions. Trends of Permafrost properties have been combined with a novel Arctic infrastructure database. Settlements prone to change during the last 20 years have been identified and trends have been extrapolated to identify infrastructure which will be affected by diminishing permafrost and potential ground instability by 2050 and 2060 respectively.

*Essential Climate Variables*

- Cryosphere
  - Permafrost ground temperature
  - Active Layer Thickness

*Climate Data Records:*

ESA Permafrost Climate Change Initiative (Permafrost\_cci): Permafrost version 2 data products, Obu, J.; Westermann, S.; Barboux, C.; Bartsch, A.; Delaloye, R.; Grosse, G.; Heim, B.; Hugelius, G.; Irrgang, A.; Kääb, A.M.; Kroisleitner, C.; Matthes, H.; Nitze, I.; Pellet, C.; Seifert, F.M.; Strozzi, T.; Wegmüller, U.; Wieczorek, M.; Wiesmann, A. (2020): ESA Permafrost Climate Change Initiative (Permafrost\_cci): Permafrost version 2 data products. Centre for Environmental Data Analysis, 15.05.2024. <http://catalogue.ceda.ac.uk/uuid/1f88068e86304b0fb34456115b6606f>

*Agencies*

- European Space Agency (ESA) Climate Change Initiative (CCI)

*Satellite observations*

- MODIS Landsurface temperature

*Description*

The accelerating climatic changes and new infrastructure development across the Arctic require more robust risk and environmental assessment, but thus far there was no consistent record of human impact. A first panarctic satellite-based record of expanding infrastructure and anthropogenic impacts along all permafrost affected coasts (100 km buffer,  $\approx 6.2$  Mio km<sup>2</sup>), named the Sentinel-1/2 derived Arctic Coastal Human Impact (SACHI) dataset, was developed and combined with Permafrost\_cci records.

An existing processing chain (Bartsch et al 2020a) was used as a first step to obtain results from two different classification approaches. It includes a pixel-based classification using a Gradient Boosting Machine and a windowed semantic segmentation approach (U-Net convolutional neural network architecture) using the deep learning framework Keras with the Tensorflow backend. A Theil-Sen regression was used for trend retrievals from 2 m ground temperature, active layer thickness (ALT), and permafrost fraction. In case of Landsat derived NDVI, the trends have been obtained with Ordinary Least Square regression. For NDVI, changes per decade, and for all other parameters, changes per year were extracted. For each object the average change was derived. This was carried out for all classes together as well as separately. The analyses were made on different levels: the entire Arctic and by country/region (in both cases subset with the 100 km buffer).

At least 15% (180 km<sup>2</sup>) of SACHI objects correspond to new or increased detectable human impact since 2000 according to a Landsat-based normalized difference vegetation index trend comparison within the analysis extent.

More than 50% of settlements occurs over continuous permafrost and more than 30% over discontinuous permafrost. Most identified areas in Canada and US are located on continuous permafrost. For Russia this applies to less than half of them. Almost 97% of all mapped areas showed a positive trend in ground temperature and 93% for ALT. Temperatures were increasing by 0.8 °C per decade on average over the human-impacted area identified within the analysis extent. The ALT increase was 11 cm per decade (average ALT in 2019 was 84 cm). About 8% changed from a permafrost fraction of 100% to a lower value between 1997 and 2019.

The changes in ground temperature during the last two decades tend to be larger in colder permafrost than for ground with temperatures near zero degree C (as determined for the year 2019, Figure 11), which agrees with prior findings (Romanovsky et al 2017, Biskaborn et al 2019, Box et al 2019). As the magnitude for the latter is still on the order of one degree C for this time period, the expected impact during the upcoming decades is large if the trend continues. 55% and 67% of human-impacted areas will be located on ground with larger than zero degree C mean annual ground temperature down to 2 m depth in 2050 and 2060 respectively. Most affected is Russia and some areas in the US (Alaska) (figure 13).

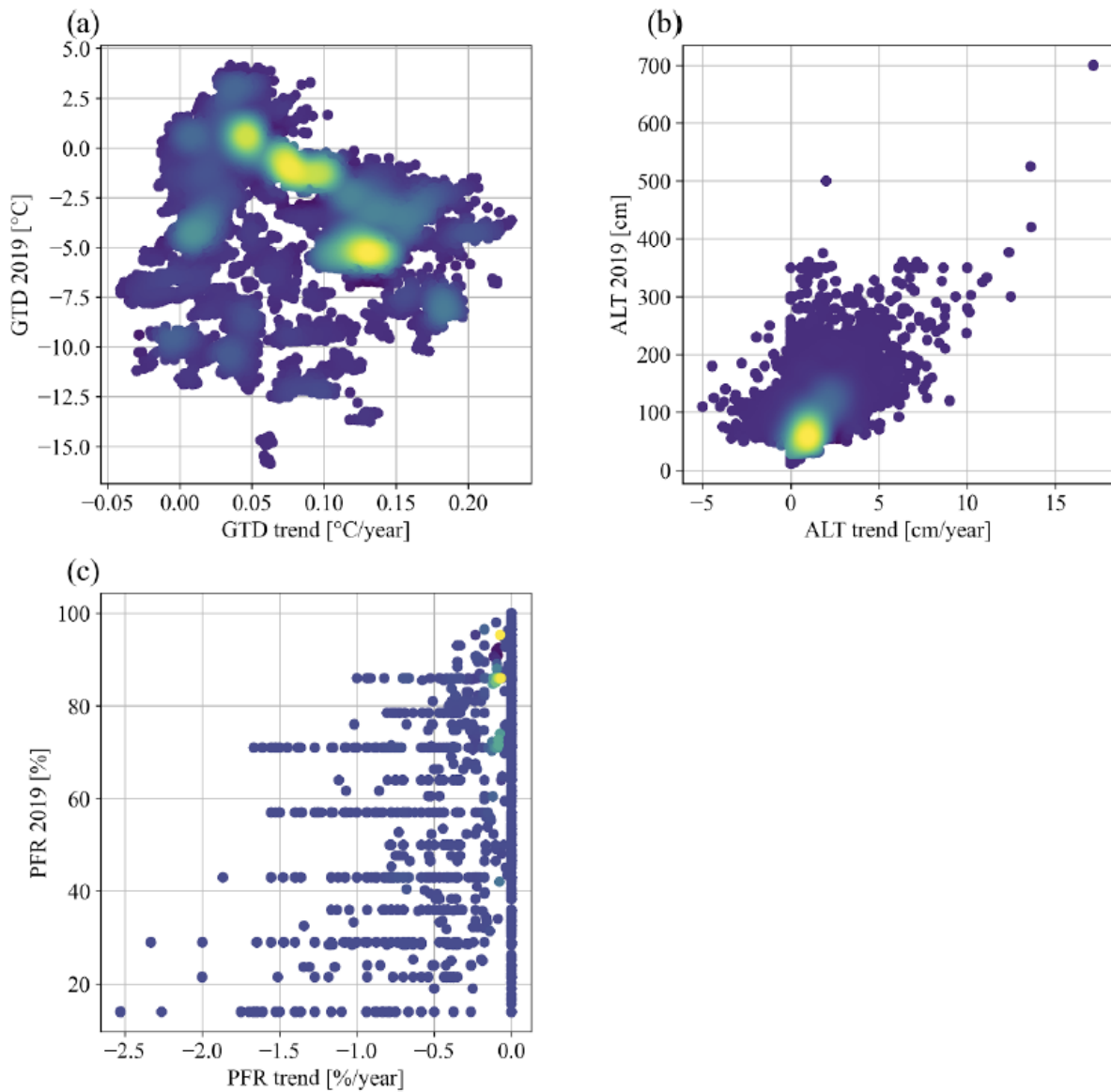


*Figure 11: Scatterplots of trend versus 2019 status for (a) ground temperature at 2 m depth, (b) active layer thickness and (c) permafrost fraction. Each point represents the average for a distinct object (human impacted area) as mapped with Sentinel-1 and -2 (Bartsch et al 2021b, dataset on ZENODO). Calculations are based on Obu et al (2021a, 2021b, 2021c) respectively. (Source: Bartsch et al. 2021a, ERL)*

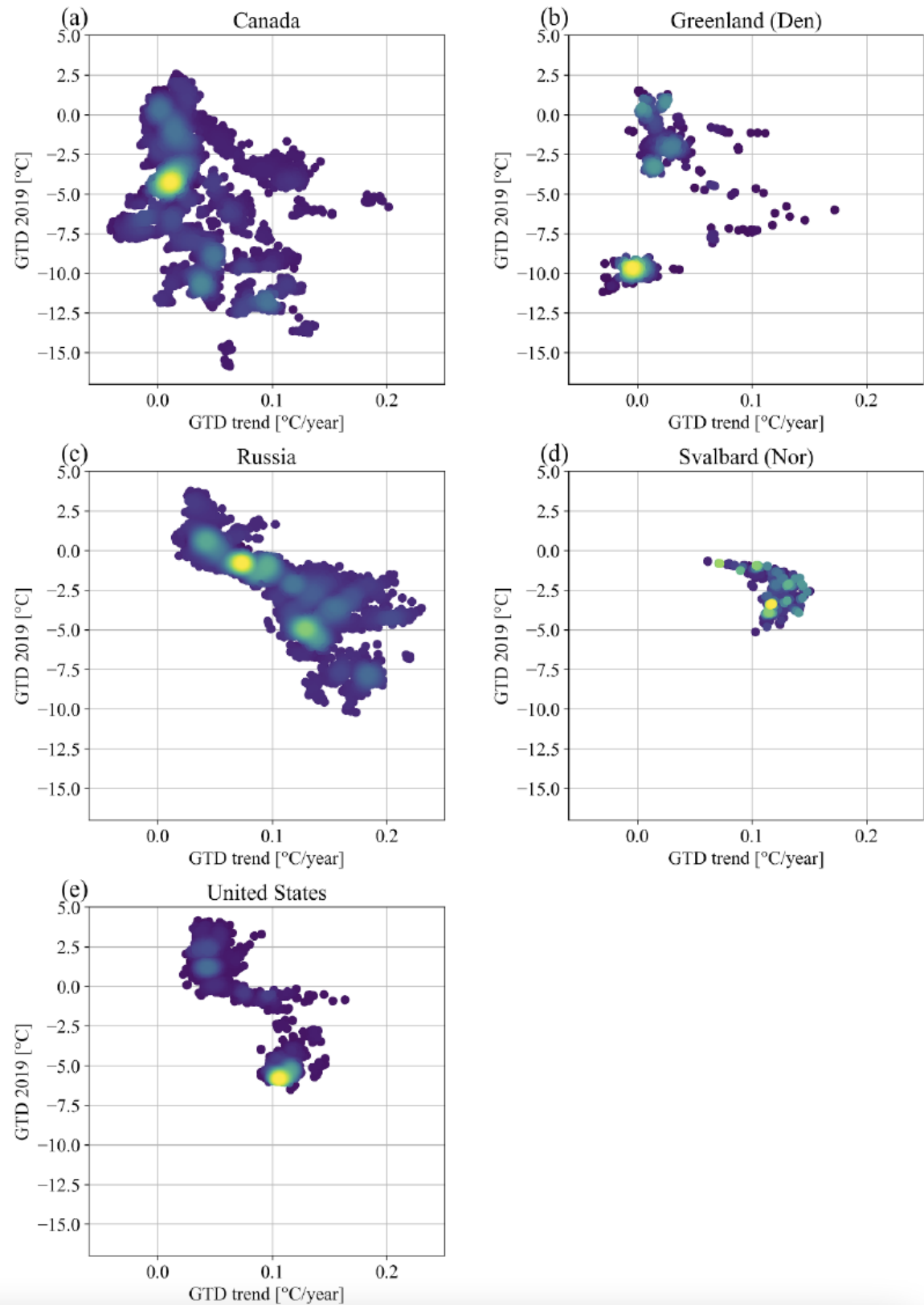


Figure 12: Scatterplots of ground temperature (GTD; 2 m depth) trend versus 2019 status for different countries/regions (analysis extent only). Each point represents the average for a distinct object (human impacted area) as mapped with Sentinel-1 and -2 (Bartsch et al 2021b). (Source: Bartsch et al. 2021a, ERL)

### 3.5 Use Case Study 4 - Permafrost trends: affected Arctic Coastal Infrastructure

- Tanguy, R., Bartsch, A., Nitze, I., Irrgang, A., Petzold, P., Widhalm, B., von Baeckmann, C., Boike, J., Martin, J., Efimova, A., Vieira, G., Whalen, D., Heim, B., Wieczorek, M., Grosse, G. (2024). Pan-Arctic assessment of coastal settlements and infrastructure vulnerable to coastal erosion, sea-level rise, and permafrost thaw. *Earth's Future*, 12, e2024EF005013. <https://doi.org/10.1029/2024EF005013>.

*Key points:*

- A first panarctic satellite-based record of coastal settlements affected by multiple risks was developed among others considering Permafrost\_cci records.
- By 2100, 77% of coastal infrastructure will see ground temperature at 2 m shift from negative to positive, based on 2000–2019 trend
- On average, coastal permafrost GT is increasing by 0.8°C per decade, and ALT is increasing by 6 cm per decade.

*Service:*

- Adaptation
- Disaster Risk reduction

*End user (s)*

- Local communities
- Policy makers
- Government agencies
- Researchers

*Intermediate user (s)*

- Research institutes and academia

*Applications*

Permafrost is permanently frozen ground. Warming of the Arctic results in widespread increase of ground temperatures and permafrost degradation is occurring in many regions. Trends of Permafrost properties have been combined with an updated Arctic infrastructure database, a novel coastal erosion dataset and projected sea level rise. Settlements at risk this century have been identified based on extrapolated trends. Settlements prone to multiple risks could be determined in combination with the other datasets.

*Essential Climate Variables*

- Cryosphere
  - Permafrost ground temperature
  - Active Layer Thickness

*Climate Data Records:*

ESA Permafrost Climate Change Initiative (Permafrost\_cci): Permafrost version 3 data products, Obu, J.; Westermann, S.; Barboux, C.; Bartsch, A.; Delaloye, R.; Grosse, G.; Heim, B.; Hugelius, G.; Irrgang, A.; Kääb, A.M.; Kroisleitner, C.; Matthes, H.; Nitze, I.; Pellet, C.; Seifert, F.M.; Strozzi, T.; Wegmüller, U.; Wieczorek, M.; Wiesmann, A. (2021): ESA Permafrost Climate Change Initiative (Permafrost\_cci): Permafrost active layer thickness for the Northern Hemisphere, v3.0. NERC EDS Centre for Environmental Data Analysis, 28 June 2021. doi:10.5285/67a3f8c8dc914ef99f7f08eb0d997e23. <https://dx.doi.org/10.5285/67a3f8c8dc914ef99f7f08eb0d997e23>

Obu, J.; Westermann, S.; Barboux, C.; Bartsch, A.; Delaloye, R.; Grosse, G.; Heim, B.; Hugelius, G.; Irrgang, A.; Kääb, A.M.; Kroisleitner, C.; Matthes, H.; Nitze, I.; Pellet, C.; Seifert, F.M.; Strozzi, T.; Wegmüller, U.; Wieczorek, M.; Wiesmann, A. (2021): ESA Permafrost Climate Change Initiative (Permafrost\_cci): Permafrost Ground Temperature for the Northern Hemisphere, v3.0. NERC EDS Centre for Environmental Data Analysis, 28 June 2021. doi:10.5285/b25d4a6174de4ac78000d034f500a268. <https://dx.doi.org/10.5285/b25d4a6174de4ac78000d034f500a268>

#### *Agencies*

- European Space Agency (ESA) Climate Change Initiative (CCI)

#### *Satellite observations*

- MODIS Landsurface temperature

#### *Description*

This study assessed the vulnerability of Arctic coastal settlements and infrastructure to coastal erosion, Sea-Level Rise (SLR) and permafrost warming. For the first time, we characterize coastline retreat consistently along permafrost coastal settlements at the regional scale for the Northern Hemisphere. A new method to automatically derive long-term coastline change rates for permafrost coasts is provided. In addition, the total number of coastal settlements and associated infrastructure that could be threatened by marine and terrestrial changes was identified using remote sensing techniques. The Arctic Coastal Infrastructure data set (SACHI) was extended to include road types, airstrips, and artificial water reservoirs. The analysis of coastline, Ground Temperature (GT) and Active Layer Thickness (ALT) changes from 2000 to 2020, in addition with SLR projection, allowed to identify exposed settlements and infrastructure for 2030, 2050, and 2100. We validated the SACHI-v2, GT and ALT data sets through comparisons with in-situ data.

Validation was done for ALT using new in-situ thaw-depth measurements (T-MOSAiC, Boike et al., 2021; CALM et al., 2024; Martin et al., 2023). The data and procedure are described in the Supporting Information S1. The comparison revealed regional biases associated with the spatial resolution (near 1 km) of the modeled data sets, which do not capture land-cover spatial variability at a finer scale (Figure 13). GT and ALT for 2019 and trends were extracted from the permafrost\_cci products (Obu et al., 2021a, 2021b) at infrastructure extent (Figure 14) as well as for the entire study extent. Linear trend extrapolation for 2030, 2050, and 2100 was applied to understand the distribution and magnitude of potential change in future decades.

60% of the detected infrastructure is built on low-lying coast (<10 m a.s.l). The results show that in 2100, 45% of all coastal settlements will be affected by SLR and 21% by coastal erosion. On average, coastal permafrost GT is increasing by 0.8°C per decade, and ALT is increasing by 6 cm per decade. In 2100, GT will become positive at 77% of the built infrastructure area. The results highlight the circumpolar and international amplitude of the problem and emphasize the need for immediate adaptation measures to current and future environmental changes to counteract a deterioration of living conditions and ensure infrastructure sustainability.

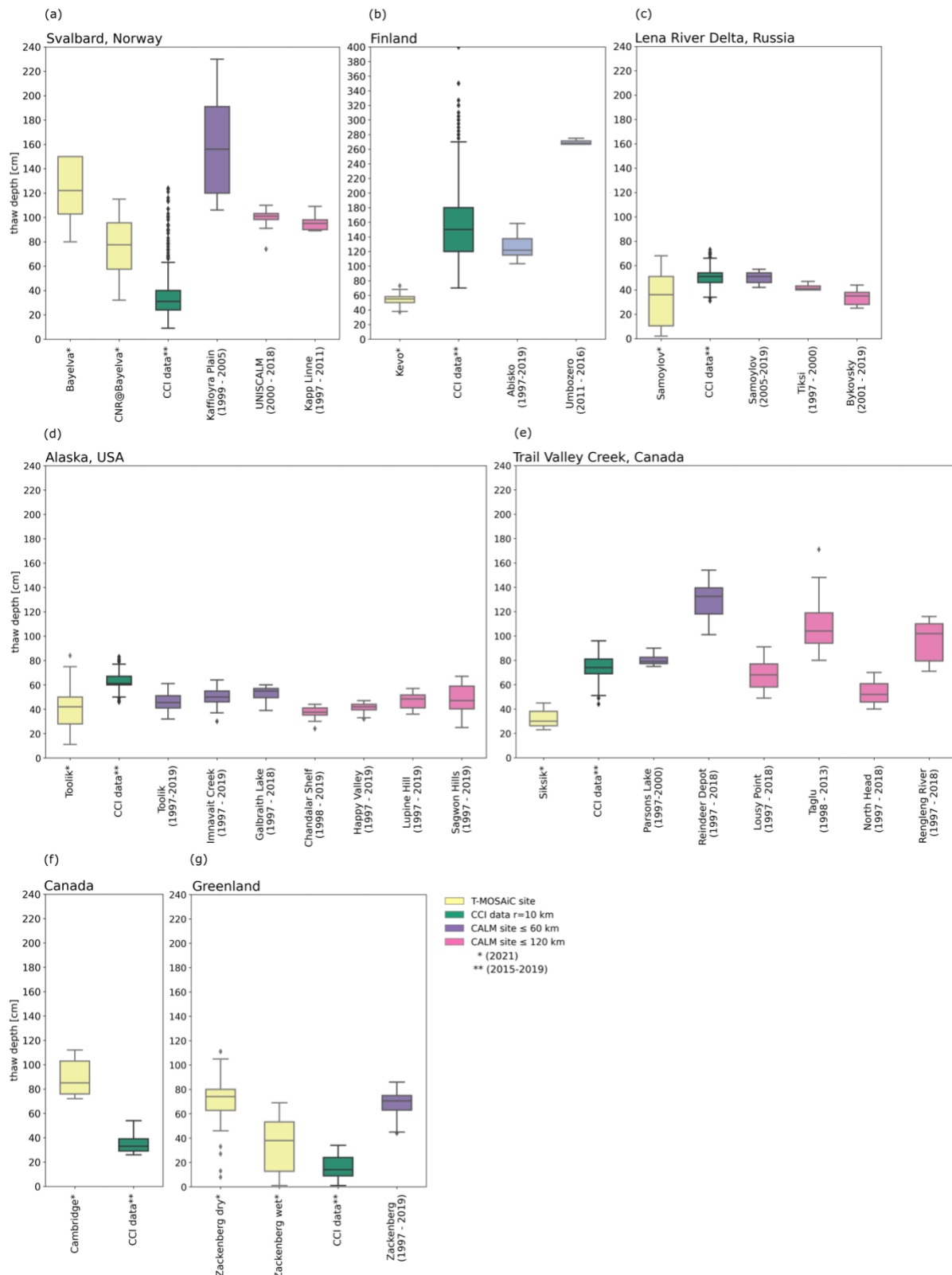
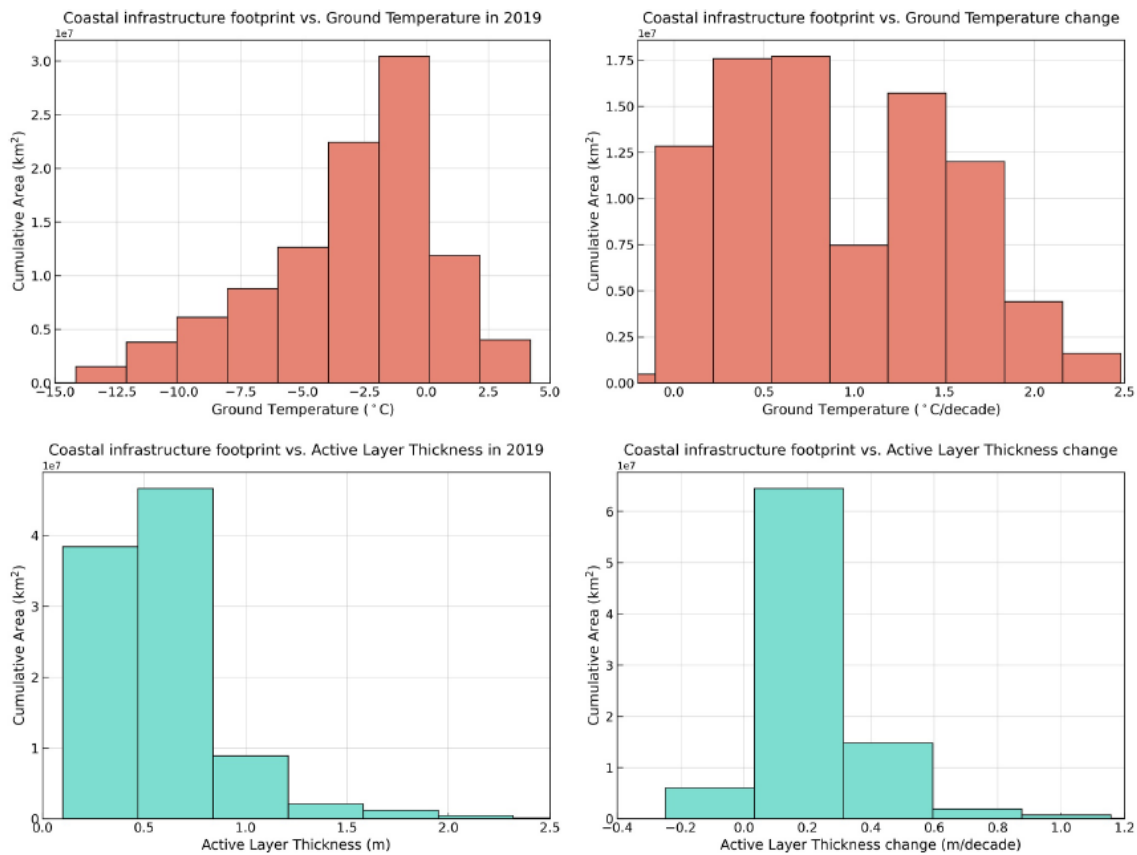


Figure 13: Comparison between T-Mosaic in situ thaw depth and Permafrost CCI records; averaged over the surroundings (source: supplement of Tanguy et al. 2024)



*Figure 14: Distribution of GT and ALT for 2019 and annual change rate at the extent of coastal infrastructure. The change rates were calculated over the 2000–2019 period. Trends were derived from Permafrost\_cci data (Obu et al., 2021a, 2021b)*

### 3.6 Use Case Study 5 - Permafrost variations: understanding Arctic change through identification similarities with sea ice

Bartsch, A., Tanguy, R., Bergstedt, H., von Baeckmann, C., Tømmervik, H., Macias-Fauria, M., Lemmetyinen, J., Rautiainen, K., Gruber, C., and Forbes, B. C.: Similarities between sea ice area variations and satellite-derived terrestrial biosphere and cryosphere parameters across the Arctic, *The Cryosphere*, 19, 4929–4967, <https://doi.org/10.5194/tc-19-4929-2025>, 2025.

*Key points:*

- A first pan-arctic satellite-based record of similarities between permafrost and sea ice variations was developed.
- A high proportion of significant correlation was found in many regions, with values over 80% for Svalbard and the Laptev Sea adjacent land area
- In the case of MAGT, high significant correlations were found for more distant sea ice basins than for the NDVI derivatives, indicating influences of large-scale atmospheric circulation patterns.

*Service:*

- Adaptation
- Disaster Risk reduction

*End user (s)*

- Local communities
- Policy makers
- Government agencies
- Researchers

*Intermediate user (s)*

- Research institutes and academia

*Applications*

Mean annual ground temperature representing 2 meter depth for 2000-2019 were analysed. Initially trends were derived for all area north of 60°N. The original time series has been detrended before comparison to monthly sea ice area datasets. The month and corresponding sea ice basin with the highest (high ground temperature with high sea ice extent) and lowest correlation (high ground temperature and low sea ice extent) has been determined for each Permafrost\_cci data grid point. Data points with significant correlations have been included into the Arctic Sea Ice and Land Parameter Correlations database (ASILaC). The ASILaC dataset provides information on both previously regionally documented and additional potential linkages, close and distant, and thus a baseline for future studies on common drivers of essential climate variables and dependencies across the Arctic.

*Essential Climate Variables*

- Cryosphere
  - Permafrost ground temperature

*Climate Data Records:*

ESA Permafrost Climate Change Initiative (Permafrost\_cci): Permafrost version 3 data products:

Obu, J.; Westermann, S.; Barboux, C.; Bartsch, A.; Delaloye, R.; Grosse, G.; Heim, B.; Hugelius, G.; Irrgang, A.; Kääb, A.M.; Kroisleitner, C.; Matthes, H.; Nitze, I.; Pellet, C.; Seifert, F.M.; Strozzi, T.; Wegmüller, U.; Wieczorek, M.; Wiesmann, A. (2021): ESA Permafrost Climate Change Initiative (Permafrost\_cci): Permafrost active layer thickness for the Northern Hemisphere, v3.0. NERC EDS Centre for Environmental Data Analysis, 28 June 2021.

doi:10.5285/67a3f8c8dc914ef99f7f08eb0d997e23. <https://dx.doi.org/10.5285/67a3f8c8dc914ef99f7f08eb0d997e23>

Obu, J.; Westermann, S.; Barboux, C.; Bartsch, A.; Delaloye, R.; Grosse, G.; Heim, B.; Hugelius, G.; Irrgang, A.; Kääb, A.M.; Kroisleitner, C.; Matthes, H.; Nitze, I.; Pellet, C.; Seifert, F.M.; Strozzi, T.; Wegmüller, U.; Wieczorek, M.; Wiesmann, A. (2021): ESA Permafrost Climate Change Initiative (Permafrost\_cci): Permafrost Ground Temperature for the Northern Hemisphere, v3.0. NERC EDS Centre for Environmental Data Analysis, 28 June 2021.

doi:10.5285/b25d4a6174de4ac78000d034f500a268. <https://dx.doi.org/10.5285/b25d4a6174de4ac78000d034f500a268>

#### *Agencies*

- European Space Agency (ESA) Climate Change Initiative (CCI)

#### *Satellite observations*

- MODIS Land surface temperature

#### *Description*

Satellite time series availability for the Arctic Ocean and adjacent land areas allows for cross-comparisons for cryosphere vs. vegetation parameters. Previous studies focused on correlation analyses between vegetation indices (time-integrated and maximum normalized difference vegetation index, TINDVI and MaxNDVI) of tundra regions and sea ice extent for selected months. These analyses were refined through consideration of distinct sea ice basins and all months, extension to south of the treeline, and included cryosphere essential climate variables such as snow water equivalent (SWE; March as proxy for annual maximum) and mean annual ground temperature (MAGT) in permafrost areas. The focus was on 2000-2019 reflecting data availability. As a first step, trends were derived. Changes across all the different parameters could be specifically determined for Eastern Siberia. Then, timeseries were de-trended and correlations determined.

The relationship between sea ice extent and MAGT differed among the investigated regions, months, and Arctic ocean basins. In general, the correlations were negative; that is, as sea ice area declines, ground temperatures increase. Northern central Siberia (Yamal to Lena Delta - Kara to Laptev sea region) and the Canadian Archipelago had the strongest relationship with sea ice in July to October. Not only summer but also most cold season months SIA were relevant for Eastern Siberia (October to May, except December) and specifically for Svalbard and NE Greenland (December to May).

The fractions of land areas with significant correlations were in many cases lowest for December and highest for May to October. MAGT variations for most of Western Siberia and North West Russia were linked to sea ice patterns of the relatively close Fram Strait in August to September and of the Kara Sea in October and November. Average correlations for tundra were around -0.5. The Chukchi Sea ice showed strong statistical links to changes in adjacent land areas and Eastern Siberia in several months, specifically in transition periods. Negative correlations occurred in early winter, with >50% of pixels with significant values. The Chukchi Sea CAVM region MAGT was relatively highly negatively correlated with cold season SIA of the Chukchi Sea in addition to the East Siberian SIA in Autumn.

Significant correlations with more distant basins were found in many cases. Chukchi Sea and Beaufort sea ice variations were inversely correlated MAGT (< -0.5 on average, 63% significant) in parts of Western Siberia (Kara) for October. Central Siberian MAGT correlated with the East Siberian Sea ice in August to October and the Beaufort SIA for January to June. Variations were also similar for the Canadian Archipelago MAGT and the Kara Sea SIA from March to June in addition to the Beaufort SIA in September and October. Northern Fennoscandia showed partial similarities with Barents and

Kara SIA from January to September. Some sites in its western part correlated with Eastern Siberian Sea, Chukchi Sea and Beaufort Sea ice variations in October to December. The MAGT of the Laptev Sea tundra regions co-varies with sea ice along its coast from May to October. In addition, Summer to Autumn SIA of the Beaufort Sea is significantly negatively correlated across the Laptev Sea tundra. The entire northern hemisphere SIA from spring to autumn negatively correlated most with the Laptev Sea CAVM region, with up to 80% significant pixels, which are the highest values for all analysed parameters. Higher values are only reached in case of the linkage between the Svalbard and Barents SIA with the Svalbard unglaciated area.

In case of MAGT, high significant correlations were found for more distant sea ice basins than for the NDVI derivatives, indicating influences of large-scale atmospheric circulation patterns. Negative and positive significant correlations were found for March SWE depending on SIA month and region. Also, other months than September (sea ice extent minimum) were found to have high correlations vs. land-based variables, with distinct differences across sea ice basins.

The fraction of data points with significant correlations north of 60°N was higher for SWE and MAGT than for the NDVI derivatives. Fractions for SWE were higher for Eurasia than Northern America. Autumn (incl. October and November) and mid-winter (incl. February, March) were most relevant for both investigated cryosphere-related parameters MAGT and SWE. The datasets provide a baseline for future studies on common drivers of essential climate parameters and causative effects across the Arctic.

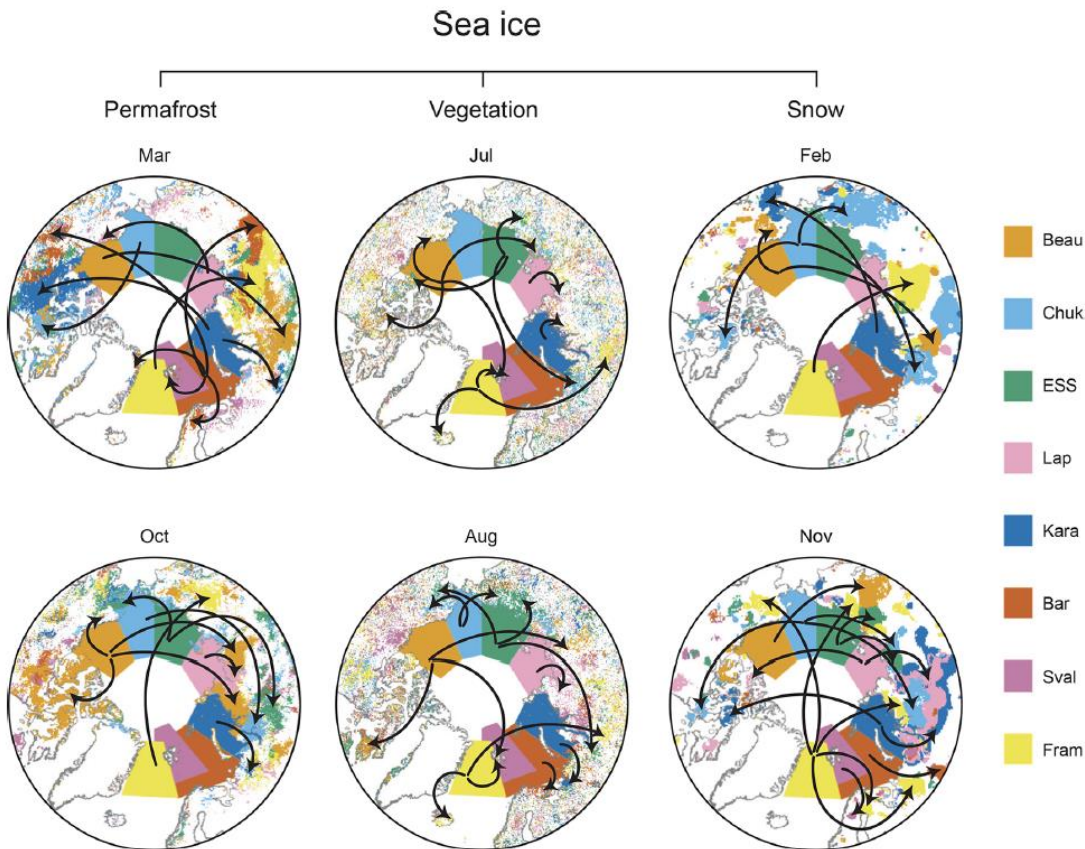


*Figure 15: Areas with significant correlations for selected months and annotations (arrows) highlighting linkages. Permafrost: mean annual ground temperature at 2m depth; Vegetation top: MaxNDVI (maximum normalized difference vegetation index); Vegetation bottom: TINDVI (time-integrated normalized difference vegetation index); Snow: March SWE (snow water equivalent).*

### 3.7 Use Case Study 6 – Analysis of Permafrost\_cci Rock Glacier Inventories (RoGI)

Rouyet, L., Bolch, T., Brardinoni, F., Caduff, R., Cusicanqui, D., Darrow, M., Delaloye, D., Echelard, T., Lambiel, C., Pellet, C., Ruiz, L., Schmid, L., Sirbu, F. and Strozzi, T. (2025). Rock Glacier Inventories (RoGIs) in 12 areas worldwide using a multi-operator consensus-based procedure. *Earth System Science Data*, 17(8), 4125-4157. <https://doi.org/10.5194/essd-17-4125-2025>

*Key points:*

- RoGI guidelines were applied in a multi-operator exercise involving 41 people working in 12 areas worldwide. Morphological analysis and kinematic interpretation using spaceborne InSAR were combined to document the location, extent and characteristics of the rock glaciers.
- In total, 337 “certain” rock glaciers were identified and characterised, and 222 additional landforms were identified as “uncertain”. The study documents and discusses the diversity and level of uncertainty within and across the 12 areas.
- Several applications are identified for future community developments in the field: 1) further investigation in selected areas and RoGI upscaling, 2) rock glacier selection for RGV

monitoring, 3) education training tools for enhancing systematic RoGI generation, 4) training data for automated RoGI techniques.

*Service:*

- Adaptation
- Disaster Risk reduction

*End user (s)*

- Local communities
- Government Agencies
- Researchers

*Intermediate user (s)*

- Research institutes and academia

*Applications*

The Use Case analyses the Rock Glacier Inventory (RoGI) products delivered in the Climate Research Data Package (CRDP) from the European Space Agency Climate Change Initiative (ESA CCI) Permafrost (<https://climate.esa.int/en/projects/permafrost/>). The study evaluates the value of the multi-operator application of the guidelines for mapping rock glaciers using both common morphological criteria and kinematic data using spaceborne Interferometric Synthetic Aperture Radar (InSAR) primarily based on Sentinel-1 SAR.

*Essential Climate Variables*

- Cryosphere
  - Permafrost – Rock Glacier Velocity

*Climate Data Records*

Rouyet, L., Pellet, C., Echelard, T., Schmid, L., Delaloye, R., Brardinoni, F., Sirbu, F., Onaca, A., Poncos, V., Brardinoni, F., Wendt, L., Lauknes, T. R., Kääb, A., Strozzi, T., Bernhard, P., Bartsch, A. 2025. ESA CCI+ Permafrost Phase 2 – CCN4 Mountain Permafrost: Rock Glacier Inventories (RoGI) and Rock glacier Velocity (RGV) Products. D3.2 Climate Research Data Package (CRDP), v2.0. European Space Agency.

*Agencies*

- European Space Agency (ESA) Climate Change Initiative (CCI)

*Satellite observations*

- Sentinel-1
- ERS-1/2
- ALOS-1/2 PALSAR-2

- SAOCOM
- Cosmo-SkyMed
- TerraSAR-X

### Description

The use case study #6 focuses on inter-comparing the findings of the Rock Glacier Inventories (RoGIs) generated in Permafrost\_cci Phase 2 (CRDP [RD-11]) and evaluates the value of applying common RoGI guidelines including InSAR data to assign a kinematic attribute to the inventoried rock glaciers. The findings are presented and discussed in an article published in Earth System Science Data (Rouyet et al., 2025).

The RoGIs from the 12 regions of Permafrost\_cci Phase 2 are compared. Three regions are in the European Alps: Western Swiss Alps (Switzerland), Southern Venosta Valley (Italy) and Vanoise Massif (France). One area is in the Carpathian Mountains (Romania). Five areas are in the sub-Arctic and high-Arctic regions: Troms and Finnmark (Northern Norway), Nordenskiöld Land (Svalbard), Disko Island (Greenland) and Brooks Range (Alaska, USA). One region is in Central Asia: northern Tien Shan (Kazakhstan). Two regions are in the Southern Hemisphere: Central Andres (Argentina) and Southern Alps (Aotearoa New Zealand).

The RoGI procedure is based on the RGIK RoGI guidelines [RD-9], with support from Permafrost\_cci for the InSAR guidelines [RD-10]. The workflow presented by Rouyet et al. (2025) (Figure 14) corresponds to the methodology presented in the Permafrost\_cci Phase 2 ATBD [RD-14], in agreement with the RGIK guidelines [RD-9].

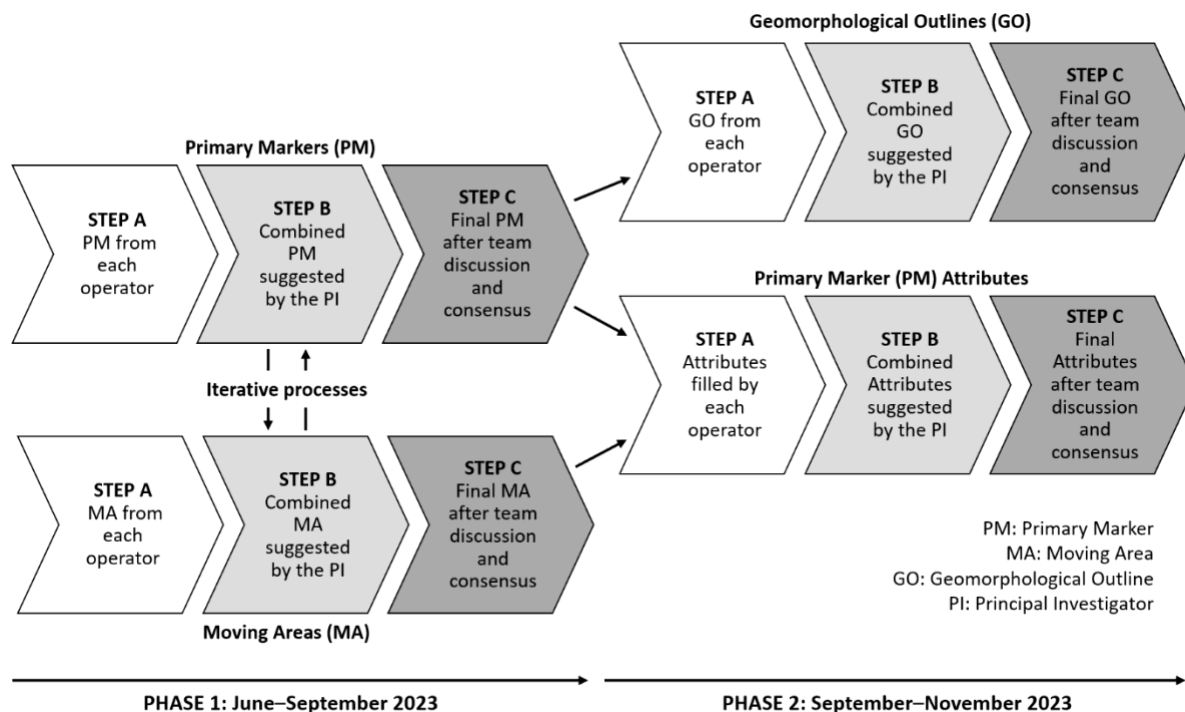
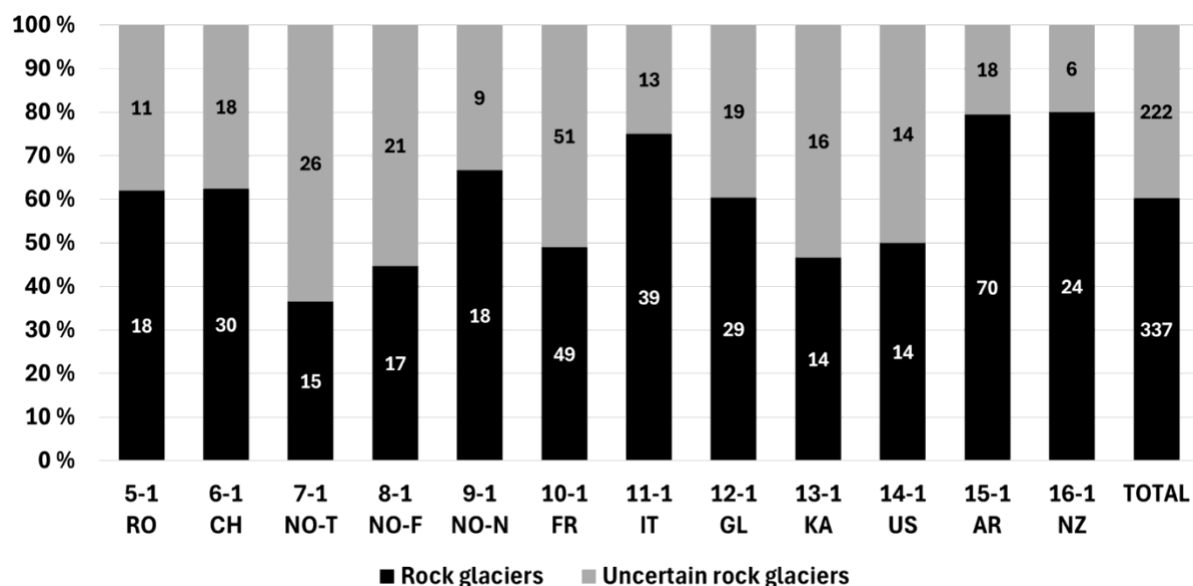


Figure 16: Consensus-based RoGI procedure applied in Rouyet et al. (2025).

The analysis builds on the work performed by Bertone et al. (2022) but focuses on smaller areas to reduce the level of subjectivity and discrepancies using an iterative consensus-based approach with many mapping operators. In total, 337 “certain” rock glaciers were identified and characterised, and 222 additional landforms were identified as “uncertain” (Figure 15). The level of uncertainty varies and reflects the geomorphological complexity of each area. On average, about 40 % of the landforms remain “uncertain”. The InSAR-based Moving Areas (MAs) have a wide range of velocities, both between and within the areas (Figure 16). The MA layers were used to assign the kinematic attribute of each rock glacier unit, which then was used to assess the activity. The study highlights the values of having operators with different skills and backgrounds to include a diversity of points of view and experiences and therefore improve the quality of the final products. The study also concludes that InSAR was useful for identifying moving rock glaciers in addition to providing a semi-quantitative information about their creep rates. When used iteratively with Primary Marker (PM) detection, the MA step allowed for including landforms that would have been overlooked based on geomorphological criteria only.



*Figure 17: Relative distribution of the rock glacier units (RGUs) identified as “certain” (black) or “uncertain” (grey) in each RoGI area resulting from the consensus-based final Primary Marker (PM) layers. The numbers written in the bars correspond to the absolute numbers of landforms. The area numbers and the acronyms of the corresponding countries are based on the Permafrost\_cci naming convention.*

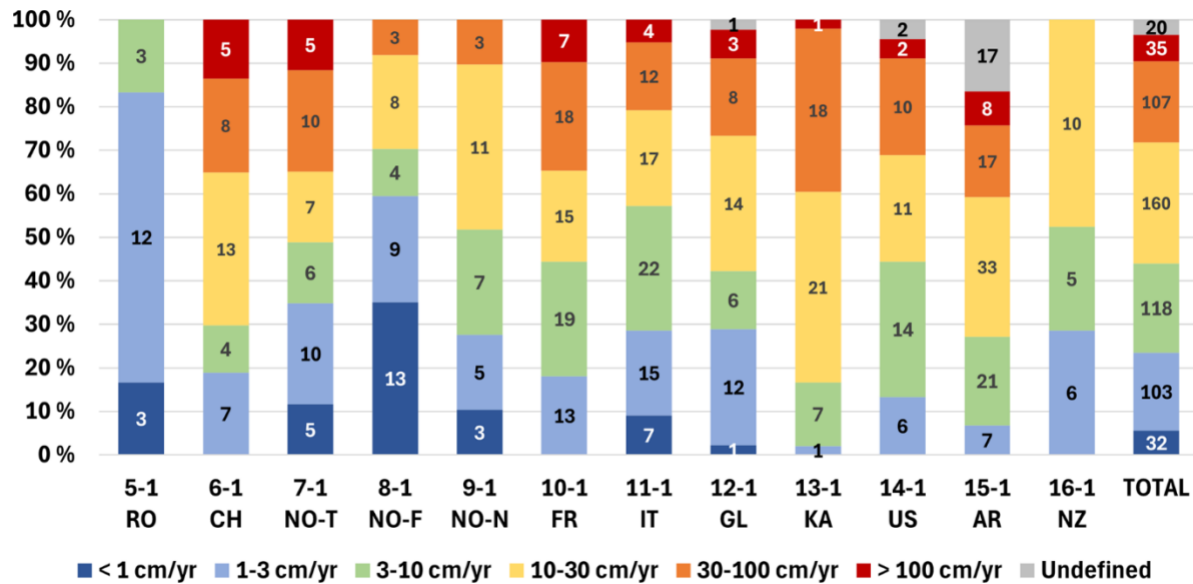


Figure 18: Relative distribution of the RGU activity (active, active uncertain, transitional, transitional uncertain, relict, relict uncertain, uncertain) documented as an attribute in the consensus-based final primary marker (PM) layers. The numbers written in the bars correspond to the absolute numbers of landforms. The area numbers and the acronyms of the corresponding countries are based on the Permafrost\_cci naming convention.

### 3.8 Use Case Study 7 – Global compilation of Rock Glacier Velocity (RGV)

Pellet, C., Bodin, X., Cusicanqui, D., Delaloye, R., Kääb, A., Kaufmann, V., Thibert, E., Vivero, S., & Kellerer-Pirklbauer, A. 2025. Rock glacier velocity. In State of Climate in 2024, Bull. Amer. Meteor. Soc., 106(8), pp. 48–49. <https://doi.org/10.1175/2025BAMSSStateoftheClimate.1>

*Key points:*

- Rock Glacier Velocity is an ECV Permafrost Quantity that is included in the annual release of the State of Climate from the Bulletin of the American Meteorological Society (BAMS).
- An overall increasing RGV trend has been observed in mountain ranges worldwide since the 1950s. This conclusion is based on in-situ data since the 2000s, complemented by optical remote sensing for long-term monitoring from the 1950s.
- The State of Climate in 2024 includes RGVs from Tien Shan and the United States, based on two studies supported by Permafrost\_cci (Kääb et al., 2022; Kääb and Røste 2024). Similarly to the other regions worldwide, the reported trends in North America are consistent with the increase of permafrost temperatures to which RGV respond more or less synchronously.

*Service:*

- Adaptation
- Disaster Risk reduction
- Protocol monitoring

*End user (s)*

- Government Agencies
- Policymakers
- Researchers

*Intermediate user (s)*

- Research institutes and academia

*Applications*

The Use Case builds on the recommendations and methods developed in Permafrost\_cci, presented in the Algorithm Theoretical Basis Document (ATBD) and the Climate Research Data Package (CRDP) from the European Space Agency Climate Change Initiative (ESA CCI) Permafrost (<https://climate.esa.int/en/projects/permafrost/>).

*Essential Climate Variables*

- Cryosphere
  - Permafrost – Rock Glacier Velocity

*Climate Data Records*

Rouyet, L., Pellet, C., Echelard, T., Schmid, L., Delaloye, R., Brardinoni, F., Sirbu, F., Onaca, A., Poncos, V., Brardinoni, F., Wendt, L., Lauknes, T. R., Kääb, A., Strozzi, T., Bernhard, P., Bartsch, A. 2025. ESA CCI+ Permafrost Phase 2 – CCN4 Mountain Permafrost: Rock Glacier Inventories (RoGI) and Rock glacier Velocity (RGV) Products. D3.2 Climate Research data Package (CRDP), v2.0. European Space Agency.

*Agencies*

- European Space Agency (ESA) Climate Change Initiative (CCI)

*Satellite observations**Description*

The use case study #7 corresponds to first global compilation of RGV products that is updated annually to serve as climate change indicator. The RGV section in the BAMS State of Climate in 2024 includes time series from 19 sites in European, American and Asian mountains. The time series are based on in-situ geodetic surveys and optical photogrammetry. The RGV section currently does not include SAR data acquired from spaceborne sensors due to the recent launch of the operational missions, and therefore short data series, compared to the time scale shown in Figure 19. However, the work builds on data standards that have been developed by RGIK [RD-15] [RD-16], with support from Permafrost\_cci [RD-11] [RD-14]. The optical remote sensing data from Tien Shan and The United States are both part of studies supported by Permafrost\_cci (Kääb et al., 2022; Kääb and Røste 2024).

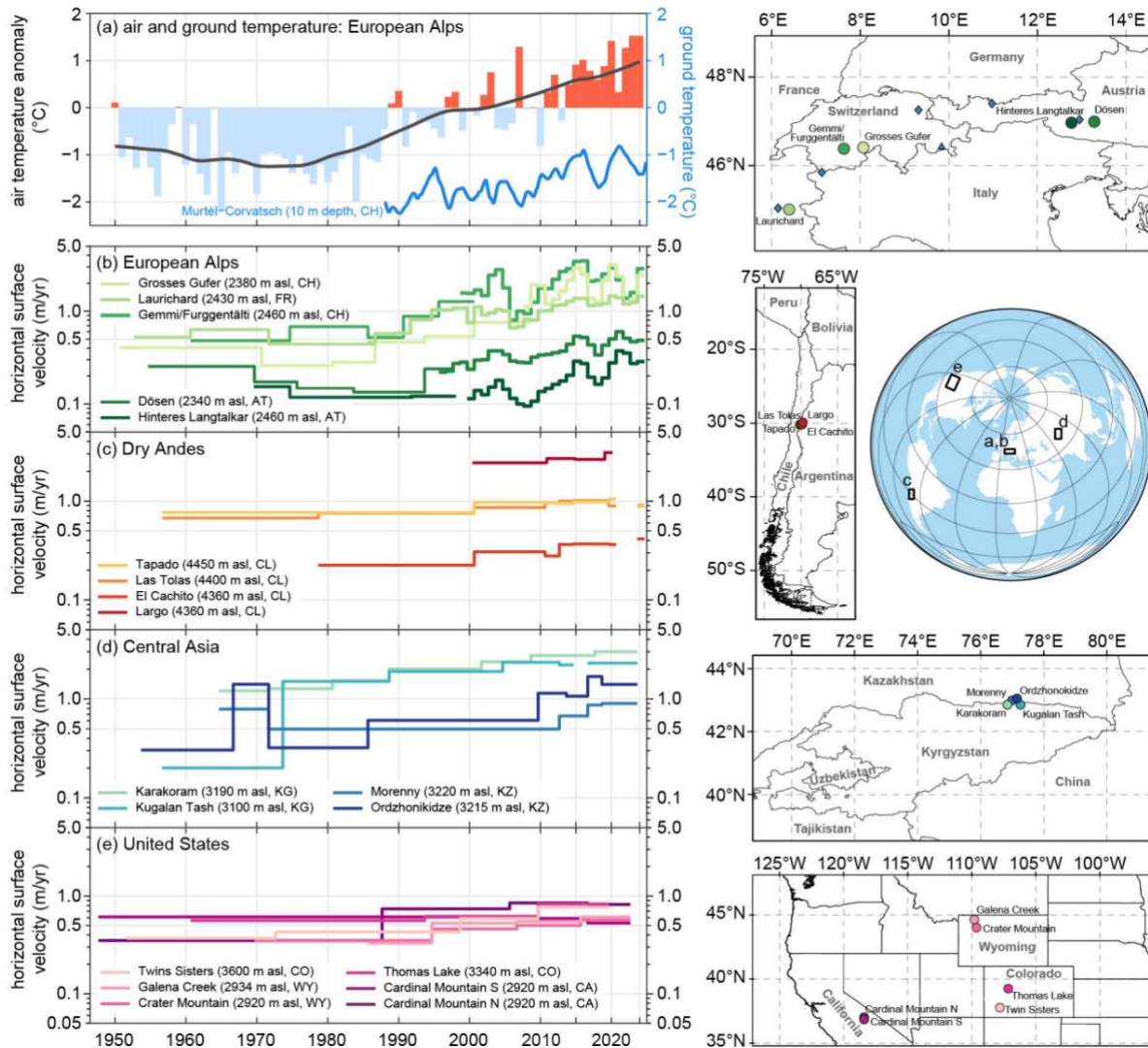


Figure 19: Key figure from Pellet et al. (2024) compilating Rock Glacier Velocity and climate data in Europa, America and Asia.

### 3.9 Further documented use

#### Permafrost\_cci ground temperature

- Damseaux, A., Matthes, H., Dutch, V. R., Wake, L., and Rutter, N.: Impact of snow thermal conductivity schemes on pan-Arctic permafrost dynamics in the Community Land Model version 5.0, *The Cryosphere*, 19, 1539–1558, <https://doi.org/10.5194/tc-19-1539-2025>, 2025.
- Gartler, S., Scheer, J., Meyer, A., K. Abass, A. Bartsch, N. Doloisio, J. Falardeau, G. Hugelius, A. Irrgang, J. H. Ingimundarson, L. Jungsberg, H. Lantuit, J. Nymand Larsen, R. Lodi, V. S. Martin, L. Mercer, D. Nielsen, P. Overduin, O. Povoroznyuk, A. Rautio, P. Schweitzer, N. J. Speetjens, S. Tomaškovičová, U. Timlin, J.-P. Vanderlinden, J. Vonk, L. Westerveld & T. Ingeman-Nielsen (2025). A transdisciplinary, comparative analysis reveals key risks from

Arctic permafrost thaw. *Commun Earth Environ*, 6, 21. <https://doi.org/10.1038/s43247-024-01883-w>

- Bartsch, A., Strozzi, T., and Nitze, I. (2023). Permafrost Monitoring from Space. *Surveys in Geophysics*. <https://link.springer.com/article/10.1007/s10712-023-09770-3>
- Miner, K., Turetsky, M., Malina, E., Bartsch, A., Tamminen, J., McGuire, A.D., Fix, A., Sweeney, C., Elder, C.D., and Miller, C.E. (2022). Permafrost carbon emissions in a changing Arctic, *Nature Reviews Earth & Environment*, 3, 55–67. <https://doi.org/10.1038/s43017-021-00230-3>
- Bartsch A, Ley S, Nitze I, Pointner G and Vieira G (2020). Feasibility Study for the Application of Synthetic Aperture Radar for Coastal Erosion Rate Quantification Across the Arctic. *Front. Environ. Sci.* 8:143. <https://doi.org/10.3389/fenvs.2020.00143>

#### Permafrost\_cci active layer thickness

- Brouillette, M. (2021). How microbes in permafrost could trigger a massive carbon bomb. Genomics studies are helping to reveal how bacteria and archaea influence one of Earth's largest carbon stores as it begins to thaw. News Feature. *Nature*, 591(7850), 360–362. <https://doi.org/10.1038/d41586-021-00659-y>
- Tamm., J. (2021): Remote-sensing based assessment of post-fire changes in land surface temperature in Arctic-Boreal permafrost regions. Master Thesis, University of Potsdam. 74pp.

#### GlobPermafrost Permafrost extent use examples

- Ramage, J., Jungsberg, L., Wang, S., Westermann, S., Lantuit, H. & Heliak, T. (2021), 'Population living on permafrost in the Arctic', *Population and Environment*. <https://doi.org/10.1007/s11111-020-00370-6>
- Julian Murton, Periglacial Processes and Deposits, Editor(s): David Alderton, Scott A. Elias, Encyclopedia of Geology (Second Edition), Academic Press, 2021, 857-875, ISBN 9780081029091, <https://doi.org/10.1016/B978-0-12-409548-9.11925-6>
- Kåresdotter, E., Destouni, G., Ghajarnia, N., Hugelius, G., & Kalantari, Z. (2021). Mapping the vulnerability of Arctic wetlands to global warming. *Earth's Future*, 9, e2020EF001858. <https://doi.org/10.1029/2020EF001858>
- Lapierre Poulin, F., Fortier, D., & Berteaux, D. (2021). Low vulnerability of Arctic fox dens to climate change-related geohazards on Bylot Island, Nunavut, Canada. *Arctic Science*, 1–16. <https://doi.org/10.1139/as-2019-0007>
- Webb, E. E., Loranty, M. M., & Lichstein, J. W. (2021). Surface water, vegetation, and fire as drivers of the terrestrial Arctic-boreal albedo feedback. *Environmental Research Letters*, 16(8), 084046. <https://doi.org/10.1088/1748-9326/ac14ea>
- Horizon2020 project Nunataryuk (GRID Arendal): Foldable map of permafrost around the world <https://www.grida.no/news/13>
- Ardelean, F., Onaca, A., Chețan, M.-A., Dornik, A., Georgievski, G., Hagemann, S., Timofte, F., & Berzescu, O. (2020). Assessment of Spatio-Temporal Landscape Changes from VHR Images in Three Different Permafrost Areas in the Western Russian Arctic. *Remote Sensing*, 12(23), 3999. <https://doi.org/10.3390/rs12233999>

Climate modelling:

- Burke, E.J., Zhang, Y., Krinner, G. (2020): Evaluating permafrost physics in the Coupled Model Intercomparison Project 6 (CMIP6) models and their sensitivity to climate change, *The Cryosphere*, 14, 3155–3174. <https://doi.org/10.5194/tc-14-3155-2020>

Rock glaciers:

- Bertone, A., Jones, N., Mair, V., Scotti, R., Strozzi, T., and Brardinoni, F. (2024). A climate-driven, altitudinal transition in rock glacier dynamics detected through integration of geomorphologic mapping and InSAR-based kinematic information. *The Cryosphere*, 18, 2335–2356. <https://doi.org/10.5194/tc-18-2335-2024>
- Bertone, A., Barboux, C., Bodin, X., Bolch, T., Brardinoni, F., Caduff, R., Christiansen, H. H., Darrow, M., Delaloye, R., Etzelmüller, B., Humlum, O., Lambiel, C., Lilleøren, K. S., Mair, V., Pellegrinon, G., Rouyet, L., Ruiz, L., and Strozzi, T. 2022. Incorporating InSAR kinematics into rock glacier inventories: insights from 11 regions worldwide, *The Cryosphere*, 16, 2769–2792. <https://doi.org/10.5194/tc-16-2769-2022>.
- Brardinoni, F., Vivero, S., Barboux, C., Bodin, X., Cicoira, A., Echelard, T., Hu, Y., Jones, N., Lambiel, C., MacDonell, S., Pellet, C., Rouyet, L., Ruiz, L., Schaffer, N., Wehbe, M. and Delaloye, R. (2025). RGIK guidelines for compiling consistent rock glacier inventories. *Geomorphology*, 110050. <https://doi.org/10.1016/j.geomorph.2025.110050>
- Hu, Y., Arenson, L. U., Barboux, C., Bodin, X., Cicoira, A., Delaloye, R., Gärtner-Roer, I., Kääb, A., Kellerer-Pirkbauer, A., Lambiel, C., Liu, L., Pellet, C., Rouyet, L., Schoeneich, P., Seier, G., and Strozzi, T. (2025). Rock glacier velocity: An essential climate variable quantity for permafrost. *Reviews of Geophysics*, 63(1), e2024RG000847. <https://doi.org/10.1029/2024RG000847>
- Kääb, A., Strozzi, T., Bolch, T., Caduff, R., Trefall, H., Stoffel, M., & Kokarev, A. (2021). Inventory and changes of rock glacier creep speeds in Ile Alatau and Kungöy Ala-Too, northern Tien Shan, since the 1950s. *The Cryosphere*, 15(2), 927–949. <https://doi.org/10.5194/tc-15-927-2021>
- Kääb, A., & Røste, J. (2024). Rock glaciers across the United States predominantly accelerate coincident with rise in air temperatures. *Nature Communications*, 15(1), 7581. <https://doi.org/10.1038/s41467-024-52093-z>
- Lambiel, C., Strozzi, T., Paillex, N., Vivero, S. and Jones, N. 2023. Inventory and kinematics of active and transitional rock glaciers in the Southern Alps of New Zealand from Sentinel-1 InSAR, Arctic, Antarctic, and Alpine Research, 55(1), 2183999. <https://doi.org/10.1080/15230430.2023.2183999>.
- Lilleøren, K. S., Etzelmüller, B., Rouyet, L., Eiken, T., Slinde, G., and Hilbich, C.: Transitional rock glaciers at sea level in northern Norway, *Earth Surf. Dynam.*, 10, 975–996, 2022. <https://doi.org/10.5194/esurf-10-975-2022>
- Onaca, A., Sîrbu, F., Poncoş, V., Hilbich, C., Strozzi, T., Urdea, P., Popescu, R., Berzescu, O., Etzelmüller, B., Vespremeanu-Stroe, A., Vasile, M., Teleagă, D., Birtaş, D., Lopătiță, I., Filhol, S., Hegyi, A., & Ardelean, F. (2025). Slow-moving rock glaciers in marginal periglacial environment of Southern Carpathians. *Earth Surface Dynamics*, 13(5), 981–1001. <https://doi.org/10.5194/esurf-13-981-2025>
- Pellet, C., Bodin, X., Cusicanqui, D., Delaloye, R., Kääb, A., Kaufmann, V., Thibert, E., Vivero, S., & Kellerer-Pirkbauer, A. 2025. Rock glacier velocity. In *State of Climate in 2024*, Bull. Amer. Meteor. Soc., 106(8), pp. 48–49. <https://doi.org/10.1175/2025BAMSStateoftheClimate.1>

- Rouyet, L., Lilleøren, K. S., Böhme, M., Vick, L. M., Delaloye, R., Etzelmüller, B., Lauknes, T. R., Larsen, Y., and Blikra, L. H. (2021). Regional Morpho-Kinematic Inventory of Slope Movements in Northern Norway, *Front. Earth Sci.* 9, 6810881. <https://doi.org/10.3389/feart.2021.681088>.
- Strozzi T., R.Caduff, N. Jones, C. Barboux, R, Delaloye, X. Bodin, A. Kääb, E. Mätzler, L. Schrott (2020). Monitoring Rock Glacier Kinematics with Synthetic Aperture Radar. *Remote Sensing*, 12(3), 559. <https://doi.org/10.3390/rs12030559>

### 3.9 Permafrost\_cci utility based on evaluation results for GRD, ALT and EXT

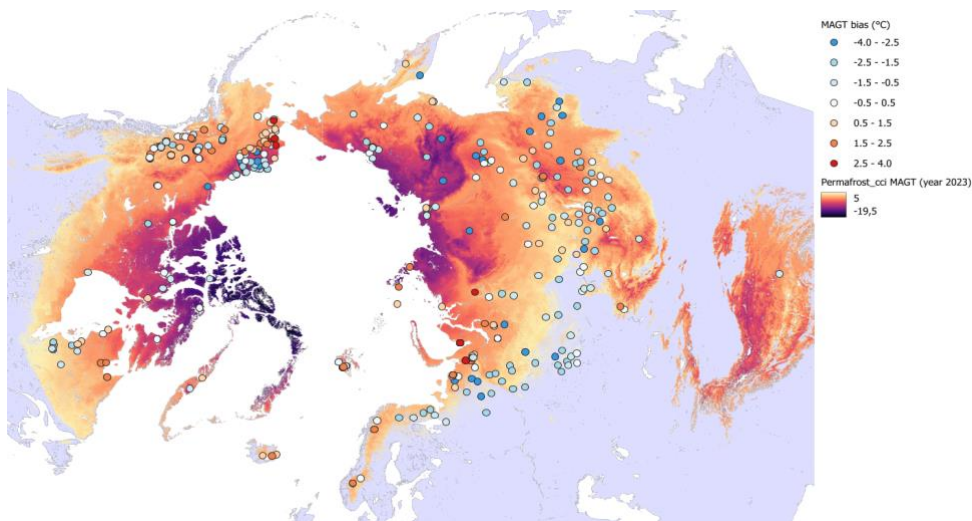
This science case study is the utility assessment of the Permafrost\_cci ECV products. The independent validation is carried out with strong support of the user community, with in situ measurements characterised by community-wide management best practices with open data access and a collaborative user environment within an international framework: WMO and GCOS delegated the global monitoring of the ECV Permafrost to the Global Terrestrial Network for Permafrost (GTN-P) that is managed by the International Permafrost Association (IPA). GTN-P/IPA established the Thermal State of Permafrost Monitoring (TSP) for permafrost temperature and the Circumpolar Active Layer Monitoring program (CALM) for active layer thickness monitoring. The national-wide Russian meteorological monitoring network ROSHYDROMET additionally provides long-term ground temperature records close to meteorological stations openly available until 2014. GTN-P and ROSHYDROMET time series and data collections from additional networks provide reference data sets, however no easy-to use or readily available time-series depth data that are data-fit for validation. We assembled standardised reference data from 1997 to 2023 spanning permafrost regions from Scandinavia to higher latitude permafrost and all altitude ranges from lowland to mountain permafrost across a wide range of latitudes, altitudes, climate zones, land cover, and lithologies.

Permafrost\_cci CRDPv4 provides 1 km pixel resolution ECV products on mean annual ground temperature (MAGT) at discrete depths (product name Ground Temperature per Depth, GTD), Active Layer Thickness (product name ALT) and Permafrost Fraction (product name PFR). All products cover the Northern hemisphere north of 30 °N and new the inland-ice free permafrost regions in Antarctica. Permafrost\_cci GTD, ALT and PFR time series from 1997 to 2023 come with an annual resolution. The growing demand for mapped permafrost products needs to accommodate user requirements that span permafrost regions from Scandinavia, Mongolia, Tibetan plateau (China) to higher latitude permafrost in North America, Greenland, Siberia and all altitude ranges from lowland to mountain permafrost. This results in high difficulties of assessing how the Permafrost\_cci products perform in all regions across a wide range of latitudes, altitudes, climate zones, land cover, and lithologies.

Permafrost\_cci products are evaluated using standard match-up statistical approaches, supported by expert knowledge. The match-ups were executed using a pixel-based approach. Permafrost\_cci GTD is provided in 0.0, 1.0, 2.0, 5.0, and 10.0 m depth and depth-interpolated to fit the depths of the extensive in situ data set. We highly standardized the match-up data, but still the reference data contains a large variability of match-up pairs in time, region, and MAGT reference depths. The mountain permafrost monitoring program PERMOS in Switzerland is specifically assessing the Permafrost\_cci products for high-mountain permafrost regions, using in situ observations of surface temperature and borehole temperatures and the ESA GlobPermafrost slope movement inventory in the Swiss Alps and the Permafrost\_cci rock glacier inventory in the Alps and worldwide at case study sites. In addition, the

validation and evaluation efforts innovatively apply the Freeze-Thaw to Temperature (FT2T) product, an EO microwave-derived ground temperature, for comparison with the Permafrost\_cci permafrost temperature product.

Permafrost\_cci GTD evaluation shows a mean cold bias of  $-0.76^{\circ}\text{C}$  (std  $\pm 1.73^{\circ}\text{C}$ ), a median cold bias of  $-0.95^{\circ}\text{C}$  (5 %  $-3.32$  to 95 %  $2.26^{\circ}\text{C}$ ) for the bulk data set and a mean cold bias of  $-0.87^{\circ}\text{C}$  (std  $\pm 1.69^{\circ}\text{C}$ ), and median cold bias of  $-1.12^{\circ}\text{C}$  (5 %  $-3.27$  to 95 %  $2.14^{\circ}\text{C}$ ) for the depth-interpolated bulk data set. Match-up pairs from the cold temperature subgroup ( $\text{MAGT} < 1^{\circ}\text{C}$ ) show an even better performance with a small mean bias of  $0.03^{\circ}\text{C}$  (std  $\pm 1.94^{\circ}\text{C}$ ) and a median warm bias of  $0.23^{\circ}\text{C}$  (5 %  $-3.25$  to 95 %  $2.89^{\circ}\text{C}$ ). This cold temperature subgroup shows for the depth-interpolated dataset a small mean bias of  $0.06^{\circ}\text{C}$  (std  $\pm 1.967^{\circ}\text{C}$ ) and a median warm bias of  $0.26^{\circ}\text{C}$  (5 %  $-3.25$  to 95 %  $2.93^{\circ}\text{C}$ ). The trends over years generally match well between the in situ measurements and Permafrost\_cci GTD, with a high Gleichläufigkeit (median glk~ 70%) and temporal bias stability ( $\text{ts} \pm 0.5^{\circ}\text{C}$ ) in all years. Figure 20 shows the spatial distribution and characteristics of the GTD bias and the residuals.



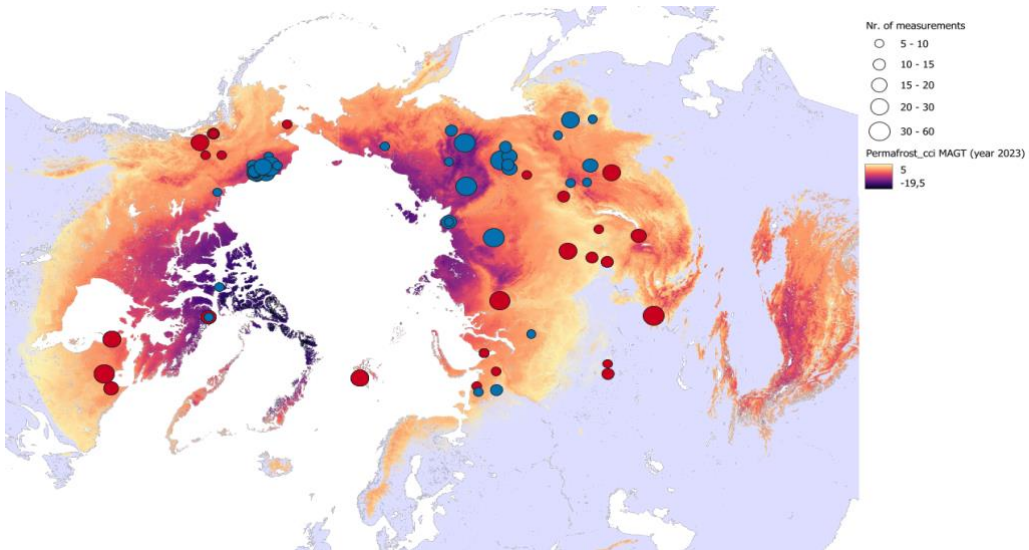


Figure 20: (upper panel) GTD bias and (lower panel) location of residuals  $> 95\%$  quantile (red) and  $< 5\%$  quantile (blue) over mapped Permafrost\_cci GTD 2023 (2 m). The size of the circle represents the number of samples with specific residuals at the particular location.

In case of the Permafrost\_cci PFR assessments, the majority of match-up pairs (88.64 % for case  $\text{PFR} \leq 14\%$ ) is in agreement between the in situ proxies for permafrost abundance and Permafrost\_cci abundance yes / no. Notably, Permafrost\_cci PFR = 100 % and PFR = 0 % show high percentage of agreement, with 98.93 % and 90.09 % match, respectively. Geographically, most mismatches are located in the Eurasian and Alaskan and Canadian southern boundary of the permafrost extent. The high agreement in the 100 % and 0 % Permafrost\_cci PFR groups is stable across years.

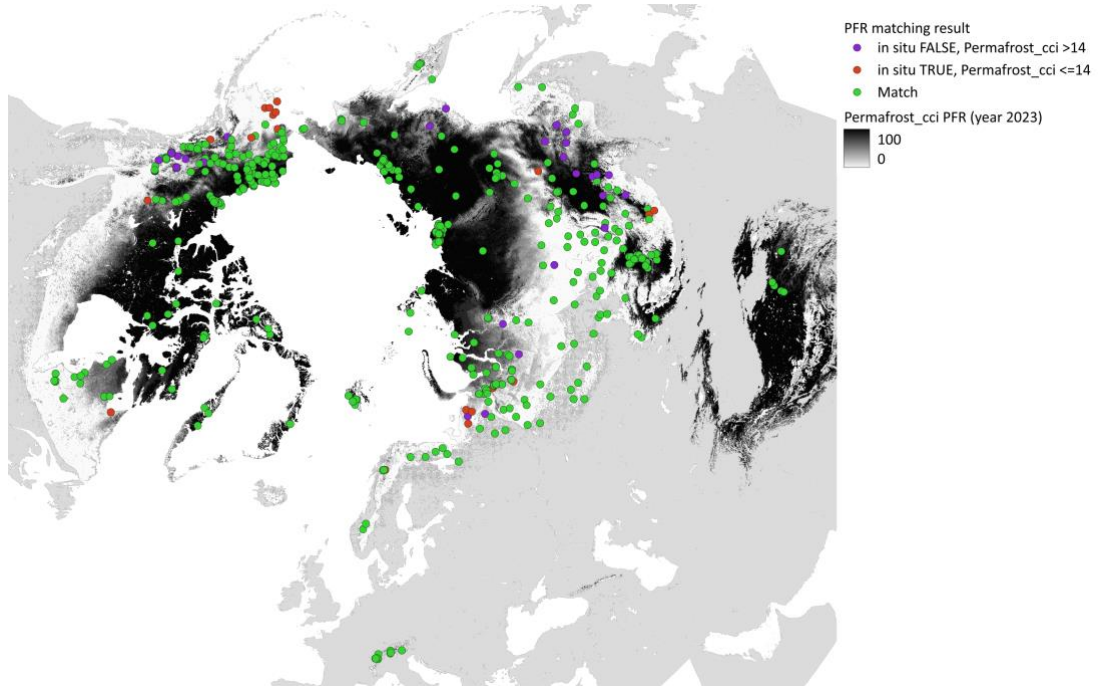


Figure 21: PFR match-up sites (color-coded point symbols grouped by matching characteristics with color-coded green points representing 'Match') over mapped Permafrost\_cci PFR 2023 in the Northern hemisphere.

For the Permafrost\_cci ALT assessments, we excluded all sites in Central Asia, Mongolia, on the Tibetan Plateau and in high mountain regions, such as the Alps, due to their different not parameterised lithologies and very high ALT depths. Permafrost\_cci ALT performance in high latitude permafrost regions is characterised by a mean bias of 0.07 m, however with a large standard deviation of  $\pm 0.56$  m and a median bias of 0.03 m, MAD of 0.57 m, and RMSE of 0.56 m. High magnitude positive bias  $> 1$  m (deep Permafrost\_cci ALT versus shallow in situ ALT) occurs only in a few match-up pairs in Alaska, Canada and Russia in the southern boundaries of the permafrost zone and high magnitude negative bias  $> -1.5$  m mainly in Svalbard and northern Scandes in rocky and pebble terrain (shallow Permafrost\_cci ALT versus deep in situ ALT). The mean temporal stability shows stable ranges around 0.01 m, with variation mainly in the range of  $\pm 0.56$  m and gleichläufigkeit (glk, fraction of same-directional year-to-year changes) shows a robust temporal stability around 73 %.

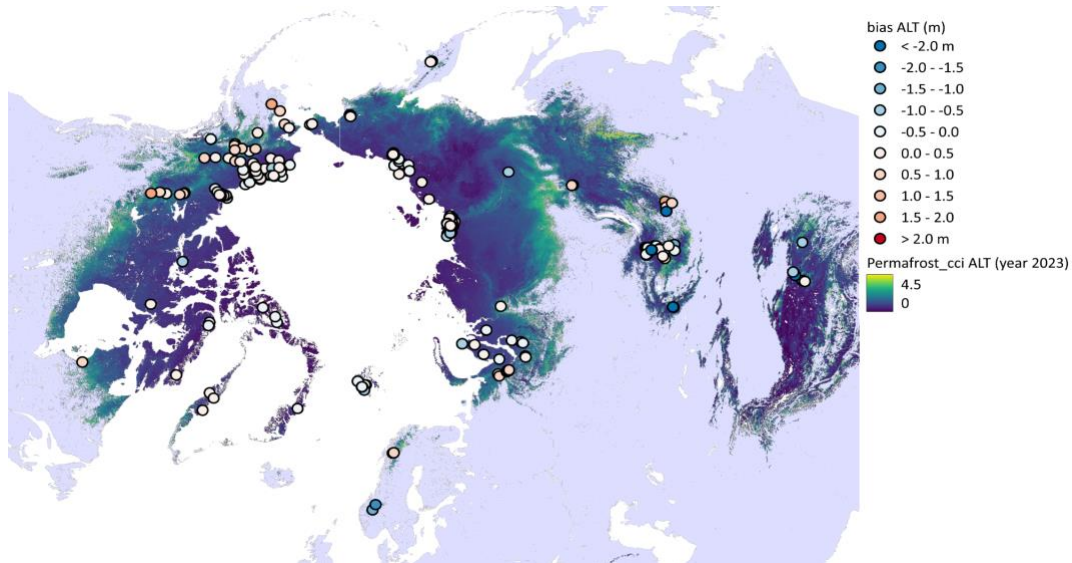


Figure 22: ALT bias (color-coded point symbols) over mapped Permafrost\_cci ALT 2023 in the Northern hemisphere.

The mountain permafrost monitoring program PERMOS in Switzerland is specifically assessing the Permafrost\_cci products for high-mountain permafrost regions, using in situ observations of surface temperature and borehole temperature time series and the ESA GlobPermafrost slope movement inventory. PERMOS investigations in the Swiss Alps show that the performance of Permafrost\_cci GTD and Permafrost\_cci PFR improved for mountain regions worldwide. Permafrost\_cci GTD in the Swiss Alps shows a slight cold bias of -0.08 °C only, RMSE is +0.32 °C). At larger depth, Permafrost\_cci GTD shows a warm bias of 1.06 °C at 10 m depth. Permafrost\_cci GTD fits best with the in situ observations near the surface with the bias increasing with depth at all sites. Although the absolute values are different, both PERMOS in situ measurements and Permafrost\_cci GTD show the consistent warming trend over the period 1997 to 2023. Permafrost\_cci GTD matches well the inter-annual variability at the surface (i.e. warmer GTD due to the extreme warm years in 2003 and colder GTD due to snow poor winters in 2017 and 2021). At depth, Permafrost\_cci GTD product fails to reproduce the measured inter-annual variability. When Permafrost\_cci GTD values are below about -0.5 °C, interannual temperature variations are small and when Permafrost\_cci GTD values are within about -0.5 and 0 °C there are no variations.

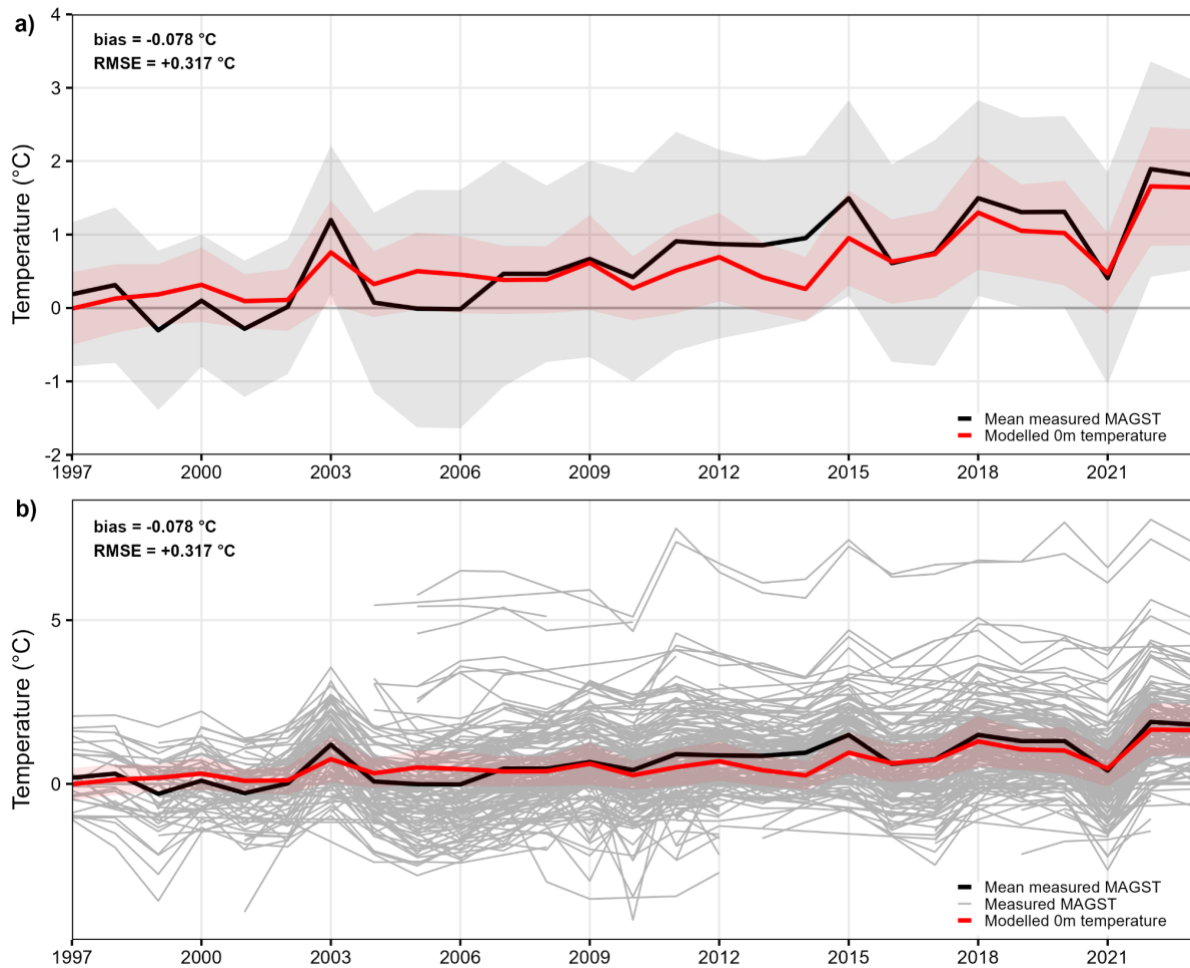


Figure 23: Temporal evolution from 1997 to 2023 of the mean in situ measured MAGST (black) in Switzerland (a) and measured MAGST at each logger (b) compared to the mean Permafrost\_cci GTD at 0 m depth (red) over the entire Swiss Alps between 2500 and 3000 m a.s.l. The shaded area represents  $\pm$  one standard deviation.

Permafrost\_cci PFR permafrost extent fits well with the distribution of the majority of inventoried ESA GlobPermafrost slope movement products as well as the active rock glaciers inventoried in CCI phase I and II (Figure 24)

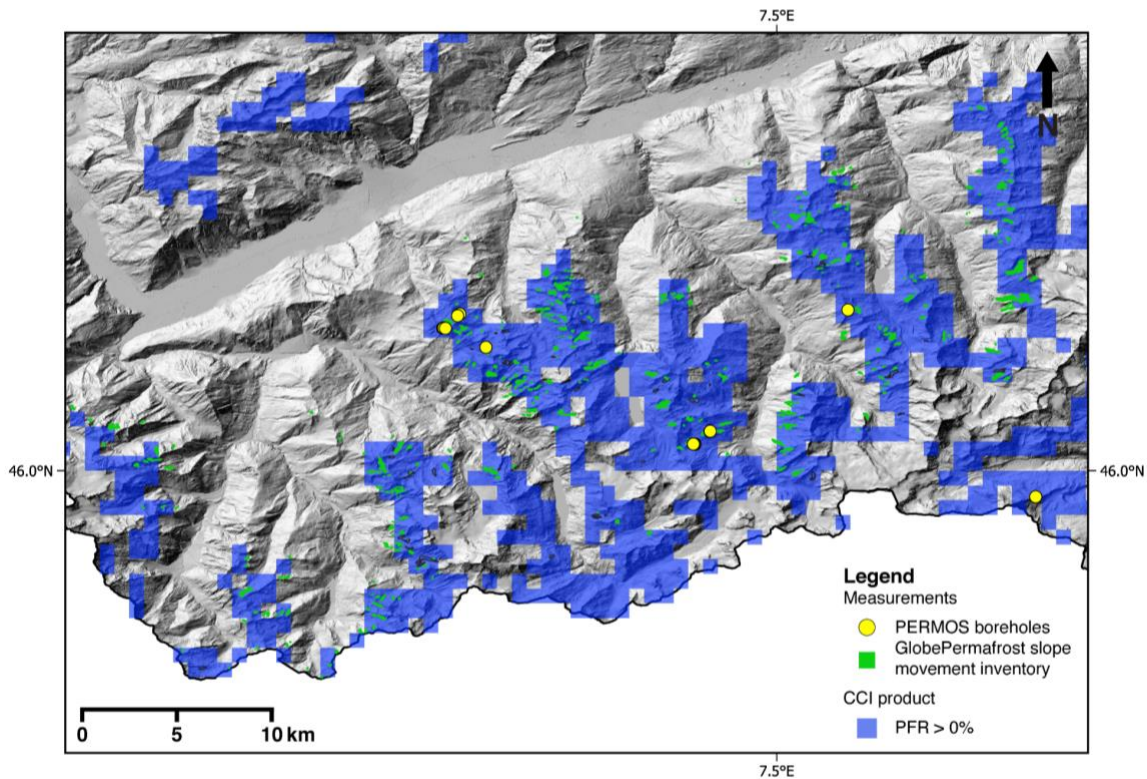
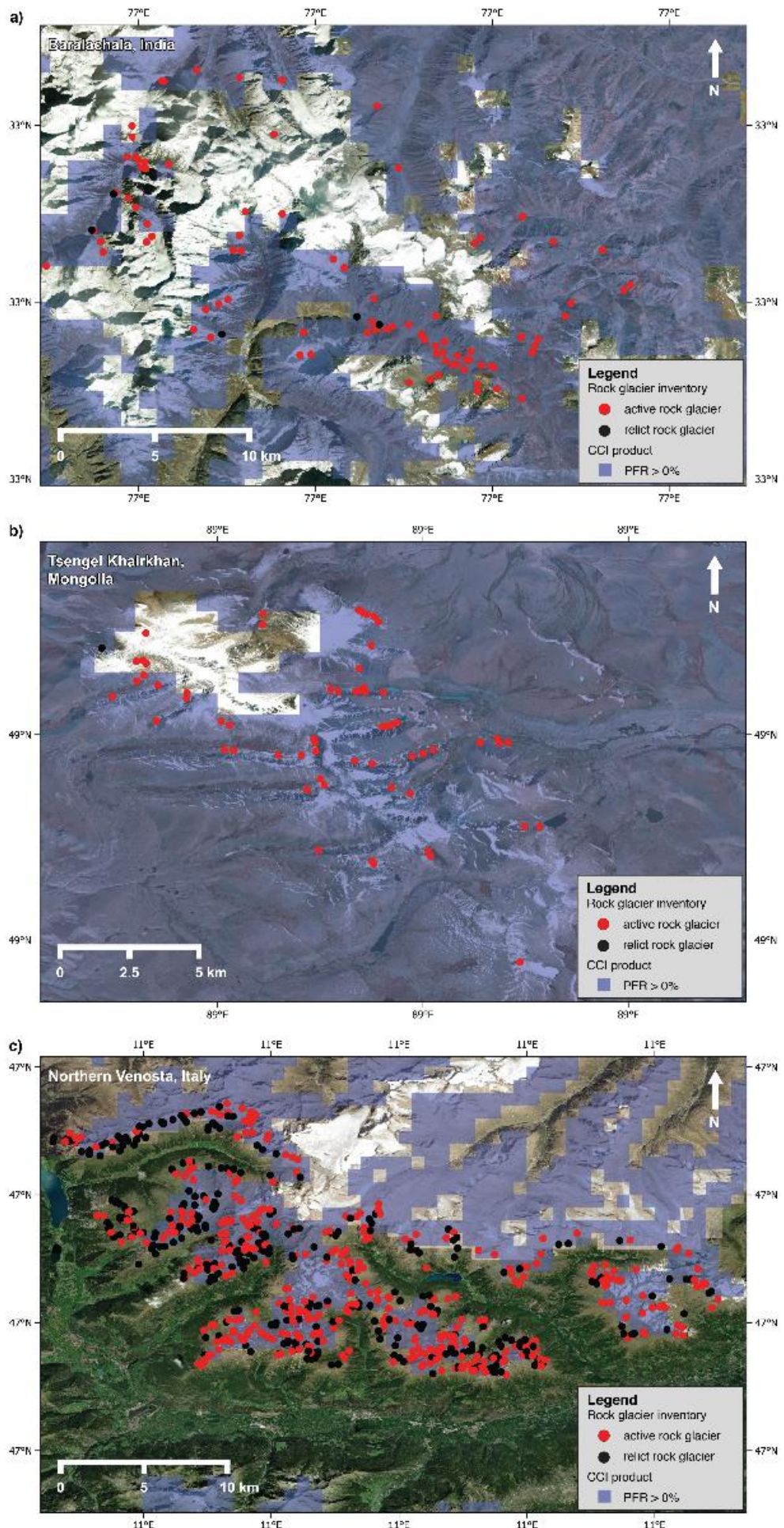
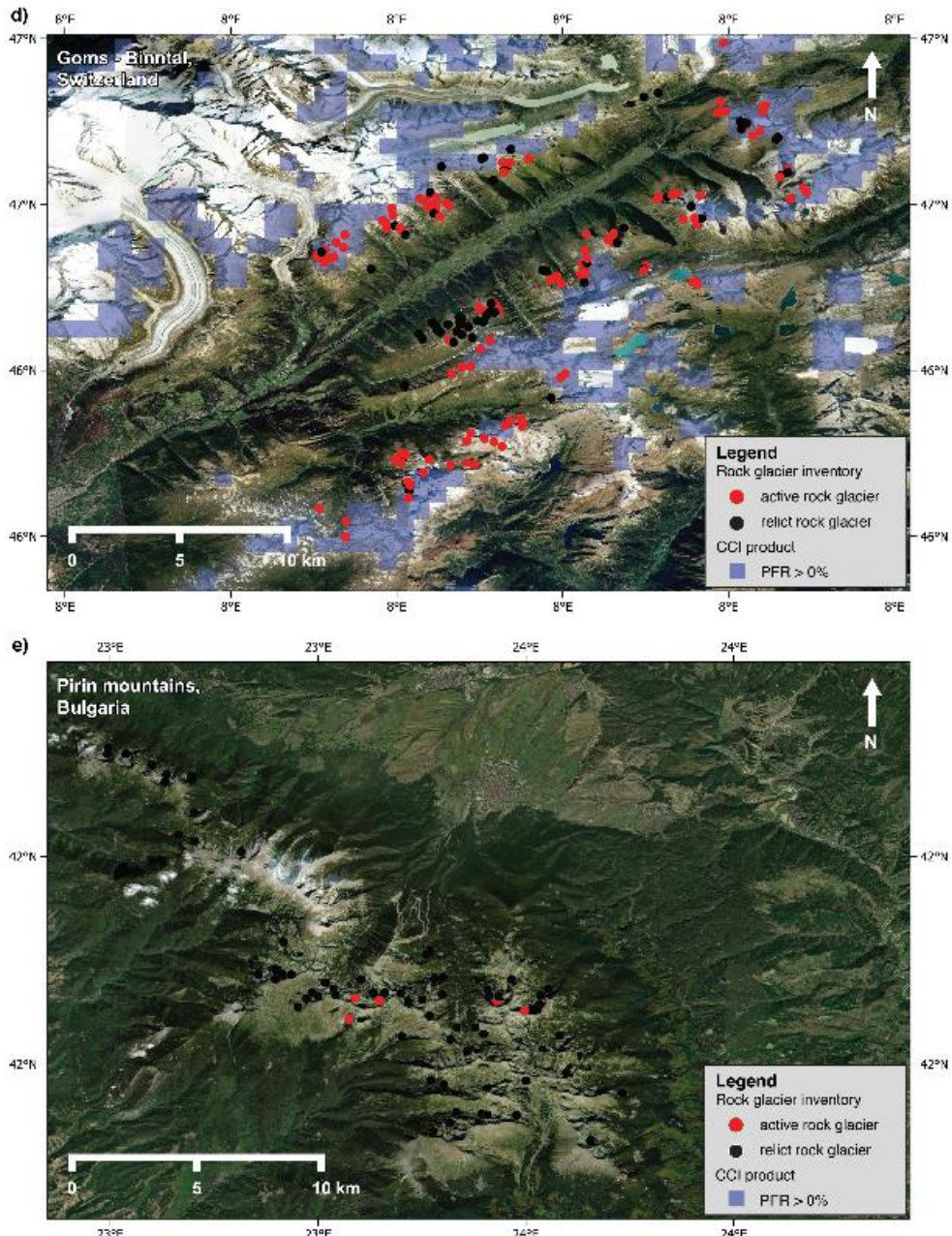


Figure 24: Overview of the simulated Permafrost\_cci PFR in 2023 in Bas-Valais (CH) compared to the ESA GlobPermafrost slope movement inventory and PERMOS permafrost monitoring borehole locations.

Looking worldwide (Figure 25), one can see that the Permafrost\_cci PFR permafrost extent fits well with the Permafrost\_cci phase II rock glacier inventory products in general. Active rock glaciers can be used as indicators of the occurrence of permafrost whereas relict landforms indicate its absence. In most areas, the 1 km<sup>2</sup> grid cell resolution Permafrost\_cci PFR fails to reproduce the small scale topographical variations and the Permafrost\_cci PFR permafrost extent is slightly overestimated in the zones of continuous permafrost. This is true for Disko Island (Western Greenland) and Brooks range (North Alaska). In the discontinuous European permafrost zone of the Troms area (North Norway), at mid-latitudes in Central Asia in the Tien Shan area (Khazastan) and in the Himalayas (India, Nepal and Bhutan) the Permafrost\_cci PFR permafrost extent fits well with the inventoried rock glacier and no systematic bias is detected. In the Alps (Goms-Binntal, Southern and Northern Venosta and Vanoise regions), Permafrost\_cci PFR shows slightly underestimated permafrost extent, although the majority of the inventoried landforms indicative for permafrost are well represented. In the mountain area of the Carpathians and Pirin mountains, no permafrost is present in the Permafrost\_cci PFR product which is consistent with the inventory, where only relict and transitional landforms have been identified.





*Figure 25: overview of Permafrost\_cci PFR permafrost extent in 2023 compared to the Permafrost\_cci phase II rock glacier inventories in Baralachala region (India) (a), Tsengel Khairkhan (Mongolia) (b), Northern Venosta (Italy) (c), Goms and Binntal (Switzerland) (d) and Pirin mountains (Bulgaria) (e). The active and transitional rock glaciers are indicated in red circles, the relict rock glaciers are indicated in black circles.*

In addition, we innovatively apply the Freeze-Thaw to Temperature (FT2T) product, an EO microwave-derived ground temperature, for comparison with Permafrost\_cci GTD. Ground temperature averages partially correlate with  $R^2 = 0.34$  in Alaska and in Canada. No correlation can be observed for Russia and Greenland. An offset can be observed in case of all selected regions. This bias ranges from  $1.42\text{ }^{\circ}\text{C}$  (Canada) to  $2.1\text{ }^{\circ}\text{C}$  (Alaska). Similar temporal patterns can be however partially observed.

For the inland ice-free permafrost regions in Antarctica, data are not sufficient for a thorough statistical analysis. In general, the in-situ data locations represent a wide gradient: cold permafrost between MAGT around  $\text{MAGT} \sim -10^\circ\text{C}$  and warm permafrost  $\sim -2^\circ\text{C}$ . The tendency of Permafrost\_cci GTD compared to the available in situ data is negative, i.e. Permafrost\_cci performs with too cold GTD (mean cold bias  $-2.76^\circ\text{C} \pm 1.10$ ; median cold bias  $-3^\circ\text{C}$ ). The tendency of the Permafrost\_cci dataset compared to the available in situ data is negative, i.e. Permafrost\_cci performs with too cold GTD and too shallow ALT depths.

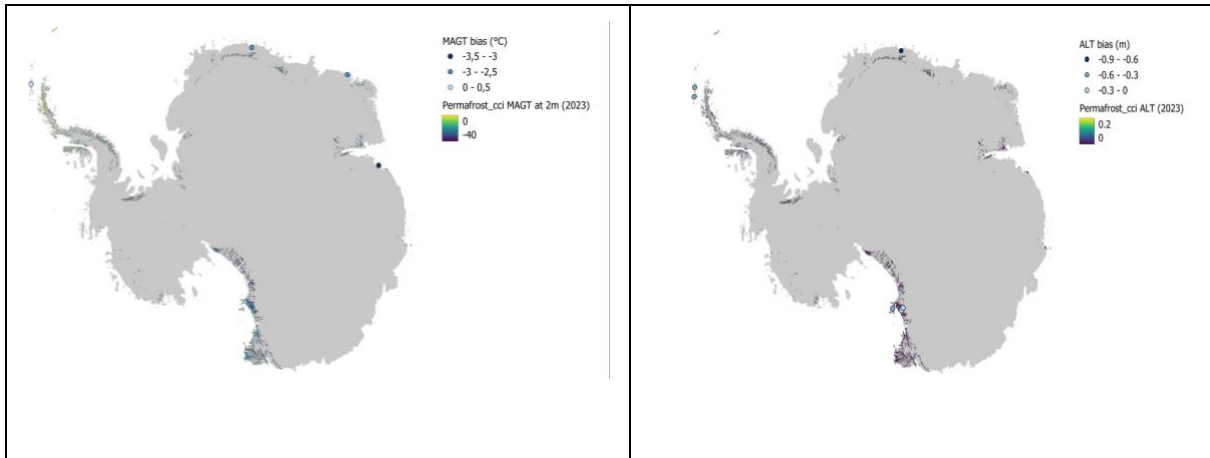


Figure 26: Antarctica (left) GTD bias (color-coded point symbols) over mapped Permafrost\_cci GTD 2023 (2 m). (right) ALT bias (color-coded point symbols) over mapped Permafrost\_cci ALT 2023. (source background map: Quantarctica, Matsuoka et al. 2021)

The temporal trend of GTD is well captured by Permafrost\_cci at three from five measurement sites. One site is warming too fast, while a second one shows no variability in Permafrost\_cci GTD.

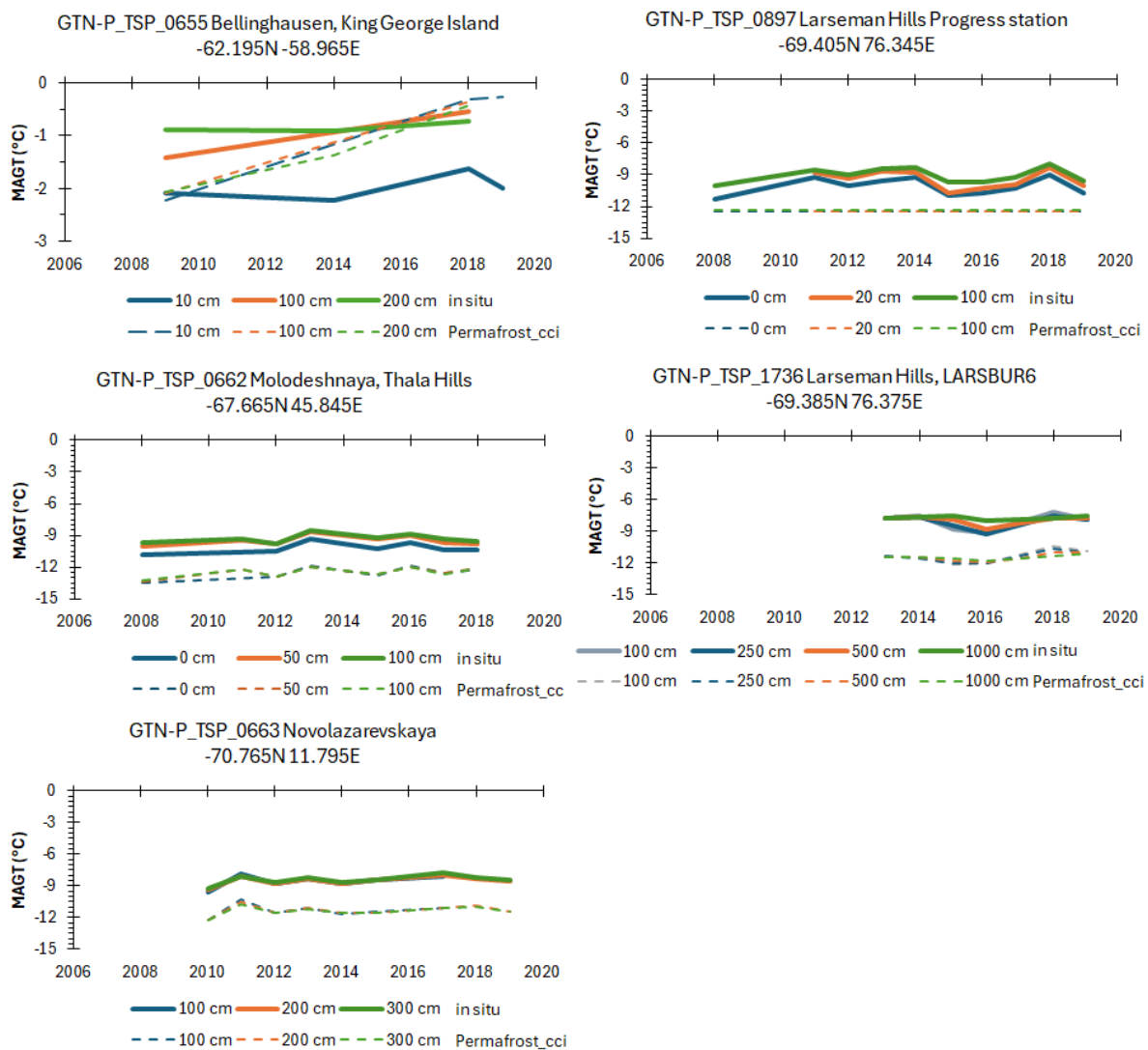


Figure 27: Temporal trends of in situ MAGT (solid) and Permafrost\_cci GTD (dashed) temperature at different depths for five sites in Antarctica.

In summary, Permafrost\_cci GTD  $< 1^{\circ}\text{C}$  shows good performance with a cold median bias of  $-0.23^{\circ}\text{C}$  (mean bias of  $0.03^{\circ}\text{C} \pm 1.94$ ) across all depths and high temporal stability resulting in a well usable CCI ECV product for the climate research communities. Users of Permafrost\_cci GTD products should consider that Permafrost\_cci GTD  $> 1^{\circ}\text{C}$  outside of the permafrost zones is characterised by a cold median bias of  $-1.33^{\circ}\text{C}$  (mean bias  $-1.16^{\circ}\text{C} \pm 1.48$ ). This leads in turn to an overestimation of the areal extent of permafrost at the southern boundaries of Permafrost in discontinuous, and sporadic permafrost regions. We consider Permafrost\_cci GTD and PFR products for the Northern hemisphere to be most reliable in the permafrost temperature range with GTD  $< 1^{\circ}\text{C}$ .

#### Community reference data publication in Permafrost\_cci cooperation

Kholodov, A.L, Wieczorek, M., Heim, B. and Romanovsky, V.E, 2025, Eleven years of Mean Annual Ground Temperatures across depths from eastern and central Siberia (2008-2018). PANGAEA, <https://doi.org/10.1594/PANGAEA.972733>

Lewkowicz, A.G., Wieczorek, M., Bartsch, A. and Heim, B., 2025, Twenty years of Mean Annual Ground Temperature (MAGT) across latitudinal and elevational gradients in the Yukon Territory (NW Canada). PANGAEA, <https://doi.org/10.1594/PANGAEA.971276>

Martin, J., Boike, J., Chadburn, S., Zwieback, S., Anselm, N., Goldau, M., Hammar, J., Abramova, E. N., Lisovski, S., Coulombe, S., Dakin, B., Wilcox, E. J., Giamberini, M., Rader, F., Suominen, O., Rudd, D. A., Mastepanov, M. and Young, A., 2023, T-MOSAiC 2021 myThaw data set. PANGAEA, <https://doi.org/10.1594/PANGAEA.956039>

Streletskei, D.A., Wieczorek, M., Heim, B. and Bartsch, A., 2025, GTN-P CALM: 35 years of Active Layer Thickness (ALT) across latitudinal and elevational gradients in the Northern Hemisphere. PANGAEA, <https://doi.org/10.1594/PANGAEA.972777>

Veremeeva, A., Morgenstern, A., Gottschalk, M., Jünger, J., Laboor, S., Abakumov, E., Adrian, I., Angelopoulos, M., Antonova, S., Boike, J., Bornemann, N., Cherepanova, A., Evgrafova, S., Fedorov-Davydov, D., Fuchs, M., Grigoriev, M.N., Günther, F., Hugelius, G., Kizyakov, A., Kut, A., Lashchinskiy, N., Lupachev, A., Maksimov, G.T., Meyer, H., Miesner, F., Minke, M., Nitzbon, J., Opel, T., Overduin, P.P., Ramage, J.L., Liebner, S., Polyakov, V.I., Rivkina, E., Runge, A., Schirrmeyer, L., Schwamborn, G., Siewert, M.B., Tarbeeva, A., Ulrich, M., Wetterich, S., Zubrzycki, S. and Grosse, G., 2025, ALLena: Thaw depth measurements of the active layer in the Lena River Delta region from 1998 to 2022, Northeastern Siberia. PANGAEA. <https://doi.org/10.1594/PANGAEA.973813>, In: Veremeeva, A et al. (2025): ALLena: Compilation of thaw depth measurements of the active layer in the Lena River Delta region from 1998 to 2022, Northeastern Siberia. PANGAEA, <https://doi.org/10.1594/PANGAEA.974408>

Wieczorek, M., Lewkowicz, A.G., Kholodov, A.L., Romanovsky, V.E., Nicolsky, D., Streletskei, D.A., Boike, J., Heim, B., Bartsch, A., Biskaborn, B.K., Christiansen, H.H., Elger, K. and Irrgang, A.M., 2025, GTN-P: 41 years of Mean Annual Ground Temperature (MAGT) across latitudinal and elevational gradients in the Northern Hemisphere. PANGAEA, <https://doi.pangaea.de/10.1594/PANGAEA.972992> (dataset in review)

### 3.10 Assessment of utility of Rock Glacier Inventory (RoGI) Products

In the first iteration of Permafrost\_cci Phase 2 (2023-2024), a RoGI multi-operator exercise performed between June and November 2023 resulted in a dataset of InSAR-based Moving Areas (MA), Rock Glacier Unit (RGU) Primary Markers (PM) and outlines for all the 12 selected areas [RD-11]. The assessment is based on feedbacks from the PIs from 10 institutions in 8 countries: The University of Fribourg (Switzerland), Gamma Remote Sensing AS (Switzerland), NORCE Norwegian Research Centre (Norway), The University of Bologna (Italy), West University of Timisoara (WUT) (Romania), The University of Savoie Mont-Blanc / The University of Grenoble Alps (France), The University of Alaska Fairbanks (USA), Argentine Institute of Nivology, Glaciology and Environmental Sciences (IANGLA) (Argentina), Graz University of Technology (TU Graz) (Austria) and The University of Lausanne (Switzerland). The comments of the results and RoGI process are based on several rounds of discussions with a large group of operators (5–10 operators in each area, 41 persons in total). The primary conclusions, strengths and limitations of the produced RoGI are detailed in the PVIR [RD-12] and PUG [RD-13]. Based on the findings of the exercise, we have also encouraged the external partners institutions to build on the findings of the exercise, to correct, upscale and further analyse their inventories. Several related publications are already published or in preparation (see Section 5).

The feedback from the PIs and operator teams are overall very positive. The steps and instructions of the exercise were generally assessed as clear and easy to follow. Most PIs/teams reported that they liked the structure and clarity of the provided GIS and data packages, which is promising for a future use as training tools. Most PIs report positive involvement and motivation from their operators. Each team had two multi-operator meetings, with about 3–10 people attending. The size of the team was ideal for a such exercise, more people would have been challenging to have good discussions. In some cases, the digital meetings have been complemented with complementary modes of communication (email discussions, sharing of comments in documents, prints screens, powerpoints, sending recording of meetings). The discussion at the meetings (and through other communication modes) were found very valuable; both for personal learning purpose and for improving the quality of the final products. Having operators with different skills and backgrounds brings value to the results. All involved institutions and PIs agree that the combination of different points of view and experiences from several regions around the World ensures that various morpho-kinematic elements are identified and taken into consideration. Although InSAR interpretation has been identified as the most challenging step due to little experience for some operators, several teams report that the data is useful at different levels, e.g. simply to detect landforms that may not be so obvious on optical images only, even when not focusing on quantifying their movement rates.

The analysis of the CRDP [RD-11] highlighted the value of the datasets for various usage: further detailed analysis in the considered area, selection of landforms for RGV generation, training dataset for machine learning, dissemination as online exercise for educational purpose. Several limitations and suggestions to improve the current procedure/guidelines are detailed in the PVIR [RD-12] and PUG [RD-13] and discussed in the Use Case Study 6..

In the second iteration of Permafrost\_cci Phase 2 (2024-2025), we started a collaboration with third parties to use the results from the first iteration as training data for RoGI using machine learning. This activity is in synergy with a RGIK working group on the same topic. The conclusions of the first iteration also contributed to the development of extra training material and adjustment of the RoGI instructions and GIS tools.. The RoGI procedure have been applied in eight extra regions. The RoGI process is completed in four regions (Switzerland, Italy, Mongolia and India). In two regions (Bolivia-Chile,

Bulgaria), the work is finished in part of the region, but the RoGI will be geographically extended. In two regions (Nepal and Bhutan), the last steps of the RoGI process are ongoing.

In the Permafrost\_cci extension phase (2026), the focus must be placed on finalising the RoGI products of iteration 2, releasing the data and supporting the publication of associated scientific articles. In addition, a suitable solution for data collection, storage and sharing must be implemented. This is aligned with the objective the RGIK RoGI working group, currently focusing on developing a RoGI database that will provide a valuable tool to compile and promote the Permafrost\_cci outcomes. We will keep improving the GIS tools and templates, and developing alternative educational and training tools for enhancing the RoGI production by third parties.

### 3.8 Assessment of utility of Rock Glacier Velocity (RGV) Products

In the first iteration of Permafrost\_cci Phase 2 (2024-2025), four different InSAR-RGV were produced at selected sites in the Swiss Alps [RD-10]. For the four sites, the relative velocity changes are homogenous. On average, the four rock glaciers all accelerated during the observation period, which matches both the trend shown by all UNIFR monitored rock glaciers in Valais and Central Swiss Alps and the trend from all rock glaciers monitored by the Swiss Permafrost Monitoring Network PERMOS [RD-11]. In general, all sites fit well with the trend documented by the regional and PERMOS averages. The results also match with the findings of Kellerer-Pirklbauer et al. (2024), who observed accelerating trends between 2018 and 2021 on multiple rock glaciers in the European Alps. Based on InSAR-RGV, all sites increase the most between 2018 and 2019, as for the PERMOS results (PERMOS, 2023).

We proposed an easily transferable method to automate the production of RGV by averaging unwrapped Sentinel-1 interferograms. The developed method appears to be suitable to produce consistent InSAR-RGV, which are comparable to GNSS-RGV, although we need to include more years of data to confirm this primary conclusion. The InSAR-RGV products can be extracted for single pixels, or represent an average of several pixels on the main moving areas of each rock glacier, providing a better spatial representativity than single GNSS points. In addition, because of the availability of historical data, time series can be computed since 2015 and 2017 with 6-days and 12-days interferograms, respectively, whereas in-situ measurements are only available from the first measurement onwards. As long as regular open access data is available, the RGV time series can be updated each year.

In the second iteration of Permafrost\_cci Phase 2 (2024-2025), the InSAR-RGV production has been extended to 21 sites in the Alps. The comparison with GNSS data shows that the results are promising, but also highlight limitations related to the detection capability of the method and the impact of unwrapping errors on rapid rock glaciers (see P VIR [RD-12] and PUG [RD-13]). The validation at the site scale remains preliminary. The analysis has only been performed for 6 of the 21 sites, due to current lack of suitable data to compare on the remaining sites. At the regional scale, the comparison show that the InSAR-RGV results highlight overall similar accelerating (2018-2020) and decelerating (2020-2022) periods, comparable with GNSS-RGV. Several questions regarding the spatial and temporal representativeness of the final products are still to be answered (e.g. criteria for pixel selection and spatial averaging based on quality measures; impact of the observation time window in case of large seasonal variability of the velocity).

We went further in the definition of processing criteria and processing chain for the operationalization and upscaling of the InSAR-RGV production. The RGV guidelines are still under development, but the last years have shown rapid advances in this field, under the umbrella of the RGIK community. The InSAR procedure applied in the European Alps still needs to be tested on more rock glaciers and the time series should be further compared with other techniques (e.g. optical remote sensing). An international working group has been kicked off to produce and intercompare RGV generated with different techniques (in situ, optical remote sensing, radar remote sensing) on similar selected rock glaciers. The kick-off meeting was organized the 10<sup>th</sup> of April 2024 and a dedicated workshop on this topic was held in November 2024 (see [RGV Working Group information on ESA website](#)). A second workshop is planned for December 2025. The current focus is on drafting technical Best Practice documents for RGV generation. The document is expected to be released in 2026, to become Appendixes of the generic RGV guidelines [RD-15] [RD-16].

In the Permafrost\_cci extension phase (2026), the focus must be placed on extending the number of RGV-documented landforms in the Alps, while further investigating the suitable InSAR-RGV

processing settings, especially in respect to the spatial and temporal representativeness of the products. The site selection should follow a more careful and conservative analysis to perform the processing only on sites where we can ensure high quality. For ensuring long time series, 12d repeat-pass is required but the corresponding maximal detectable velocity (half wavelength: 28 cm/12 days, i.e. 85 cm/yr) is too low for many alpine rock glaciers. On the long-run, the upcoming availability of SAR data with better suited radar frequency (L-band) will allow for an enhanced detection capability, valuable for InSAR-RGV production. In preparation of ROSE-L, processing tests based on SAOCOM and NISAR are planned. We will further investigate the suitable processing settings, especially in respect to the spatial and temporal representativeness of the products. The impact of the observation time window has also to be further tested, especially for cases with very strong seasonal variations.

In the long run, Permafrost\_cci contributes to the objective to complement in-situ monitoring sites with a large set of remotely sensed RGV in more regions and on more landforms in each region. The effort of data collection and comparison has started (see Use Case Study 7) but is recent and the analysis is currently based on few sites worldwide. Systematic generation using the Permafrost\_cci InSAR-RGV methodology and further development of similar approaches for other remote sensing techniques will contribute to enlarge the set of comparable RGVs. Further analyse in respect to climate variables and other ECV products (PT, ALT) in similar regions will allow for comprehensive evaluation of the RGV significance as climate change indicator.

## 4 Progress in regard to user requirements

### 4.1 Algorithm selection

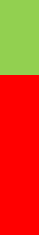
The process of the algorithm selection as detailed in the User Requirements Documents (URD) [RD-4,7] has been driven by the requirements of the climate research community. The user community deemed the selected algorithm as appropriate for their applications.

### 4.2 Product specification

In Table 4, we specify user requirements from the URD [RD-4] for the CryoGrid products and show the respective status of achievement. We aimed to complete as many requirements as possible, which are marked in green. Table 5 addresses the rock glacier product requirements.

*Table 4: Summary of user requirements. Background (BG) means that this is a continuous activity, production (P), and dissemination (D) means that the related requirement has to be considered during production, and dissemination, respectively. Parameters are Permafrost Extent (PE), Ground Temperature (GT) and Active Layer Thickness (ALT). The last column indicates the achievement status for the fourth project year (Y4=year 4; red: not started, yellow: ongoing, green: completed).*

ID	Parameter	Requirements	Source	Type	Y4
URQ_01	PE/GT/ALT	higher spatial resolution than a map scale of 1:10,000,000	IPA Mapping group report	BG	
URQ_02	PE/GT/ALT	data need to be related to a time stamp	IPA Mapping group report	P	
URQ_03	PE/GT/ALT	form of delivery for maps and data need to be flexible	IPA Mapping group report	D	
URQ_04	PE/GT/ALT	high data quality	IPA Mapping group report	BG	
URQ_05	PE/GT/ALT	benchmark dataset needs to be developed	IPA Mapping group report, GlobPermafrost/IPA mapping group workshop	P	
URQ_06	PE/GT/ALT	evaluation through community	GlobPermafrost/IPA mapping group workshop	P	
URQ_07	PE/GT/ALT	terminology for modelling output 'potential'	GlobPermafrost/IPA mapping group workshop	D	
URQ_08	GT/ALT	depth of active layer, permafrost temperature in	GCOS	BG	

		K and seasonal soil freeze/thaw needs to be addressed			
<b>URQ_09</b>	PE	Threshold: uncertainty 10-25%, hor. res. 10-100 km, temp. res. 3-5 days, timeliness 5-6 days;	OSCAR	BG	
		breakthrough uncertainty 7-8.5%, hor. res. 0.85 - 1 km, temp. res. 14-36 hours, timeliness 14-36 h			
<b>URQ_10</b>	PE/GT/ALT	Distribution as NetCDF	CMUG	D	
<b>URQ_11</b>	PE/GT/ALT	Development of a new ground stratigraphy product for the permafrost domain	GlobPermafrost survey	P/D	
<b>URQ_12</b>	GT	Threshold: pan-arctic, yearly, last decade, 10km, RMSE<2.5°C,	Permafrost_cci survey	BG	
		Target, global, monthly, 1979- present, 1km, subgrid variability, RMSE < 0.5°C			
<b>URQ_13</b>	ALT	Threshold: pan-arctic, yearly, last decade, 10km, RMSE<25cm, Target, global, monthly, 1979- present, 1km, subgrid variability, RMSE<10cm	Permafrost_cci survey	BG	

**Table 5.** Summary of user requirements for the Rock Glacier Inventories (RoGI) and the Rock Glacier Velocity (RGV) products [RD-7]. In the column ‘Type’, Background (BG) means that the requirement relates to the initial selection of the study areas, data and/or methods. Production (P) means that the related requirements must be considered during the production phase. Evaluation (E) means that the requirements are related to the quality assessment of the products. The colours show the achievement status at the end of the Phase II iteration 2 (in black: **Threshold Requirement**; in blue: **Breakthrough Requirement**; in green: **Goal Requirement**). \*\*\*Note that no Breakthrough Requirement was initially defined for URq\_03 but the products reached an intermediate level between Threshold and Goal, corresponding to a Breakthrough level. The last column indicates the achievement status for the fourth project year (Y5=year 5; red: not started, yellow: ongoing, green: completed).

ID	PARAMETER	USER REQUIREMENTS	TYPE	Y4
URq_01	RoGI	Relevant geographical coverage at the local-regional scale (valley side, drainage basin, mountain range).	BG	
URq_02	RoGI	Inventory based on several recent datasets over the 5-10 past years.	BG	
URq_03 ***	RoGI	Identification by a primary marker (point) and rock glacier outline as a polygon following the extended and/or restricted geomorphological footprints).	P	
URq_04	RoGI	Differentiation of rock glacier units (RGU) and mono-unit or multi-unit systems (RGS), based on distinct timing of formation, different connections to the upslope unit or distinct activities/kinematics.	P	
URq_05	RoGI	Mandatory documentation of the temporal properties (acquisition data, time frame/window) of the data sources used for RoGI generation, required for comparison and potential future update.	P/E	
URq_06	RoGI	Updated activity categorization: active, transitional, or relict. Uncertainty between categories can be documented.	P	
URq_07	RoGI	Optional destabilization attribute, only documented when geomorphological or kinematic evidence is available.	BG/P	
URq_08	RoGI	Semi-quantitative velocity classes, depending on the applied technique: For InSAR: 1-3 cm/yr, 3-10 cm/yr, 10-30 cm/yr, 30-100 cm/yr, etc.	BG/P	
URq_09	RoGI	Semi-quantitative ‘half an order-of-magnitude’ categories: cm-dm/yr, dm/yr, dm-m/yr, m/yr, etc.	P	

<b>URq_10</b>	RoGI	The data properties (data source, dimensionality, time window/frame) must be documented for all attributes. The reliability and spatial representativeness of moving areas and kinematic attributes must be qualitatively assessed (low, medium, high).	P/E	
<b>URq_11</b>	RGV	Multiple sites in a defined region, allowing for preliminary analysis of similar/dissimilar trends.	BG	
<b>URq_12</b>	RGV	Active or transitional rock glaciers with movement related to permafrost creep. Sites where long-term monitoring is feasible. Rock glacier units fully characterised following RoGI requirements.	BG	
<b>URq_13</b>	RGV	1 year, i.e. measured or computed once a year.	BG/P	
<b>URq_14</b>	RGV	Observation time window < 1 year (e.g. summer period only). At least 1 month and consistent over time (max. $\approx$ 15 days of difference).	BG/P	
<b>URq_15</b>	RGV	Temporal extent: past 5-10 years	BG/P	
<b>URq_16</b>	RGV	Annual mean velocity value. Unit: m/yr	P	
<b>URq_17</b>	RGV	The velocity is aggregated from flow field or several discrete points covering a large part of the rock glacier unit. The aggregation procedure and the considered area should be consistent over time.	P	
<b>URq_18</b>	RGV	Maximal relative error of the velocity data: 20%. If the error exceeds 20%, the site must be discarded, or alternative techniques should be considered in accordance with the absolute velocity measured/computed of the selected rock glacier.	E	
<b>URq_19</b>	RGV	The RGV consistency needs to be ensured.	E	

### 4.3 Plan for operationalization of PE, GT and ALT

The ESA Permafrost\_cci processing chain is currently implemented on the network of Norwegian supercomputing clusters managed by the company Sigma2 ([www.sigma2.no](http://www.sigma2.no)). As such, operational services for Permafrost ECV generation can be conducted as-is on the Sigma2 infrastructure, although higher rates will be charged for both CPU hours and storage for commercial users than for universities and research institutes. Furthermore, the processing chain is partly implemented in Matlab, so that access to licenses could eventually become a cost factor, especially for commercial entities. In the following, we summarize principal requirements for an operational processing system, as well as changes to the processing chain that have been or should ideally be implemented to achieve operational services.

*Constraints on processing system:* Hardware: supercomputing cluster with at least 100 cores with 4GB fast memory per core, about 15 TB storage for input data sets. Software: Matlab; slurm for management of supercomputing cluster.

*Steps implemented towards operationalization:* In the first iterations of Permafrost\_cci ECV generation, only the ECV parameters are stored, e.g. annual averages of ground temperatures. In order to compute a new time period (e.g. another year), the entire processing for all previous years must be repeated, as it is not possible to store the “raw” model state due to memory limitations. In the year 4 processing in Permafrost\_cci, the possibility to restart simulations from the raw model state at a particular point in time has been implemented. In particular, this makes it possible to compute, update and continue an existing ECV time series when new EO data become available. We estimate that this reduces the amount of computation by about a factor of 50 compared to recomputing the entire time period, which makes operational releases of the Permafrost\_cci ECV products much more feasible.

*Further changes to consolidate operationalization:* While there is no principal problem using Matlab-based code for processing, it may introduce complications and potentially costs for operational entities. Recoding the processing chain in a faster open-source language would therefore be desirable, but the complexity of the processing chain makes this re-coding difficult and potentially costly. Recoding in C++ is the most feasible option as there is an automatic C++ code converter available in Matlab. At present, not all code structures required for the processing system are supported, in particular recursive data structures of objects like linked lists. However, the capabilities of the code converter have steadily improved from year to year: in particular, in the 2024a version of Matlab, code containing arrays of objects can for the first time be automatically converted C++ code, which in previous versions was a key shortcoming of the automatic code conversion. We expect support for other important data structures employed in the processing chain, such as recursive relationships, in the coming years which would strongly reduce the working time and thus the costs required to re-implement the Permafrost\_cci processing chain in C++. We emphasize that changes to the processing system are much easier to implement in the current Matlab-based processing chain which is specially designed for modularity. Therefore, unless fast automatic code conversion becomes fully available, re-coding of the processing system in C++ or other languages should only be commenced when the processing system is fully consolidated.

## 5 Publications and outreach

### 5.1 Peer-reviewed scientific articles

#### Accepted/Published

Aga, J., Boike, J., Langer, M., Ingeman-Nielsen, T., and Westermann, S. (2023). Simulating ice segregation and thaw consolidation in permafrost environments with the CryoGrid community model, *The Cryosphere*, 17, 4179–4206, <https://doi.org/10.5194/tc-17-4179-2023>

Ardelean, F.; Onaca, A.; Chețan, M.-A.; Dornik, A.; Georgievski, G.; Hagemann, S.; Timofte, F.; Berzescu, O. (2020). Assessment of Spatio-Temporal Landscape Changes from VHR Images in Three Different Permafrost Areas in the Western Russian Arctic. *Remote Sensing*, 12(23), 3999. <https://doi.org/10.3390/rs12233999>

Bartsch, A., Ley, S., Nitze, I., Pointner, G., & Vieira, G. (2020). Feasibility study for the application of Synthetic Aperture Radar for coastal erosion rate quantification across the Arctic. *Frontiers in Environmental Science*, 8(143). <https://doi.org/10.3389/fenvs.2020.00143>

Bartsch, A. G. Pointner, H. Bergstedt, B. Widhalm, A. Wendleder, A. Roth (2021). Utility of polarizations available from Sentinel- 1 for tundra mapping. *IGARSS 2021* proceedings.

Bartsch, A., Strozzi, T., & Nitze, I. (2023). Permafrost Monitoring from Space. *Surveys in Geophysics*, 44(5), 1579–1613. <https://doi.org/10.1007/s10712-023-09770-3>

Bartsch, A., Efimova, A., Widhalm, B., Muri, X., von Baeckmann, C., Bergstedt, H., Ermokhina, K., Hugelius, G., Heim, B., and Leibman, M. (2024). Circumarctic land cover diversity considering wetness gradients, *Hydrol. Earth Syst. Sci.*, 28, 2421–2481. <https://doi.org/10.5194/hess-28-2421-2024>.

Bartsch, A., Muri, X., Hetzenecker, M., Rautiainen, K., Bergstedt, H., Wuite, J., Nagler, T., and Nicolsky, D. (2025). Benchmarking passive microwave satellite derived freeze/thaw datasets, *The Cryosphere*, 19, 459–483. <https://doi.org/10.5194/tc-19-459-2025>.

Bartsch, A., Tanguy, R., Bergstedt, H., von Baeckmann, C., Tømmervik, H., Macias-Fauria, M., Lemmettyinen, J., Rautiainen, K., Gruber, C., and Forbes, B. C. (2025). Similarities between sea ice area variations and satellite-derived terrestrial biosphere and cryosphere parameters across the Arctic, *The Cryosphere*, 19, 4929–4967. <https://doi.org/10.5194/tc-19-4929-2025>.

Bergstedt, H., Bartsch, A., Neureiter, A., Höfler, A., Widhalm, B., Pepin, N., and Hjort, J. (2020). Deriving a Frozen Area Fraction From Metop ASCAT Backscatter Based on Sentinel-1. *IEEE Transactions on Geoscience and Remote Sensing*, Volume: 58, Issue: 9. <https://doi.org/10.1109/TGRS.2020.2967364>

Bergstedt, H., Bartsch, A., Duguay, C. R., & Jones, B. M. (2020). Influence of surface water on coarse resolution C-band backscatter: Implications for freeze/thaw retrieval from scatterometer data. *Remote Sensing of Environment*, 247, 111911. <https://doi.org/10.1016/j.rse.2020.111911>

Bertone, A., Jones, N., Mair, V., Scotti, R., Strozzi, T., and Brardinoni, F. (2024). A climate-driven, altitudinal transition in rock glacier dynamics detected through integration of geomorphological mapping and synthetic aperture radar interferometry (InSAR)-based kinematics, *The Cryosphere*, 18, 2335–2356. <https://doi.org/10.5194/tc-18-2335-2024>.

Bertone, A., Barboux, C., Bodin, X., Bolch, T., Brardinoni, F., Caduff, R., Christiansen, H. H., Darrow, M., Delaloye, R., Etzelmüller, B., Humlum, O., Lambiel, C., Lilleøren, K. S., Mair, V., Pellegrinon, G., Rouyet, L., Ruiz, L., and Strozzi, T. (2022). Incorporating InSAR kinematics into rock glacier

inventories: insights from 11 regions worldwide, *The Cryosphere*, 16, 2769–2792. <https://doi.org/10.5194/tc-16-2769-2022>.

Brouillette, M. (2021). How microbes in permafrost could trigger a massive carbon bomb. *Nature*, 591, 360–362. <https://www.nature.com/articles/d41586-021-00659-y>

Biskaborn, B. K.; Smith, S. L.; Noetzli, J.; Matthes, H.; Vieira, G.; Streletschi, D. A.; Schoeneich, P.; Romanovsky, V. E.; Lewkowicz, A. G.; Abramov, A.; Allard, M.; Boike, J.; Cable, W. L.; Christiansen, H. H.; Delaloye, R.; Diekmann, B.; Drozdov, D.; Etzelmüller, B.; Grosse, G.; Guglielmin, M.; Ingeman-Nielsen, T.; Isaksen, K.; Ishikawa, M.; Johansson, M.; Johannsson, H.; Joo, A.; Kaverin, D.; Kholodov, A.; Konstantinov, P.; Kröger, T.; Lambiel, C.; Lanckman, J.-P.; Luo, D.; Malkova, G.; Meiklejohn, I.; Moskalenko, N.; Oliva, M.; Phillips, M.; Ramos, M.; Sannel, A. B. K.; Sergeev, D.; Seybold, C.; Skryabin, P.; Vasiliev, A.; Wu, Q.; Yoshikawa, K.; Zheleznyak, M.; Lantuit, H. (2019). Permafrost is warming at a global scale. *Nature Communications*, 10, 264. <https://doi.org/10.1038/s41467-018-08240-4>

Biskaborn, B. K., Lanckman, J.-P., Lantuit, H., Elger, K., Streletschi, D. A., Cable, W. L., and Romanovsky, V. E. (2015). The new database of the Global Terrestrial Network for Permafrost (GTN-P). *Earth Syst. Sci. Data*, 7, 245–259. <https://doi.org/10.5194/essd-7-245-2015>

Brardinoni, F., Vivero, S., Barboux, C., Bodin, X., Cicoira, A., Echelard, T., Hu, Y., Jones, N., Lambiel, C., MacDonell, S., Pellet, C., Rouyet, L., Ruiz, L., Schaffer, N., Wehbe, M. and Delaloye, R. (2025). RGIK guidelines for compiling consistent rock glacier inventories. *Geomorphology*, 110050. <https://doi.org/10.1016/j.geomorph.2025.110050>

Brovkin, V., Bartsch, A., Hugelius, G., Calamita, E., Lever, J.J., Goo, E., Kim, H., Stacke, T., de Vrese, P. (2025). Permafrost and Freshwater Systems in the Arctic as Tipping Elements of the Climate System. *Surv Geophys*. <https://doi.org/10.1007/s10712-025-09885-9>.

Burke, E. J., Zhang, Y., & Krinner, G. (2020). Evaluating permafrost physics in the Coupled Model Intercomparison Project 6 (CMIP6) models and their sensitivity to climate change. *The Cryosphere*, 14(9), 3155–3174. <https://doi.org/10.5194/tc-14-3155-2020>

Burn, C., Bartsch, A., Chakraborty, E., Das, S., Frauenfelder, R., Gärtnner-Roer, I., Gisnås, K., Herring, T., Jones, B., Kokelj, S., Langer, M., Lathrop, E., Murton, J., Nielsen, D., Niu, F., Olson, C., O'Neill, H., Opfergelt, S., Overduin, P., Schaefer, K., Schuur, E., Skierszkan, E., Smith, S., Stuenzi, S., Tank, S., van der Slujs, J., Vieira, G., Westermann, S., Wolfe, S. and Yarmak, E. (2024). Developments in Permafrost Science and Engineering in Response to Climate Warming in Circumpolar and High Mountain Regions, 2019–2024. *Permafrost and Periglac Process*. <https://doi.org/10.1002/ppp.2261>.

Frost GV, Bhatt US, Macander MJ, Berner LT, Walker DA, Raynolds MK, Magnússon RÍ, Bartsch A, Bjerke JW, Epstein HE, Forbes BC, Goetz SJ, Hoy EE, Karlsen SR, Kumpula T, Lantz TC, Lara MJ, López-Blanco E, Montesano PM, Neigh CSR, Nitze I, Orndahl KM, Park T, Phoenix GK, Rocha AV, Rogers BM, Schaepman-Strub G, Tømmervik H, Verdonen M, Veremeeva A, Virkkala A-M and Waigl CF (2025). The changing face of the Arctic: four decades of greening and implications for tundra ecosystems. *Front. Environ. Sci.* 13:1525574. <https://doi.org/10.3389/fenvs.2025.1525574>.

Hu, Y., Arenson, L. U., Barboux, C., Bodin, X., Cicoira, A., Delaloye, R., Gärtnner-Roer, I., Kääb, A., Kellerer-Priklbauer, A., Lambiel, C., Liu, L., Pellet, C., Rouyet, L., Schoeneich, P., Seier, G., and Strozzi, T. (2025). Rock glacier velocity: An essential climate variable quantity for permafrost. *Reviews of Geophysics*, 63(1), e2024RG000847. <https://doi.org/10.1029/2024RG000847>

Ishikawa, M., Westermann, S., Jambaljav, Y., Dashtseren, A., Hiyama, T., Endo, N., & Etzelmüller, B. (2024). Transient Modeling of Permafrost Distribution From 1986 to 2016 in Mongolia. *Permafrost and Periglac Process*. <https://doi.org/10.1002/ppp.2231>.

Jones, B. M. , Arp, C. D. , Grosse, G. , Nitze, I. , Lara, M. J., Whitman, M. S. , Farquharson, L. M. , Kanevskiy, M. , Parsekian, A. D. , Breen, A. L. , Ohara, N. , Rangel, R. C. and Hinkel, K. M. (2020). Identifying historical and future potential lake drainage events on the western Arctic coastal plain of Alaska. *Permafrost and Periglacial Processes*, 31 (1), 110-127. <https://doi.org/10.1002/ppp.2038>

Jones, B. M., Schaeffer Tessier, S., Tessier, T., Brubaker, M., Brook, M., Schaeffer, J., Ward Jones, M. K., Grosse, G., Nitze, I., Rettelbach, T., Zavoico, S., Clark, J. A., & Tape, K. D. (2023). Integrating local environmental observations and remote sensing to better understand the life cycle of a thermokarst lake in Arctic Alaska. *Arctic, Antarctic, and Alpine Research*, 55(1), 2195518. <https://doi.org/10.1080/15230430.2023.2195518>

Jones, B. M., Irrgang, A. M., Farquharson, L. M., Lantuit, H., Whalen, D., Ogorodov, S., Grigoriev, M., Tweedie, C., Gibbs, A. E., Strzelecki, M. C., Baranskaya, A., Belova, N., Sinitsyn, A., Kroon, A., Maslakov, A., Vieira, G., Grosse, G., Overduin, P., Nitze, I., Maio, C., Overbeck, J., Bendixen, M., Zagórski, P., Romanovsky, V.E. (2020). NOAA Arctic Report Card 2020, Coastal Permafrost Erosion, Administrative Report. <https://doi.org/10.25923/E47W-DW52>

Kääb, A., Strozzi, T., Bolch, T., Caduff, R., Trefall, H., Stoffel, M., & Kokarev, A. (2021). Inventory and changes of rock glacier creep speeds in Ile Alatau and Kungöy Ala-Too, northern Tien Shan, since the 1950s. *The Cryosphere*, 15(2), 927–949. <https://doi.org/10.5194/tc-15-927-2021>

Kääb, A., & Røste, J. (2024). Rock glaciers across the United States predominantly accelerate coincident with rise in air temperatures. *Nature Communications*, 15(1), 7581. <https://doi.org/10.1038/s41467-024-52093-z>

Kholodov, A.L, Wieczorek, M., Heim, B. and Romanovsky, V.E (2025). Eleven years of Mean Annual Ground Temperatures across depths from eastern and central Siberia (2008-2018). PANGAEA, <https://doi.org/10.1594/PANGAEA.972733>

Lambiel, C., Strozzi, T., Paillex, N., Vivero, S. and Jones, N. (2023). Inventory and kinematics of active and transitional rock glaciers in the Southern Alps of New Zealand from Sentinel-1 InSAR, Arctic, Antarctic, and Alpine Research, 55(1), 2183999. <https://doi.org/10.1080/15230430.2023.2183999>

Langer, M., von Deimling, T.S., Westermann, S., Rolph, R., Rutte, R., Antonova, S., Rachold, V., Schultz, M., Oehme A., Grosse G. (2023). Thawing permafrost poses environmental threat to thousands of sites with legacy industrial contamination. *Nat Commun* 14, 1721. <https://doi.org/10.1038/s41467-023-37276-4>

Lenton, T.M., Abrams, J.F., Bartsch, A. et al. (2024). Remotely sensing potential climate change tipping points across scales. *Nat Commun* 15, 343. <https://doi.org/10.1038/s41467-023-44609-w>

Lewkowicz, A.G, Wieczorek, M., Bartsch, A. and Heim, B. (2025). Twenty years of Mean Annual Ground Temperature (MAGT) across latitudinal and elevational gradients in the Yukon Territory (NW Canada). PANGAEA, <https://doi.org/10.1594/PANGAEA.971276>

Lilleøren, K. S., Etzelmüller, B., Rouyet, L., Eiken, T., Slinde, G., and Hilbich, C. (2022). Transitional rock glaciers at sea level in northern Norway, *Earth Surf. Dynam.*, 10, 975–996. <https://doi.org/10.5194/esurf-10-975-2022>

Lissak, C., Bartsch, A., De Michele, M., Gomez, C., Maquaire, O., Raucoules, D., & Roulland, T. (2020). Remote Sensing for Assessing Landslides and Associated Hazards. *Surveys in Geophysics*, 41(6), 1391–1435. <https://doi.org/10.1007/s10712-020-09609-1>

Loriani, S., Bartsch, A., Calamita, E., Donges, J. F., Hebden, S., Hirota, M., Landolfi, A., Nagler, T., Sakschewski, B., Staal, A., Verbesselt, J., Winkelmann, R., Wood, R., Wunderling, N. (2025). Monitoring the Multiple Stages of Climate Tipping Systems from Space: Do the GCOS Essential Climate Variables Meet the Needs? *Surveys in Geophysics*. <https://doi.org/10.1007/s10712-024-09866-4>

Martin, L. C. P., Nitzbon, J., Scheer, J., Aas, K.S., Eiken, T., Langer, M., Filhol, S., Etzelmüller, B., & Westermann, S. (2021). Lateral thermokarst patterns in permafrost peat plateaus in northern Norway. *The Cryosphere*, 15, 3423–3442. <https://doi.org/10.5194/tc-15-3423-2021>

Nitzbon, J., Schneider von Deimling, T., Aliyeva, M., Chadburn, S., Grosse, G., Laboor, S., Lee, H., Lohmann, G., Steinert, N., Stuenzi, S., Werner, M., Westermann, S., and Langer M. (2024). No respite from permafrost-thaw impacts in the absence of a global tipping point, *Nat. Clim. Chang.* <https://doi.org/10.1038/s41558-024-02011-4>.

Nitze, I., Cooley, S. W., Duguay, C. R., Jones, B. M., & Grosse, G. (2020). The catastrophic thermokarst lake drainage events of 2018 in northwestern Alaska: Fast-forward into the future. *The Cryosphere*, 14(12), 4279–4297. <https://doi.org/10.5194/tc-14-4279-2020>

Nitze, I., Heidler, K., Barth, S., & Grosse, G. (2021). Developing and Testing a Deep Learning Approach for Mapping Retrogressive Thaw Slumps. *Remote Sensing*, 13(21). <https://doi.org/10.3390/rs13214294>

Obu, J. (2021). How Much of the Earth's Surface is Underlain by Permafrost? *Journal of Geophysical Research: Earth Surface*, 126(5). <https://doi.org/10.1029/2021JF006123>

Onaca, A., Sîrbu, F., Poncoş, V., Hilbich, C., Strozzi, T., Urdea, P., Popescu, R., Berzescu, O., Etzelmüller, B., Vespremeanu-Stroe, A., Vasile, M., Teleagă, D., Birtaş, D., Lopătiă, I., Filhol, S., Hegyi, A., & Ardelean, F. (2025). Slow-moving rock glaciers in marginal periglacial environment of Southern Carpathians. *Earth Surface Dynamics*, 13(5), 981–1001. <https://doi.org/10.5194/esurf-13-981-2025>

Pellet, C., Bodin, X., Cusicanqui, D., Delaloye, R., Kääb, A., Kaufmann, V., Thibert, E., Vivero, S., & Kellerer-Pirklbauer, A. (2025). Rock glacier velocity. In *State of Climate in 2024*, Bull. Amer. Meteor. Soc., 106(8), pp. 48–49. <https://doi.org/10.1175/2025BAMSSStateoftheClimate.1>

Popp, T., M.I. Hegglin, R. Hollmann, F. Ardhuin, A. Bartsch, A. Bastos, V. Bennett, J. Boutin, C. Brockmann, M. Buchwitz, E. Chuvieco, P. Ciais, W. Dorigo, D. Ghent, R. Jones, T. Lavergne, C.J. Merchant, B. Meyssignac, F. Paul, S. Quegan, S. Sathyendranath, T. Scanlon, M. Schröder, S.G.H. Simis, U. Willén (2020). Consistency of satellite climate data records for Earth system monitoring. *Bulletin of the American Meteorological Society*. <https://doi.org/10.1175/BAMS-D-19-0127.1>

Renette, C., Aalstad, K., Aga, J., Zweigel, R. B., Etzelmüller, B., Lilleøren, K. S., Isaksen, K., and Westermann, S. (2023). Simulating the effect of subsurface drainage on the thermal regime and ground ice in blocky terrain in Norway, *Earth Surf. Dynam.*, 11, 33–50, <https://doi.org/10.5194/esurf-11-33-2023>

Rouyet, L., Lilleøren, K. S., Böhme, M., Vick, L. M., Delaloye, R., Etzelmüller, B., Lauknes, T. R., Larsen, Y., and Blikra, L. H. (2021). Regional Morpho-Kinematic Inventory of Slope Movements in Northern Norway, *Front. Earth Sci.* 9, 6810881. <https://doi.org/10.3389/feart.2021.681088>

Rouyet, L., Liu, L., Strand, S. M., Christiansen, H. H., Lauknes, T. R., & Larsen, Y. (2021). Seasonal InSAR Displacements Documenting the Active Layer Freeze and Thaw Progression in Central-Western Spitsbergen, Svalbard. *Remote Sensing*, 13(15), 2977. <https://doi.org/10.3390/rs13152977>

Rouyet, L., Bolch, T., Brardinoni, F., Caduff, R., Cusicanqui, D., Darrow, M., Delaloye, D., Echelard, T., Lambiel, C., Pellet, C., Ruiz, L., Schmid, L., Sirbu, F. and Strozzi, T. (2025). Rock Glacier Inventories (RoGIs) in 12 areas worldwide using a multi-operator consensus-based procedure. *Earth System Science Data*, 17(8), 4125–4157. <https://doi.org/10.5194/essd-17-4125-2025>

Runge, A. and Grosse, G. (2020). Mosaicking Landsat and Sentinel-2 Data to Enhance LandTrendr Time Series Analysis in Northern High Latitude Permafrost Regions. *Remote Sensing*, 12(15), 2471. <https://doi.org/10.3390/rs12152471>

Runge, A., Nitze, I., & Grosse, G. (2022). Remote sensing annual dynamics of rapid permafrost thaw disturbances with LandTrendr. *Remote Sensing of Environment*, 268, 112752. <https://doi.org/10.1016/j.rse.2021.112752>

Sasgen, I., Steinhoefel, G., Kasprzyk, C., Matthes, H., Westermann, S., Boike, J., Grosse, G. (2024). Atmosphere circulation patterns synchronize pan-Arctic glacier melt and permafrost thaw, *Commun Earth Environ*, 5, 375, 2024. <https://doi.org/10.1038/s43247-024-01548-8>.

Schickhoff, M., de Vrese, P., Bartsch, A., Widhalm, B. and Brovkin, V. (2024). Effects of land surface model resolution on fluxes and soil state in the Arctic, *Environ. Res. Lett.* 19 104032. <https://doi.org/10.1088/1748-9326/ad6019>.

Strauss, J., Fuchs, M., Hugelius, G., Miesner, F., Nitze, I., Opfergelt, S., Schuur, E., Treat, C., Turetsky, M., Yang, Y., & Grosse, G. (2024). Organic matter storage and vulnerability in the permafrost domain. In *Reference Module in Earth Systems and Environmental Sciences* (p. B9780323999311001641). Elsevier. <https://doi.org/10.1016/B978-0-323-99931-1.00164-1>

Streletskiy, D.A., Maslakov, A., Grosse, G., Shiklomanov, N., Farquharson, L.M., Zwieback, S., Iwahana, G., Bartsch, A., Liu, L., Strozzi, T., Lee, H., Debolskiy, M. V. (2025). Thawing permafrost is subsiding in the Northern Hemisphere - review and perspectives. *Environmental Research Letters*, Volume 20, Number 1. <https://doi.org/10.1088/1748-9326/ada2ff>.

Streletskiy, D.A., Wieczorek, M., Heim, B. and Bartsch, A. (2025). GTN-P CALM: 35 years of Active Layer Thickness (ALT) across latitudinal and elevational gradients in the Northern Hemisphere. PANGAEA, <https://doi.org/10.1594/PANGAEA.972777>

Strozzi T., R.Caduff, N. Jones, C. Barboux, R. Delaloye, X. Bodin, A. Kääb, E. Mätzler, L. Schrott (2020). Monitoring Rock Glacier Kinematics with Synthetic Aperture Radar. *Remote Sensing*, 12(3), 559. <https://doi.org/10.3390/rs12030559>

Swingedouw, D., Speranza, C., Bartsch, A., Durand, G., Jamet, C., Beaugrand, G., Conversi, A. (2020). Early Warning from Space for a Few Key Tipping Points in Physical, Biological, and Social-Ecological Systems. *Surveys in Geophysics*. <https://doi.org/10.1007/s10712-020-09604-6>

Tanguy, R., Bartsch, A., Nitze, I., Irrgang, A., Petzold, P., Widhalm, B., von Baeckmann, C., Boike, J., Martin, J., Efimova, A., Vieira, G., Whalen, D., Heim, B., Wieszorek, M., Grosse, G. (2024). Pan-Arctic Assessment of Coastal Settlements and Infrastructure Vulnerable to Coastal Erosion, Sea-Level Rise, and Permafrost Thaw, *Earth's Future*. <https://doi.org/10.1029/2024EF005013>.

Tape, K. D., Clark, J. A., Jones, B. M., Kantner, S., Gaglioti, B. V., Grosse, G., & Nitze, I. (2022). Expanding beaver pond distribution in Arctic Alaska, 1949 to 2019. *Scientific Reports*, 12(1), 7123. <https://doi.org/10.1038/s41598-022-09330-6>

von Baeckmann, C., Bartsch, A., Bergstedt, H., Efimova, A., Widhalm, B., Ehrich, D., Kumpula, T., Sokolov, A., and Abdulmanova, S. (2024). Land cover succession for recently drained lakes in permafrost on the Yamal Peninsula, Western Siberia, *The Cryosphere*, 18, 4703–4722. <https://doi.org/10.5194/tc-18-4703-2024>.

Veremeeva, A., Morgenstern, A., Gottschalk, M., Jünger, J., Laboor, S., Abakumov, E., Adrian, I., Angelopoulos, M., Antonova, S., Boike, J., Bornemann, N., Cherepanova, A., Evgrafova, S., Fedorov-Davydov, D., Fuchs, M., Grigoriev, M.N., Günther, F., Hugelius, G., Kizyakov, A., Kut, A., Lashchinskiy, N., Lupachev, A., Maksimov, G.T., Meyer, H., Miesner, F., Minke, M., Nitzbon, J., Opel, T., Overduin, P.P., Ramage, J.L., Liebner, S., Polyakov, V.I., Rivkina, E., Runge, A., Schirrmeyer, L., Schwamborn, G., Siewert, M.B., Tarbeeva, A., Ulrich, M., Wetterich, S., Zubrzycki, S. and Grosse, G. (2025). ALLena: Thaw depth measurements of the active layer in the Lena River Delta region from 1998 to 2022, Northeastern Siberia. PANGAEA. <https://doi.org/10.1594/PANGAEA.973813>, In: Veremeeva, A et al. (2025). ALLena: Compilation of thaw depth measurements of the active layer in the Lena River Delta region from 1998 to 2022, Northeastern Siberia. PANGAEA, <https://doi.org/10.1594/PANGAEA.974408>

Veremeeva, A., Nitze, I., Günther, F., Grosse, G., & Rivkina, E. (2021). Geomorphological and Climatic Drivers of Thermokarst Lake Area Increase Trend (1999–2018) in the Kolyma Lowland Yedoma Region, North-Eastern Siberia. *Remote Sensing*, 13(2), 178. <https://doi.org/10.3390/rs13020178>

Westermann, S., Ingeman-Nielsen, T., Scheer, J., Aalstad, K., Aga, J., Chaudhary, N., Etzelmüller, B., Filhol, S., Kääb, A., Renette, C., Schmidt, L. S., Schuler, T. V., Zweigel, R. B., Martin, L., Morard, S., Ben-Asher, M., Angelopoulos, M., Boike, J., Groenke, B., Miesner, F., Nitzbon, J., Overduin, P., Stuenzi, S. M., and Langer, M. (2023). The CryoGrid community model (version 1.0) – a multi-physics toolbox for climate-driven simulations in the terrestrial cryosphere. *Geosci. Model Dev.*, 16, 2607–2647. <https://doi.org/10.5194/gmd-16-2607-2023>

Wendt, L., Rouyet, L., Christiansen, H. H., Lauknes, T. R., & Westermann, S. (2024). InSAR sensitivity to active layer ground ice content in Adventdalen, Svalbard. *EGU Sphere* [preprint], accepted. <https://doi.org/10.5194/egusphere-2024-2972>

Wieczorek, M., Lewkowicz, A.G., Kholodov, A.L., Romanovsky, V.E., Nicolsky, D., Strelets, D.A., Boike, J., Heim, B., Bartsch, A., Biskaborn, B.K., Christiansen, H.H., Elger, K. and Irrgang, A.M. (2025). GTN-P: 41 years of Mean Annual Ground Temperature (MAGT) across latitudinal and elevational gradients in the Northern Hemisphere. PANGAEA, <https://doi.pangaea.de/10.1594/PANGAEA.972992>

Widhalm, B., Bartsch, A., Strozzi, T., Jones, N., Khomutov, A., Babkina, E., Leibman, M., Khairullin, R., Göckede, M., Bergstedt, H., von Baeckmann, C., and Muri, X. (2025). InSAR-derived seasonal subsidence reflects spatial soil moisture patterns in Arctic lowland permafrost regions, *The Cryosphere*, 19, 1103–1133, <https://doi.org/10.5194/tc-19-1103-2025>

Wolter, J., Jones, B. M., Fuchs, M., Breen, A. L., Bussmann, I., Koch, B. P., Lenz, J., Myers-Smith, I. H., Sachs, T., Strauss, J., Nitze, I., & Grosse, G. (2024). Post-drainage vegetation, microtopography and organic matter in Arctic drained lake basins. *Environmental Research Letters*. <https://doi.org/10.1088/1748-9326/ad2eeb>

Yang, Y., Rogers, B. M., Fiske, G., Watts, J., Potter, S., Windholz, T., Mullen, A., Nitze, I., & Natali, S. M. (2023). Mapping retrogressive thaw slumps using deep neural networks. *Remote Sensing of Environment*, 288, 113495. <https://doi.org/10.1016/j.rse.2023.113495>

Zwieback, S., Liu, L., Rouyet, L., Short, N., & Strozzi, T. (2024). Advances in InSAR analysis of permafrost terrain. *Permafrost and Periglacial Processes*, 35(4), 544–556. <https://doi.org/10.1002/ppp.2248>

### In prep./Submitted/In review/In revision

Avirmed D., Bilguun T., Delaloye R., Echelard, T., Milceva, A., Rouyet L., Strozzi T., Westermann, S. Rock glacier inventory in Tsengel Khairkhan Massif, Western Mongolia. In prep.

Heidler, K., Nitze, I., Grosse, G., & Zhu, X. X. (2024). PixelDINO: Semi-Supervised Semantic Segmentation for Detecting Permafrost Disturbances (arXiv:2401.09271). arXiv. <http://arxiv.org/abs/2401.09271>

Nitze, I., Van Der Sluijs, J., Barth, S., Bernhard, P., Huang, L., Lara, M., Kizyakov, A., Runge, A., Veremeeva, A., Ward Jones, M., Witharana, C., Xia, Z., & Liljedahl, A. (2024). A labeling intercomparison of retrogressive thaw slumps by a diverse group of domain experts. <https://doi.org/10.31223/X55M4P> Strozzi, Tazio and Jones, Nina and Boike, Julia and Antonova, Sofia and Heim, Birgit and Leinss, Silvan and Wegmüller, Urs and Westermann, Sebastian and Kääb, Andreas and Grosse, Guido and Bartsch, Annett, Seasonal Vertical Surface Thaw Displacement in

2018 on Samoylov. Available at SSRN: <https://ssrn.com/abstract=5683711> or <http://dx.doi.org/10.2139/ssrn.5683711>

### Community guidelines and white papers

RGIK, 2023. [Puigcerdà Commitment](#). IPA Action Group Rock glacier inventories and kinematics. 4 pp. <https://www.rgik.org>.

RGIK. 2023. Guidelines for inventorying rock glaciers: baseline and practical concepts (version 1.0). IPA Action Group Rock glacier inventories and kinematics, 25 pp. <https://doi.org/10.51363/unifr.srr.2023.002>.

RGIK. 2022. Optional kinematic attribute in standardized rock glacier inventories (version 3.0.1). IPA Action Group Rock glacier inventories and kinematics, 8 pp. <https://www.rgik.org>.

RGIK. 2023. InSAR-based kinematic attribute in rock glacier inventories. Practical InSAR guidelines (version 4.0). IPA Action Group Rock glacier inventories and kinematics, 33 pp. <https://www.rgik.org>.

RGIK 2023. Rock Glacier Velocity as an associated parameter of ECV Permafrost: baseline concepts (version 3.2). IPA Action Group Rock glacier inventories and kinematics, 12 pp. <https://www.rgik.org>.

RGIK. 2023. Rock Glacier Velocity as an associated parameter of ECV Permafrost: practical concepts (version 1.2). IPA Action Group Rock glacier inventories and kinematics, 17 pp. <https://www.rgik.org>.

RGIK. 2023. Instructions of the RoGI exercises in the Goms and the Matter Valley (Switzerland). IPA Action Group Rock glacier inventories and kinematics, 10 pp. <https://www.rgik.org>.

### 5.2 News Stories

February 25 .2020 ESA – Picturing permafrost in the Arctic

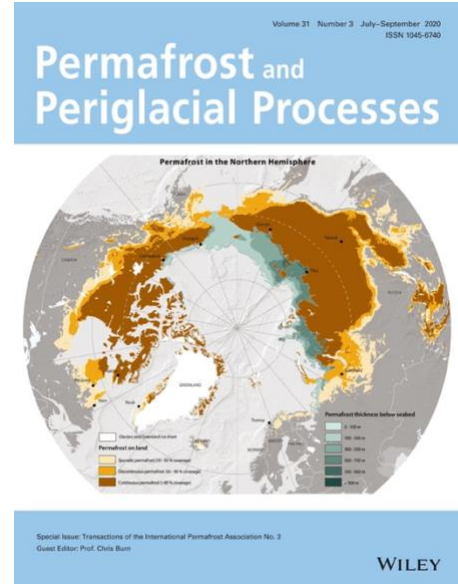
[http://www.esa.int/Applications/Observing\\_the\\_Earth/Space\\_for\\_our\\_climate/Picturing\\_permafrost\\_in\\_the\\_Arctic](http://www.esa.int/Applications/Observing_the_Earth/Space_for_our_climate/Picturing_permafrost_in_the_Arctic)

March 4, 2020. H2020 Nunataryuk

<https://nunataryuk.org/news/139-new-map-shows-extent-of-permafrost-in-northern-hemisphere>

Cover image of Permafrost and Periglacial Processes, volume 31, issue 3, July-September 2020, shows new permafrost map produced by UNEP Grid Arendal based on submarine permafrost map by Overduin et al. 2019 and land-based permafrost by Obu et al. 2019.

2022 IPA: Frozen Ground 43, the News Bulletin of the IPA,  
<https://www.permafrost.org/frozen-ground-newsletter/>



April 19, 2023: ESA - Permafrost Monitoring from Space – a review: Understanding the implications of thawing permafrost is expected to advance with enhanced data availability and products, <https://climate.esa.int/en/news-events/permafrost-monitoring-from-space-a-review>

12/12/2023: Permafrost thaw: a silent menace, ESA - European Space Agency, [https://www.esa.int/ESA\\_Multimedia/Videos/2023/12/Permafrost\\_thaw\\_a\\_silent\\_menace](https://www.esa.int/ESA_Multimedia/Videos/2023/12/Permafrost_thaw_a_silent_menace)

Stockton, E.J. and Burn, C.R. (eds.) 2024. Frozen Ground 47 (2023). International Permafrost Association (IPA). DOI: 10.52381/IPA.FG472023.1. Permafrost\_cci appears three times (third one on last page – the landcover poster in the picture).

Earth Online news, SAOCOM reveals how rock glaciers creep across the landscape, 30 September 2024, <https://earth.esa.int/eogateway/success-story/saocom-reveals-how-rock-glaciers-creep-across-the-landscape>.

New Arctic Land Cover Map Reveals Unprecedented Detail, <https://climate.esa.int/en/news-events>, published online 10 December 2024.

New Rock Glacier Velocity (RGV) Working Group kicks off!, <https://climate.esa.int/en/projects/permafrost/news-and-events/news/Rock-Glacier-Velocity-Working-Group-kicks-off>, published online 13 December 2024.

Most coastal Arctic infrastructure faces instability by 2100: <https://news.agu.org/press-release/most-arctic-infrastructure-faces-instability>.

ESA data records help underpin climate change report, 25/08/2025, [https://www.esa.int/Applications/Observing\\_the\\_Earth/Space\\_for\\_our\\_climate/ESA\\_data\\_records\\_help\\_underpin\\_climate\\_change\\_report](https://www.esa.int/Applications/Observing_the_Earth/Space_for_our_climate/ESA_data_records_help_underpin_climate_change_report).

### 5.3 User workshops

#### 1st Permafrost\_cci User Workshop

The first Permafrost\_cci user workshop took place on September 27<sup>th</sup> 2021. It was held online with 66 participants. The project status was presented first. The first block of user presentations comprised climate modelling topics. The project use case #1 (HIRHAM) was presented by Heidrun Matthes (section 3.2). Kazuyuki Saito (YAMSTEC) discussed issues regarding soil organic carbon and ground

ice dynamics in climate models. Eleanor Burke (Metoffice) showed a detailed assessment of permafrost\_cci records with respect to CMIP6 activities. Ground temperature trends are similar to past records. This block was followed by planned and ongoing activities which combine or compare to other satellite products. This included an ESA fellowship presentation (A. Runge, AWI), use case #2 (Ingmar Nitze, AWI; section 3.3) and status of RECCAP-2 (Gustaf Hugelius, University Stockholm). The last user presentation block referred to applications of the permafrost extent product of DUE GlobPermafrost. Eventually, challenges in production and validation have been presented by Permafrost\_cci team members. This covered lowland and mountain permafrost. The importance of validation in mountain areas and associated issues have been discussed. The need for documentation of how to work with the Polar Stereographic projection in GIS environment has been pointed out. In general, there was positive feedback regarding the availability as NetCDF. The final discussion specifically addressed climate modelling applications. The following requirements have been stated:

- Monthly timesteps
- High vertical resolution (also 20 and 50 cm)
- Recommendations for aggregation/resampling to modelling grids

## 1st Permafrost\_cci User Workshop of Phase 2

A series of workshops were organized during the 6th European Conference on Permafrost ([EUCOP 2023](#)) in Puigcerdà (Spain). The two tutorials of Sunday 18 June 2023 between 10 and 12 h and of Tuesday 20 June 2023 between 7.30 and 8.30 h focused on the access and use of the data generated in Phase 1 of the project, i.e. Ground Temperature, Active Layer Thickness and Permafrost Extent. The workshop of Saturday 17 June 2023 between 9 and 18 was organized by the IPA Action Group "Rock glacier inventories and kinematics" ([RGIK](#)) to discuss the background, current status, challenges and future needs of Rock glacier inventories (RoGI) and Rock glacier velocity (RGV).

A variety of options for Permafrost\_cci datasets has been presented in the CCI+ Permafrost tutorials – data access and use workshop. This included data download as well as visualisation tools. As most of the target audience had an interest in specific regions, subsetting and location specific information retrieval was demonstrated for preselected regions as well as sites proposed by the participants. The introduction to the project and datasets also included some first higher level products (time series for annual averages) foreseen as data distribution and graphics. The options have been discussed and recommendations collected during each of the two sessions. Workshop participants suggested the production of regional specific higher level datasets. In addition, public access to the tutorial has been requested. Both can be achieved within the first iteration of Phase 2 of Permafrost\_cci. However, a strategy for the distribution of the higher level datasets still needs to be developed.

The RGIK office organized the third workshop of the IPA Action Group as a side-event of EUCOP conference in Puigcerdà. The objectives were to gather the active members of the community, summarize the achievements of the IPA Action Group and outline the goal and the workplan for the coming years. Advertised to the entire network in Spring 2023 (209 people from 29 countries), the workshop gathered 35 people. The programme was divided in three parts: 1) a reminder and summary of the RGIK objectives, tasks and achievements (international guidelines, common tools and promotion of consistent rock glacier mapping and monitoring strategies); 2) group discussions regarding the challenges and knowledge gaps to generate standardized rock glacier inventories (RoGI) and rock glacier velocity (RGV) products; 3) discussion and decision regarding the future governance of the group. EUCOP6 marked the end of the support of the International Permafrost Association ([IPA](#)) to

RGIK as an Action Group after two periods lasting from June 2018 to June 2023. In the framework of the workshop a short document named the Puigcerdà Commitment was prepared to define the objectives of the RGIK community and lay the foundation for the transition of the Action Group to a sustainable structure as an IPA Standing Committee. The final version of the [Puigcerdà Commitment](#) has been approved by 60 people (status: July 23th, 2023). During the Council Meeting of the IPA on 21 June 2023, the request and the commitment of the RGIK Action Group were presented and discussed. The IPA Council unanimously approved the initiative, asking to be ready to transition to a Standing Committee within a year and to enlarge the scope of RGIK to rock glaciers in general. In addition to the continuation of the works done until present, the transition to a Standing Committee requires the nomination of an Executive Committee and an Advisory Board, as well as the development and approval of the by-laws, to be achieved before the next International Conference on Permafrost ([ICOP](#)) in June 2024.

## 2024 European Polar Science Week

3 - 6 September 2024 | The Black Diamond | Copenhagen, Denmark

Session Title: Space-borne studies of permafrost in the Arctic

Chairs: Tazio Strozzi and Annett Bartch

Date and Time: Thursday 5 September 2024 16:30 – 18:00

### Summary of session presentations and discussion

In the session we discussed the general requirements for ground temperature modelling and validation and presented various results obtained from space-borne studies of permafrost in the Arctic. Six presentations documented the rapid advances in permafrost studies from space, including modeling and in-situ observations.

### Major advances and highlights

- Improved accuracy of CCI permafrost products “Ground temperature” and “Active Layer Thickness”.
- “Rock glacier velocity” is a new product of ECV permafrost, rock glaciers predominantly accelerate with rise in air/ground temperature.
- Seasonal and multi-year Sentinel-1 subsidence have the potential to deterministically determine subsurface properties.
- Spatially and thematically detailed landcover information at full circumpolar extent provides advance for many permafrost related applications, including monitoring of thaw impacts and climate model development.
- Climate data records from satellites are potentially of high value for climate models focusing on polar issues, but the high product uncertainties in this region remain an open issue.

### Key messages and recommendations

- Permafrost temperatures are steadily increasing across the Arctic, but uncertainties in estimation need to be reduced.

- Cal/Val super-sites across all permafrost zones (continuous, discontinuous) dedicated to permafrost studies are needed.
- Resume Sentinel-1 IWS acquisitions over Siberia asap (6 days are better than 12 days).
- Consider Arctic permafrost areas as key regions in the planning of acquisitions of future missions (e.g. ROSE-L, NISAR, Harmony, ...).

## 2024 ITCH – It's The CryoGrid Hackathon

From Oct 21-25,2024, the 7th ITCH modeling workshop was held in Drøbak near Oslo, Norway. This year, topics related to remote sensing and possible applications within ESA-related projects were put in the foreground. Specifically, we conducted group work on using novel machine learning techniques to transfer the results of physically-based permafrost models in space which holds significant potential to speed up permafrost mapping, as well as to improve the spatial resolution of the resulting maps. The ITCH 2024 started with a two-day seminar held at Drøbak aquarium in which participants introduced themselves and their research interest, followed by presentations of newly funded projects using CryoGrid. In the final three days of the workshop, participants worked in groups “hackathon-style” on research topics of interest, putting practical advances of model codes and science applications in the foreground. In total 32, researchers (mainly in PostDoc/ PhD stage) from 13 institutions in 7 countries participated at the ITCH 2024 (see full participant list in the Appendix). The gender ratio of the participants was in balance (17 women, 15 men). The ITCH was organized by the University of Oslo at the premises of the biological station in Drøbak, Norway, located right on the shore of Oslofjord about 25 km from Oslo. The biological station consists of two buildings: first the research unit “Biologen” located in a historic bulding with adjacent private harbour and second the historic toll collecting station “Tollboden” which today houses laboratories for student education and a conference center. In total, the station provides accommodation for up to 24 participants at a modest price. At the same time, it is possible for participants to cook themselves, thus greatly reducing the cost of the stay and making it possible to attend for students on a small budget. As the number of registered participants at the ITCH exceeded the capacity of the meeting room at the station, a larger meeting room was rented at the facilities of the local aquarium for the first two days.

## Key messages and recommendations

- The ITCH has established itself as a meeting platform for the European permafrost modeling community. It is mainly driven by early-career researchers who have adopted the CryoGrid community model as a joint simulation tool for their research.
- The CryoGrid community model has become a well-used platform to merge and process a range of data sets for cryosphere applications, most notably remote sensing and reanalysis data. Methodology and model code developed in the ESA Permafrost\_cci project have strongly boosted the model's capabilities for spatially distributed processing which has already now attracted a growing user community with several newly funded projects.
- Development and maintenance of the CryoGrid community model is fully dependent on soft-money, such as ESA Permafrost\_cci. Maintenance and user support is almost entirely accomplished by researchers and students at the University of Oslo on project basis - there is no base funding (e.g. for technicians, programmers, data scientists) available that would ensure sustainable operations on a long-

term basis. Despite the current successes, this puts the CryoGrid community model and its user community in a volatile situation.

## 2nd User Workshop of the ESA CCI Permafrost Phase 2 Project

Virtual Meeting Wednesday 4 June 2025 09:00-12:00

Around 40 people registered and participated in the workshop.

After the welcome, the general context of the project and the data produced during Phases 1 and 2 (“Baseline” plus “Options”) were presented. Primary deliverables are so-called Climate Research Data Packages (CRDP, now Version 3), including Ground Temperature (GT), Active Layer Thickness (ALT) and permafrost extent. In addition, in-situ borehole temperature records were harmonized for calibration and validation. RGV has been integrated as a new associated quantity in 2022 and in Phase 2 we support the production of standardized Rock Glacier Inventories (RoGI) and we are making a significant contribution to develop RGV based on remote sensing, in particular InSAR. New circumarctic landcover units at 10 m resolution now supports the CryoGRID soil parameterization. Data and documentation are available on the project website and there are tools available for data visualization.

Three internal project presentations were held in the following, describing data generation with CryoGRID, the evaluation of the CryoGRID results, and rock glacier inventory generation and status. Three user presentations were then given in a first session describing different uses of permafrost CCI data, spanning all CryoGROD product types. They included support to snow modelling, satellite gravimetry compared to pan-Arctic ALT trends, and a study on changes in the composition of nitrogen yields in large Arctic rivers linked to permafrost extent. Four user presentations were subsequently held in a second session with a broader perspective. They included independent validation of active layer thaw depth, recommendations for improved regional characterization of rock glacier dynamics, a study on key risks from Arctic permafrost thaw for local communities, and high-altitude permafrost in the Dry Andes. In each of the two sessions, the possible uses of CCI\_data were discussed and recommendations collected.

It was emphasized that the uncertainties in the products need to be clearly communicated as they affect the interpretation, especially in the case of permafrost extent maps. Spatial and temporal variability must be taken into account during validation to ensure robustness. Higher resolution products are of great interest. However, the small-scale variability of groundwater, snowpack, stratigraphy and land use is difficult to document. The presence of peat soils is crucial, which is particularly problematic in forested areas. The need for coverage of the southern hemisphere has been expressed. The participants exchanged experiences with the use of the data.

## RGV workshops

- First RGV workshop, 20–22 November 2024, Fribourg, Switzerland.
- Upcoming: Second RGV workshop, 04–05 December 2025, Fribourg, Switzerland.
- Upcoming: Rock glacier student summer school, Italian Alps, September 2026.

## 5.4 Outreach activities

Option 6 results were presented as a *Webinar of the Permafrost Discovery Gateway*, 5th of October 2023: Bartsch, A. ‘The Arctic land north of the treeline at 10m’ <https://arcticdata.io/catalog/portals/permafrost/Stay-Connected> (recording published on youtube: <https://www.youtube.com/watch?v=xGGrLoUJlxk>)

The *Arctic Permafrost Atlas* from the Nunataryuk project, which contains permafrost\_cci output on several pages (e.g., 47 and 91), was released: [https://gridarendal-website-live.s3.amazonaws.com/production/documents/:s\\_document/1041/original/PermafrostAtlas\\_20oct\\_finaldraft.pdf?1697708753](https://gridarendal-website-live.s3.amazonaws.com/production/documents/:s_document/1041/original/PermafrostAtlas_20oct_finaldraft.pdf?1697708753)

Permafrost\_cci results were presented at the 13th *CCI colocation and CMUG Integration meetings*, which took place between November 7 and 9, 2023 at the ESA ECSAT conference centre in Harwell (Oxfordshire, UK).

A presentation on “The potential and limitations of remote sensing for the ECV Permafrost” was held at the *ISSI Workshop on Remote Sensing in Climatology – ECVs and their Uncertainties*, 13-17 November 2023.

A presentation on “Satellite data use for permafrost related monitoring in ESA and H2020 projects” was held at the *EC-ESA Joint Earth System Science Initiative*, 22-24 November 2023.

The project status has been further presented at

- as part of an invited talk at the Canadian Permafrost Day on the 1st of March 2023 (Bartsch et al.)
- as part of an invited talk at Arctic International Technical Conference (AITC 2023) Mapping the Arctic in Nuuk (Greenland), April 24-27 2023 (Strozzi et al.).
- the IPA Austria workshop on 28th of September 2023 (Mallnitz, Austria). (Bartsch et al.)

A presentation on “Tracking permafrost landscape dynamics in a rapidly warming Arctic” was held by Ingmar Nitze in the AI for Good webinar series. 28 February 2024.

Session at the 2024 European Polar Science Week, 3 - 6 September 2024, Copenhagen, Denmark. Title: Space-borne studies of permafrost in the Arctic; Chairs: Tazio Strozzi and Annett Bartsch; Date and Time: Thursday 5 September 2024 16:30 – 18:00.

Annett Bartsch, Magnitude of changes in the last two decades and future perspectives for monitoring methane from space, COP29 Baku, Cryosphere Pavilion, Permafrost day 18<sup>th</sup> of November 2024.

Tazio Strozzi, Rock glacier inventories and kinematics: merging scientific insights with industrial perspectives, Schweizerische Gesellschaft für Schnee, Eis und Permafrost, Vortragsabend (virtuell auf ZOOM) am 27.11.2024, “Kryosphären Aktivitäten in der Privatwirtschaft”.

*ESA Living Planet Symposium 2025, 23—27 June 2025, Vienna, Austria*

- ORAL Session A.09.06 Advances in Permafrost, Thursday morning 26.06.2025 in Room 1.85/1.86.

- POSTERS Session A.09.06 Advances in Permafrost in Room, Thursday 26.06.2025 5:45 pm to 7 pm.
- Tuesday 24th 9:30-10:00 Hall X4, Educational program -Expert:innen Talks ("Meet an Austrian EO Expert"); presentation of Permafrost and Arctic topic (in German, for school kids); Chiara Gruber, b.geos GmbH.
- Project presentation at ESA Climate initiative booth:
  - Tuesday 24th afternoon break – NH CRDP (A. Bartsch, b.geos);
  - Wednesday 25th afternoon break –rock glacier inventories (Line Rouyet, NORCE).
- Panel discussion contribution (A. Bartsch, b.geos): A.05.10 The ESA-NASA Arctic Methane Permafrost Challenge (AMPAC) community past and future review. Room 1.61/1.62, 14:00, 26.06.2025

The time series for Central Asian rock glaciers, compiled within Permafrost\_CCI, are shown and discussed in Blunden, J. and J. Reagan, Eds., 2025: "State of the Climate in 2024". Bull. Amer. Meteor. Soc., 106 (8), Si–S513 <https://doi.org/10.1175/2025BAMSStateoftheClimate.1>.

Presentations of CCI Permafrost Activities were held by Annett Bartsch, Sebastian Westermann and Line Rouyet at a workshop on Svalbard Terrestrial Cryosphere and Remote Sensing, after the Svalbard Science Conference (SSC) in Oslo (30-31 October 2025).

Rock glaciers:

- EGU RGIK splitter meeting (SPM66), 15 April 2024. Approx. 25 attendees.
- ICOP RGIK side meeting, 17 June 2024, Whitehorse, Canada.

## 5.5 Presentations at scientific conferences (Phase II)

### *6<sup>th</sup> European Conference on Permafrost (EUCOP), 18–22 June 2023, Puigcerdà, Spain*

A. Bartsch, T. Strozzi, I. Nitze. Permafrost Monitoring from Space – What Have We Learned So Far?

H. Bergstedt, A. L. Breen, B. M. Jones, L. Farquharson, J. Wolter, G. Grosse, A. Bartsch, M. Kanevskiy, C. von Baeckmann, T. Kumpula, A. Veremeeva, G. Hugelius, K. Ermokhina. Drained Lake Basins on a Panarctic Scale.

F. Brardinoni, A. Bertone, N. Jones, V. Mair, R. Scotti, T. Strozzi. A Rock Glacier Inventory Integrating Geomorphological Mapping and Sentinel-1 Satellite SAR Interferometry in Western South Tyrol, Italy.

T. Echelard, S. V. Andrade, L. Rouyet, C. Pellet, R. Delaloye, C. Barboux. Towards Practical Guidelines for Rock Glaciers Inventories (RoGI): A New 'User-friendly' GIS Tool for Training the Community.

A. Efimova, A. Bartsch, B. Widhalm, X. Muri, G. Hugelius, C. von Baeckmann. The Potential of High Resolution Landcover Classification as Proxy for Soil Properties.

K. Heidler, I. Nitze, G. Grosse, X. X. Zhu. Scaling Strategies for AI in Permafrost Remote Sensing.

B. Heim, M. Wieczorek, A. Irrgang, S. Lisovski, H. Matthes, G. Grosse, A. Haas, K. Elger, S. Westermann, C. Barboux, C. Pellet, R. Delaloye, F. M. Seifert, T. Strozzi, A. Bartsch. ESA CCI+ Permafrost - Validation Using International and National Permafrost Monitoring Networks.

A. Höhl, K. Heidler, A. Runge, G. Grosse, X. X. Zhu. Identifying and Interpreting Permafrost Vulnerability with Machine Learning.

Y. Hu, L. U. Arenson, C. Barboux, X. Bodin, A. Cicoira, R. Delaloye, I. Gärtner-Roer, A. Kääb, A. Kellerer-Pirklbauer, C. Lambiel, L. Liu, C. Pellet, L. Rouyet, P. Schoeneich, G. Seier, T. Strozzi. Rock Glacier Velocity as a New Product of the Essential Climate Variable Permafrost.

N. Jones, T. Strozzi, R. Caduff, F. Brardinoni, A. Bertone, L. Rouyet, L. Schmid, R. Delaloye. Rock Glacier Velocity in the Italian and Swiss Alps from Sentinel-1 Satellite SAR Interferometry.

T. Lübker, I. Nitze, S. Laboor, A. Irrgang, H. Lantuit, G. Grosse. A Web-based Portal for Serving Geospatial Information on Permafrost Disturbances to Permafrost Communities.

I. Nitze, M. J. Lara, G. Grosse. Continental-scale Drivers of Lake Drainage in Permafrost Regions.

A. Runge, A. Bartsch, A. Höhl, K. Heidler, B. Juhls, S. Westermann, G. Grosse. Identifying Linkages between EO-based Surface Variables and Permafrost Temperature Changes.

T. Strozzi, N. Jones, S. Westermann, A. Kääb, J. Boike, S. Antonova, A. Veremeeva, G. Grosse, A. Bartsch. Surface Deformation Monitoring of the Lena River Delta with Sentinel-1 SAR Interferometry.

A. Veremeeva, F. Guenther, T. Strozzi, A. Kizyakov, I. Nitze, C. Inauen, A. Morgenstern, N. Jones, M. Kanevskiy, A. Pismeniuk, M. Zimin, E. Rivkina, G. Grosse. Yedoma-alas Landscape Elevation Changes and Their Drivers Based on Sentinel-1 SAR Interferometry, Field Data, and High-resolution Optical Imagery, Bykovsky Peninsula, Laptev Sea Region.

A. Veremeeva, A. Morgenstern, S. Antonova, J. Boike, N. Bornemann, A. Cherepanova, M. Fuchs, M. Grigoriev, F. Guenther, A. Kizyakov, S. Laboor, F. Miesner, J. Nitzbon, E. Rivkina, A. Runge, L. Schirrmeister, U. Mathias, G. Grosse. Lena Delta Active Layer Thickness Database.

C. von Baeckmann, H. Bergstedt, A. Bartsch, B. Widhalm, A. Efimova, T. Kumpula, D. Ehrich, S. Abdulmanova, A. Sokolov. Land Cover Patterns for Drained Lake Basins across Bioclimatic Gradients.

S. Westermann, T. Ingeman-Nielsen, K. Aalstad, J. Aga, R. Zweigel, C. Willmes, L. Schmidt, B. Etzelmüller, A. Kääb, T. V. Schuler, C. Renette, L. Martin, S. Morard, M. Ben-Asher, J. Baptista, A. Bartsch, T. Strozzi, J. Boike, F. Miesner, J. Nitzbon, P. Overduin, S. Stuenzi, M. Langer. The CryoGrid Community Model - A Multi-physics Toolbox for Climate-driven Simulations in the Terrestrial Cryosphere.

B. Widhalm, A. Bartsch, T. Strozzi, N. Jones, M. Goeckede, M. Leibman, A. Khomutov, E. Babkina, E. Babkin. InSAR Application for Surface Displacement Investigations in Arctic Permafrost Regions: A Comparison of Mitigation Methods for Interfering Atmospheric Effects.

*Cryosphere 2022 International Symposium on Ice, Snow and Water in a Warming World, 21–26 August 2022, Reykjavík, Iceland*

Rouyet, L., Lauknes, T.R., Lilleøren, K.S., Etzelmüller, B., Kääb, A.M., Christiansen, H.H., Humlum, O., Delaloye, R., Strozzi, T., Bertone, A. 2022. SAR satellite remote sensing for mapping and monitoring Norwegian rock glaciers.

*American Geophysical Union (AGU) Fall Meeting 2023, 11-15 December 2023, San Francisco, USA*

Bartsch, Annett, Gustaf Hugelius, Barbara Widhalm, Aleksandra Efimova, Helena Bergstedt, Guido Grosse, Joshua Hashemi, Claire C Treat, Mathias Goeckede, Johanna Tamminen, Andreas Fix, Torsten Sachs, Sander Houweling, Dirk Schuettemeyer and AMPAC-Net Team. A51X-2297 Tackling Arctic landcover monitoring supporting The Arctic Methane and Permafrost Challenge (AMPAC) Network.

*EGU 2024 General Assembly, Vienna, Austria & Online, 14–19 April 2024*

EGU24-8327, “Multi-annual Rock Glacier Velocity (RGV) products based on InSAR” by Lea Schmid et al., Posters on site in session GM10.5 - Interaction between climate, rock glaciers, and proglacial processes across scales.

EGU24-15688, “Assessment of the Topographic Wetness Index in Permafrost landscapes” by Barbara Widhalm et al., Posters on site in session CR4.2 - Permafrost dynamics, interactions, feedbacks, disturbances and GHG's across scales: perspectives from observation to modelling.

EGU24-16785, “Status of the Circumpolar Landcover Unit database” by Rustam Khairullin et al., Posters on site in session CR4.2 - Permafrost dynamics, interactions, feedbacks, disturbances and GHG's across scales: perspectives from observation to modelling.

EGU24-14843, “Remote sensing supporting the Arctic Methane and Permafrost Challenge (AMPAC)” by Bartsch et al., Solicited presentation in US3 Bridging the scales: The Arctic methane and permafrost challenge

*International Conference on Permafrost (ICOP), 16-20 June 2024, Whitehorse, Yukon, Canada*

I. Nitze, K. Heidler, K. Maier, S. Barth, A. Liljedahl, & G. Grosse. Using Deep Learning to Advance Global Monitoring of Retrogressive Thaw Slumps at High Spatio-Temporal Resolution.

K. Maier, P. Bernhard, I. Nitze, & I. Hajnsek. Automatic Segmentation Strategies for DEM-based RTS Monitoring.

C. Inauen, G. Grosse, M. Langer, I. Nitze, S. Barth, M. Baysinger, C. Hanna, T. Luebker, T. Rettelbach, A. Runge, & I. Hajnsek. Studying Drivers of Thermo-erosional Gully Development Based on In-situ Measurements, Remote Sensing Data, and Modeling.

K. Keskitalo, N. Speetjens, P. P. Overduin, S. Westermann, F. Miesner, T. Sachs, I. Nitze, L. Bröder, J. Lattaud, N. Haghipour, T. Eglinton, & J. Vonk. Landscape Characteristics and Particulate Organic Carbon Composition in the Peel River Watershed, Canada.

P. P. Overduin, B. Juhls, K. Keskitalo, I. Nitze, F. Miesner, N. Speetjens, J. Vonk, & S. Westermann. Hydrology of the Peel River, Yukon, Canada during the Extremely Dry Summer of 2019.

A. Bartsch, C. von Baeckmann, H. Bergstedt, B. Widhalm, B. Heim, M. Wieszorek, V. Döpper. 10m Resolution Circumpolar Landcover as Proxy for Permafrost Features.

F. Brardinoni, A. Bertone, V. Mair, N. Jones, T. Strozzi. Integrating Sentinel-1 and Cosmo-SkyMed InSAR-based Information for an Improved Regional Assessment of Rock Glacier Dynamics.

I. Gärtner-Roer, A. Kneib-Walter, A. Vieli, A. Cicoira, J. Beutel, T. Strozzi. Rockglacier Dynamics on Disko Island, Western Greenland.

C. Pellet, R. Delaloye, I. Gärtner-Roer, C. Lambiel, J. Noetzli, M. Phillips, C. Scapozza. On the Influence of Ground Surface Temperature on Rock Glacier Velocity.

L. Rouyet, R. Delaloye, T. Bolch, F. Brardinoni, R. Caduff, D. Cusicanqui, M. Darrow, T. Echelard, C. Lambiel, L. Ruiz, F. Sirbu, T. Strozzi. Multi-operator Mapping Exercise for Consensus-based Generation of Rock Glacier Inventories (RoGI) in 12 Areas Worldwide.

L. Schmid, L. Rouyet, R. Delaloye, C. Pellet, N. Jones, T. Strozzi. Multiannual Rock Glacier Velocity (RGV) Products Based on InSAR.

L. Wendt, L. Rouyet, H. H. Christiansen, S. Westermann. Evaluating InSAR Sensitivity to In-situ Ground Ice Contents Across Different Landforms.

S. Westermann, C. Willmes, L. Wendt, K. Aalstad, J. Aga, R. Zweigel, J. Røste, L. Rouyet, F. Miesner, B. Heim, M. Wieczorek, A. Kääb, B. Etzelmüller, T. Strozzi, A. Bartsch. Global-scale Mapping of Permafrost in a Changing Climate.

C. Willmes, S. Westermann, K. Aalstad. Improving Simulations of the Local Ground Thermal Regime by Data Assimilation of Sentinel-2-retrieved Fractional Snow-Covered Area.

*IGARSS 2024, 7 - 12 July, 2024, Athens, Greece*

A. Bartsch, R. Tanguy, H. Bergstedt, X. Muri, Similarities in northern hemisphere permafrost ground temperature and sea ice extent change from 1997 to 2019.

*2024 European Polar Science Week, 3–6 September 2024, Copenhagen, Denmark*

Frederieke Miesner (Alfred Wegener Institute & University of Oslo), The CryoGrid community model and Permafrost\_CCI results.

Birgit Heim (Alfred Wegener Institute), Validation of Permafrost\_cci ground temperature and active layer time series using international and national permafrost monitoring networks.

Line Rouyet (NORCE Norwegian Research Centre), New ECV parameter Rock Glacier Velocity (RGV).

Annett Bartsch (B.GEOS), Landcover characterization for permafrost methane flux studies contributing to AMPAC.

Annett Bartsch (B.GEOS) for Philipp de Vrese (Max-Planck-Institut für Meteorologie), Land-surface modeling of Arctic permafrost regions - use of satellite observations in the ERC Synergy project Q-Arctic.

*American Geophysical Union (AGU) Fall Meeting 2024, 9-13 December, Washington D.C., USA*

A. Bartsch et al.: Landcover fusion for Arctic studies. AGU Fall Meeting, 10.12.2024.

A. Bartsch et al.: Advances in Processing of Synthetic Aperture Radar Data at C-Band for Benchmarking Passive Microwave Derived Surface State. AGU Fall Meeting, 12.12.2024.

*EGU General Assembly 2025, Vienna, Austria & Online, 27 April–2 May 2025*

Vivero, S., Pellet, C., Rouyet, L., Bernhard, P., Buchelt, S., Cusicanqui, D., Delaloye, R., Duvanel, T., Hartl, L., Hu, Y., Khan, M. A. R., Lambiel, C., Li, M., Schmid, L., Seier, G., Strozzi, T., Sun, Z., and Wendt, L.: Steps towards consistent production of Rock Glacier Velocity (RGV): comparison and

assessment of challenges from three technical approaches, EGU General Assembly 2025, Vienna, Austria, 27 Apr–2 May 2025, EGU25-15701, <https://doi.org/10.5194/egusphere-egu25-15701>, 2025

Dupuis, S., Metzger, N., Westermann, S., Schindler, K., Götsche, F.-M., and Wunderle, S.: Benefits of downscaled satellite-derived land surface temperature for permafrost modelling in the northern high latitudes, EGU General Assembly 2025, Vienna, Austria, 27 Apr–2 May 2025, EGU25-5216, <https://doi.org/10.5194/egusphere-egu25-5216>, 2025

Khairullin, R., Widhalm, B., Gruber, C., von Baeckmann, C., Radha Krishnan, S. R., Bartsch, A., and Khomutov, A.: Permafrost feature and wetness gradient monitoring in Northern Western Siberia, EGU General Assembly 2025, Vienna, Austria, 27 Apr–2 May 2025, EGU25-16275, <https://doi.org/10.5194/egusphere-egu25-16275>, 2025.

Lübker, T., Nitze, I., Laboor, S., Irrgang, A., Lantuit, H., and Grosse, G.: Communicating remotely sensed pan-arctic permafrost land surface changes to non-specialist audiences with the Arctic Landscape EXplorer (ALEX), EGU General Assembly 2025, Vienna, Austria, 27 Apr–2 May 2025, EGU25-18409, <https://doi.org/10.5194/egusphere-egu25-18409>, 2025.

Bergstedt, H., Bartsch, A., von Baeckmann, C., Jones, B. M., Breen, A., Wolter, J., Farquharson, L., Grosse, G., and Kanevskiy, M.: Regional differences in drained lake basindistribution and surface characteristics across the Arctic , EGU General Assembly 2025, Vienna, Austria, 27 Apr–2 May 2025, EGU25-15630, <https://doi.org/10.5194/egusphere-egu25-15630>, 2025.

*ESA Living Planet Symposium 2025, 23–27 June 2025, Vienna, Austria*

Annett Bartsch, Tazio Strozzi and Ingmar Nitze, Permafrost monitoring from space – what have we learned so far? A.09.06 Advances in Permafrost.

Bartsch A., Widhalm B., Irrgang A., Tanguy R., Vieira G., Nitze I., Heim B., Wieczorek M., Khairullin R.: Multi-hazard risk assessment for Arctic coastal environments. B.04.02 Addressing multi-hazards: Compounding and Cascading Events through Earth Observation.

Buchelt, S., Bernhard, P., Hu, Y., Li, M., Rouyet, L., Strozzi, T., Sun, Z. and Wendt L. (2025). Monitoring the Essential Climate Variable (ECV) Quantity Rock Glacier Velocity (RGV) Using InSAR: Steps Towards a Standardized and Consistent Approach. Oral presentation. ESA Living Planet Symposium, Vienna, Austria.

Antonie Haas, Birgit Heim, Annet Bartsch, Andreas Walter, Mareike Wieczoreck, Guido Grosse, Tazio Strozzi, Sebastian Westermann, Frank Martin Seifert, ESA CCI Permafrost time series maps as Essential Climate Variable (ECV) products primarily derived from satellite measurements, A.09.06 Advances in Permafrost.

Birgit Heim, Mareike Wieczoreck, Anna Irrgang, Cécile Pellet, Reynald Delaloye, Guido Grosse, Antonie Haas, Kirsten Elger, Sebastian Westermann, Line Rouyet, Frank Martin Seifert, Tazio Strozzi, Annet Bartsch: ESA CCI+ Permafrost - Validation using international and national permafrost monitoring networks, A.09.06 Advances in Permafrost.

Frederike Miesner, Simone M. Stünzi, Sebastian Westermann, Annett Bartsch: Representation of canopy effects in global-scale monitoring of permafrost.

I. Nitze, K. Hardie, C. Wang, T. Nicholson, L. Marini, B. M. Jones, M. Ward Jones, M. B. Jones, W. Li, A. Liljedahl, and G. Grosse, Near Real-Time Tracking of Lake Drainage in Arctic Permafrost Regions.

Ingo Sasgen, Grit Steinhöfel, Caroline Kasprzyk, Heidrun Matthes, Sebastian Westermann, Julia Boike, Guido Grosse: Permafrost and glacier observations in response to atmosphere circulation in the Arctic, A.09.06 Advances in Permafrost.

Lotte Wendt, Line Rouyet, Marie Bredal, Hanne H. Christiansen, Andrew Hodson, Anatoly Sinitsyn, Heidi Hindberg, Tom Rune Lauknes, Sebastian Westermann: Interannual InSAR subsidence and heave patterns in the permafrost landscape of Svalbard, A.09.06 Advances in Permafrost.

*IAG Regional Conference on Geomorphology 2025, 16-18 September 2025, Timișoara, Romania*

Annett Bartsch, Barbara Widhalm, Clemens von Baeckmann, Rustam Khairullin, Helena Bergstedt, Sree Radha Krishnan: Changing permafrost features on Yamal as seen from space.

Pellet, C., Delaloye, R., Gärtner-Roer, I., Hu, Y., Lambiel., C., Noetzli, J., Philips, M. and Scapozza, C. (2025). On the influence of ground surface temperature on rock glacier velocity. Oral presentation. IAG Regional Conference on Geomorphology, Timisoara, Romania.

Strozzi, T., Buchelt, S., Bernhard, P., Hu, Y., Li, M., Rouyet, L., Sun, Z., and Wendt, L. (2025). Monitoring Rock Glacier Velocity (RGV) using satellite SAR. Oral presentation. IAG Regional Conference on Geomorphology, Timisoara, Romania.

Tara Tripura Mantha, Sheikh Nawaz Ali, Pratima Pandey, Thomas Echelard, Volkmar Mair, Philipp Bernhard, Tazio Strozzi, Francesco Brardinoni, Building a rock glacier inventory of the Baralacha La area, Western Himalaya, India.

Brardinoni, F, Strozzi, T, Vivero, S, Conforto G, Peri, I, Scotti, R, Beyond destabilization: rapid disintegration of an active rock glacier through mass wasting and headward channel incision, Livigno, Italy.

Flavius Sîrbu, Valentin Poncos, Alexandru Onaca, Tazio Strozzi, Emil Gatchev, Cristian Ardelean, A new rockglacier inventory, based on PSI derived moving areas, in the Pirin Mountains.

## 5.6 Specific tasks

### Session chairing

Sîrbu, F., Strozzi, T., Berzescu, O. (conveners). Remote sensing and modelling of permafrost and periglacial landforms. IAG Regional Conference on Geomorphology, 16–18 September 2025, Timisoara, Romania.

Strozzi, T: Space-borne studies of permafrost in the Arctic , 2024 European Polar Science Week, 3–6 September 2024, Copenhagen, Denmark.

Helena Bergstedt, In-Won Kim, Martijn Pallandt, Louise Farquharson, David Wårldin, Annett Bartsch, Rebecca Scholten: Permafrost dynamics, interactions, feedbacks, disturbances and GHG's across scales: perspectives from observation to modelling. EGU General Assembly 2024, 14–19 April 2024, Vienna, Austria,

Garten-Roer, I., Kelkar, K., Brardinoni, F. (conveners). Open session on Rock glaciers. 12<sup>th</sup> International Conference on Permafrost (ICOP), 16–20 June 2024, Whitehorse, Canada.

Pellet, C., Vivero, S., Cusicanqui, D., Hartl, L. Kellerer-Priklbauer, A. (conveners). New insights into the dynamics of rock glaciers. EGU General Assembly 2024, 14–19 April 2024, Vienna, Austria,

Pellet, C., Rouyet, L., Hu, Y. (conveners). Open session on Rock glaciers. 6<sup>th</sup> European Conference on Permafrost (EUCOP), 18–22 June 2023, Puigcerdà, Spain.

### **Projects in synergy with the Permafrost\_cci rock glacier component**

Full-scale rock glacier inventory of Switzerland in ongoing, through the work package 1 of the **RoDynAlpS** project “Rock glacier dynamics at multiple spatio-temporal scales in Switzerland” (2023–2027), funded by the Swiss National Foundation (SNF). The ongoing work is using the GIS tools and approaches developed in the framework of RGIK and Permafrost\_cci.

The development of the database to store and disseminate RoGI and RGV products is supported by the **ORoDaPT** project “Open Rock Glacier Data Production Tools” (2024), funded SwissUniversities. ORoDaPT aims to develop tools to collect, process and analyse RoGI and RGV data, and design and implement a data management system. The project contributes to provide sustainable solutions for the dissemination and user exploitation of Permafrost\_cci products.

RoGI and RGV product generation in the Italian Alps is supported by the **PARACELSO** project “Predictive Analysis, monitoRing, and mAnagement of Climate change Effects Leveraging Satellite Observations” (2024–2026), funded by the Italian Space Agency. WP4 deals with rock glaciers in Valle d'Aosta region (Western Italian Alps). Task 4.1: Region-wide InSAR-based kinematic characterization of rock glaciers (S1, CSK and SAOCOM). Task 4.2: InSAR-based RGV time series for a selected cluster of rock glaciers that may pose risk to infrastructure.

### **5.7 Student teaching and courses**

MSc thesis from Lea Schmid (February 2024) “InSAR multi-annual velocity products on selected rock glaciers in the Swiss Alps”, University of Fribourg (UNIFR), Switzerland. Supervisors: Prof. Reynald Delaloye, Dr. Line Rouyet.

BSc practical course in Geomorphology (spring semester 2023), University of Fribourg (UNIFR), Switzerland. Teachers: Prof. Reynald Delaloye and Dr. Thomas Echelard. Project conducted with students on testing the RoGI GIS tools and approaches developed in the framework of RGIK and Permafrost\_cci in selected areas over the Swiss Alps.

Graduate GIS course (autumn semester 2023), University of Bologna (UniBo). Teacher: Ass.Prof. Francesco Brardinoni. Practical component on applying RoGI guidelines developed in the framework of RGIK and Permafrost\_cci focusing on study areas in the Italian Alps.

One-day lecture and practical exercise on Remote Sensing of Permafrost Regions, as part of the MSc/PhD AG-330/830 course on Permafrost and Periglacial Environments (spring semester 2024),

University Centre in Svalbard (UNIS). Teacher: Dr. Line Rouyet. Theory and use of InSAR in Svalbard, incl. applications on rock glaciers, as developed in Permafrost\_cci.

Remote Sensing of Permafrost Regions, MSc Module taught by G. Grosse & I. Nitze at University of Potsdam (4 hrs/week; SS 2019, WS 2019/2020, WS 2020/2021, WS 2021/2022, WS 2022/23, WS 2023/24)

HEIBRiDS Seminar Series. I.Nitze: Machine-learning for mapping permafrost landscape dynamics.  
<https://www.heibrids.berlin/>

Potsdam Summer School 2021. I.Nitze: Wetting vs. Drying of Arctic Permafrost landscapes.  
<https://potsdam-summer-school.org/>

## 6 References

### 6.1 Bibliography

Bartsch, A., Höfler, A., Kroisleitner, C., Trofaier, A.M. (2016). Land Cover Mapping in Northern High Latitude Permafrost Regions with Satellite Data: Achievements and Remaining Challenges. *Remote Sens.*, 8, 979.

Bartsch A., Ley S., Nitze I., Pointner G. and Vieira G. (2020). Feasibility Study for the Application of Synthetic Aperture Radar for Coastal Erosion Rate Quantification Across the Arctic. *Front. Environ. Sci.* 8:143. <https://10.3389/fenvs.2020.00143>

Biskaborn, B.K., Lanckman, J.-P., Lantuit, H., Elger, K., Streletschi, D.A., Cable, W.L. and Romanovsky, V.E. (2015). The new database of the Global Terrestrial Network for Permafrost (GTN-P). *Earth System Science Data*, 7(2), 245–259. <https://doi.org/10.5194/essd-7-245-2015>

Biskaborn, B.K., Smith, S.L., Noetzli, J., Matthes, H., Vieira, G., Streletschi, D.A., Schoeneich, P., Romanovsky, V.E., Lewkowicz, A.G., Abramov, A. and Allard, M. (2019). Permafrost is warming at a global scale. *Nature Communications*, 10(1), 264.

Bertone, A., Barboux, C., Bodin, X., Bolch, T., Brardinoni, F., Caduff, R., Christiansen, H. H., Darrow, M., Delaloye, R., Etzelmüller, B., Humlum, O., Lambiel, C., Lilleøren, K. S., Mair, V., Pellegrinon, G., Rouyet, L., Ruiz, L., and Strozzi, T. 2022. Incorporating InSAR kinematics into rock glacier inventories: insights from 11 regions worldwide, *The Cryosphere*, 16, 2769–2792. <https://doi.org/10.5194/tc-16-2769-2022>.

Brown R.J.E. (1970) Permafrost in Canada: Its influence on northern development. University of Toronto Press, Toronto 234 p.

Cable, W.L., Romanovsky, V.E. and Jorgenson, M.T. (2016). Scaling-up permafrost thermal measurements in western Alaska using an ecotype approach. *Cryosphere*, 10, 2517–2532.

Chadburn, S., Burke, E., Cox, P., Friedlingstein, P., Hugelius, G. and Westermann, S. (2017a). An observation-based constraint on permafrost loss as a function of global warming, *Nature Climate Change*, doi:10.1038/nclimate3262.

Chadburn, S.E., Krinner, G., Porada, P., Bartsch, A., Beer, C., Belelli Marchesini, L., Boike, J., Ekici, A., Elberling, B., Friberg, T., Hugelius, G., Johansson, M., Kuhry, P., Kutzbach, L., Langer, M., Lund, M., Parmentier, F.-J.W., Peng, S., Van Huissteden, K., Wang, T., Westermann, S., Zhu, D., and Burke, E.J. (2017b). Carbon stocks and fluxes in the high latitudes: using site-level data to evaluate Earth system models, *Biogeosciences*, 14, 5143–5169. <https://doi.org/10.5194/bg-14-5143-2017>.

Christensen, O.B., Drews, M., Christensen, J.H., Dethloff, K., Ketelsen, K., Hebestadt, I. and Rinke, A. (2007), The HIRHAM regional climate model, version 5, Tech. Rep. 06-17, Dan. Meteorol. Inst., Copenhagen, <http://www.dmi.dk/dmi/tr06-17.pdf>.

Delhasse, A., Hanna, E., Kittel, C., & Fettweis, X. (2020). Brief communication: CMIP6 does not suggest any circulation change over Greenland in summer by 2100. *The Cryosphere Discussions*, 2020, 1–8.

Dutch, V. R., Rutter, N., Wake, L., Sandells, M., Derksen, C., Walker, B., ... & Boike, J. (2022). Impact of measured and simulated tundra snowpack properties on heat transfer. *The Cryosphere*, 16(10), 4201–4222.

Flechtner, F., Morton, P., Watkins, M., & Webb, F. (2014). Status of the GRACE Follow-On mission. In *Gravity, Geoid and Height Systems* (Vol. 141, pp. 117–121). Springer International Publishing, Cham.

Gisnås, K., Westermann, S., Schuler, T.V., Litherland, T., Isaksen, K., Boike, J., and Etzelmüller, B. (2014). A statistical approach to represent small-scale variability of permafrost temperatures due to snow cover. *The Cryosphere*, 8, 2063–2074. <https://doi.org/10.5194/tc-8-2063-2014>

Grosse G., Robinson J.E., Bryant R., Taylor M.D., Harper W., DeMasi A., Kyker-Snowman E., Veremeeva A., Schirrmeyer L. and Harden J. (2013). Distribution of late Pleistocene ice-rich syngenetic permafrost of the Yedoma Suite in east and central Siberia, Russia. U.S. Geological Survey Open File Report 2013-1078, 37p.

Hanna, E., Cropper, T. E., Hall, R. J., & Cappelen, J. (2016). Greenland Blocking Index 1851–2015: A regional climate change signal. *International Journal of Climatology*, 36, 4847–4861.

Heginbottom, J.A. (1984). The mapping of permafrost. *Canadian Geographer*, Vol. 28, No.1, pp. 78-83.

Heginbottom, J.A., Radburn, L.K. (1992). Permafrost and Ground Ice Conditions of Northwestern Canada (Mackenzie Region). National Snow and Ice Data Center, Boulder, CO, USA.

IPCC (2013). Climate Change 2013: The Physical Science Basis. Contribution of Working Group I to the Fifth Assessment Report of the Intergovernmental Panel on Climate Change [Stocker, T.F., D. Qin, G.-K. Plattner, M. Tignor, S.K. Allen, J. Boschung, A. Nauels, Y. Xia, V. Bex and P.M. Midgley (eds.)]. Cambridge University Press, Cambridge, United Kingdom and New York, NY, USA, 1535 pp.

IPCC (2019). IPCC Special Report on the Ocean and Cryosphere in a Changing Climate (SROCC).

IPCC (2021). Climate Change 2021: The Physical Science Basis. Contribution of Working Group I to the Sixth Assessment Report of the Intergovernmental Panel on Climate Change [Masson-Delmotte, V., P. Zhai, A. Pirani, S.L. Connors, C. Péan, S. Berger, N. Caud, Y. Chen, L. Goldfarb, M.I. Gomis, M. Huang, K. Leitzell, E. Lonnoy, J.B.R. Matthews, T.K. Maycock, T. Waterfield, O. Yelekçi, R. Yu, and B. Zhou (eds.)]. Cambridge University Press.

Jones, B.M., Kolden, C.A., Jandt, R., Abatzoglou, J.T., Urban, F., & Arp, C.D. (2009). Fire Behavior, Weather, and Burn Severity of the 2007 Anaktuvuk River Tundra Fire, North Slope, Alaska. *Arctic, Antarctic, and Alpine Research*, 41(3), 309–316. <https://doi.org/10.1657/1938-4246-41.3.309>

Kääb, A., Strozzi, T., Bolch, T., Caduff, R., Trefall, H., Stoffel, M., and Kokarev, A. (2021). Inventory and changes of rock glacier creep speeds in Ile Alatau and Kungöy Ala-Too, northern Tien Shan, since the 1950s. *The Cryosphere*, 15, 927–949, <https://doi.org/10.5194/tc-15-927-2021>

Kääb, A., & Røste, J. (2024). Rock glaciers across the United States predominantly accelerate coincident with rise in air temperatures. *Nature Communications*, 15(1), 7581. <https://doi.org/10.1038/s41467-024-52093-z>

Kellerer-Pirklbauer-Eulenstein, A., Bodin, X., Delaloye, R., Lambiel, C., Gärtner-Roer, I., Bonnefoy-Demongeot, M., ... & Zumiani, M. (2024). Acceleration and interannual variability of creep rates in mountain permafrost landforms (rock glacier velocities) in the European Alps in 1995–2022. *Environmental Research Letters*. <https://doi.org/10.1088/1748-9326/ad25a4>.

Kelley, A.M., Epstein, H.E., and Walker, D.A. (2004). Role of vegetation and climate in permafrost active layer depth in arctic tundra of northern Alaska and Canada. *J. Glaciol. Climatol.*, 26, 269–273.

Koven, C.D., W.J. Riley, and Stern, A. (2013). Analysis of Permafrost Thermal Dynamics and Response to Climate Change in the CMIP5 Earth System Models. *J. Climate*, 26, 1877–1900

Kudryavtsev V.A., (Editor) (1978). *Obshcheye merzlotovedeniya (Geokriologiya)* (General permafrost science) In Russian. Izd. 2, (Edu 2) Moscow (Moscow), Izdatel'stvo Moskovskogo Universiteta, (Moscow University Editions), 404 pp

Lawrence, D. M., Fisher, R. A., Koven, C. D., Oleson, K. W., Swenson, S. C., Bonan, G., ... & Zeng, X. (2019). The Community Land Model version 5: Description of new features, benchmarking, and impact of forcing uncertainty. *Journal of Advances in Modeling Earth Systems*, 11(12), 4245-4287.

Matthes, H., Rinke, A. and Dethloff (2015). Recent changes in Arctic temperature extremes: warm and cold spells during winter and summer, *Environmental Research Letters*, 10(11).

Matthes, H., Rinke, A., Zhou, X., and Dethloff, K. (2017). Modelling atmosphere and permafrost in the Arctic using a new regional coupled atmosphere-land model, *Journal of Geophysical Research Atmospheres*, 122, 7755–7771.

McGuire A.D., Koven C., Lawrence D.M., Clein J.S., Xia J., Beer C., Burke E., Chen G., Chen X., Delire C., Jafarov E., MacDougall A.H., Marchenko S., Nicolsky D., Peng S., Rinke A., Saito K., Zhang W., Alkama R., Bohn T.J., Ciais P., Decharme B., Ekici A., Gouttevin I., Hajima T., Hayes D.J., Ji D., Krinner G., Lettenmaier D.P., Luo Y., Miller P.A., Moore J.C., Romanovsky V., Schädel C., Schaefer K., Schuur E.A.G., Smith B., Sueyoshi T. snf Zhuang Q. (2016:).Variability in the sensitivity among model simulations of permafrost and carbon dynamics in the permafrost region between 1960 and 2009, 2016: *Global Biogeochemical Cycles*. <https://doi:10.1002/2016GB005405>

Muller S.W. (1943). Permafrost or permanently frozen ground and related engineering problems. U.S. Engineers Office, Strategic Engineering Study, Special Report No. 62. 136p. (Reprinted in 1947, J. W. Edwards, Ann Arbor, Michigan, 231p.)

Nelson, F.E., Shiklomanov, N.I., Mueller, G.R., Hinkel, K.M., Walker, D.A., and Bockheim, J.G. (1997). Estimating Active-Layer Thickness over a Large Region: Kuparuk River Basin, Alaska, USA, *Arctic Alpine Res.*, 29, 4, <https://doi:10.2307/1551985>.

Nelson, F. E., Shiklomanov, N. I., & Nyland, K. E. (2021). Cool, CALM, collected: The Circumpolar Active Layer Monitoring program and network. *Polar Geography*, 44, 155–166.

Nitze, I., Grosse, G., Jones, B.M., Arp, C.D., Ulrich, M., Fedorov, A., and Veremeeva, A. (2017). Landsat-based trend analysis of lake dynamics across northern permafrost regions. *Remote Sensing*, 9(7), 640.

Nitze, I., Grosse, G., Jones, B.M., Romanovsky, V.E. and Boike, J. (2018a). Remote sensing quantifies widespread abundance of permafrost region disturbances across the Arctic and Subarctic. *Nature communications*, 9(1), 1-11.

Nitze, I., Grosse, G., Jones, B.M., Romanovsky, V.E and Boike, J. (2018b). Data Documentation v1. 0: Remote sensing quantifies widespread abundance of permafrost region disturbances across the Arctic and Subarctic.

Nitze, I., Cooley, S., Duguay, C., Jones, B. M. and Grosse, G. (2020). The catastrophic thermokarst lake drainage events of 2018 in northwestern Alaska: Fast-forward into the future. *The Cryosphere Discussions*, 1-33.

Obu, J., Westermann, S., Kääb, A. and Bartsch, A. (2018). Ground Temperature Map, 2000-2016, Northern Hemisphere Permafrost (p. 40 data points) [Text/tab-separated-values]. PANGAEA - Data Publisher for Earth & Environmental Science. <https://doi.org/10.1594/PANGAEA.888600>

Obu, J., Westermann, S., Bartsch, A., Berdnikov, N., Christiansen, H.H., Dashtseren, A., Delaloye, R., Elberling, B., Etzelmüller, B., Khodolov, A. and Khomutov, A. (2019). Northern Hemisphere permafrost map based on TTOP modelling for 2000–2016 at 1 km<sup>2</sup> scale. *Earth-Science Reviews*.

Obu, J. (2021). How Much of the Earth's Surface is Underlain by Permafrost? *Journal of Geophysical Research: Earth Surface*, 126(5). <https://doi.org/10.1029/2021JF006123>.

Olefeldt, D., Goswami, S., Grosse, G., Hayes, D., Hugelius, G., Kuhry, P., McGuire, A. D., Romanovsky, V. E., Sannel, A. B. K., Schuur, E. A. G., & Turetsky, M. R. (2016). Circumpolar

distribution and carbon storage of thermokarst landscapes. *Nature Communications*, 7(1), 13043. <https://doi.org/10.1038/ncomms13043>

Pellet, C., Bodin, X., Cusicanqui, D., Delaloye, R., Kaufmann, V., Noetzli, J., Thibert, E., Vivero, S., & Kellerer-Pirklbauer, A. 2023. Rock glacier velocity. In *State of Climate 2022* (Vol. 104, pp. 41–42). <https://doi.org/10.1175/2023BAMSSStateoftheClimate.1>.

PERMOS 2023. Swiss Permafrost Bulletin 2022. Noetzli, J. and Pellet, C. (eds.) 22 pp. <https://doi.org/10.13093/permos-bull-2023>.

Romanovsky, V.E., Smith, S.L., and Christiansen, H.H. (2010). Permafrost thermal state in the polar Northern Hemisphere during the international polar year 2007–2009: A synthesis. *Permafrost and Periglacial Processes*, 21(2), 106–116.

Sasgen, I., Steinhöfel, G., Kasprzyk, C., Matthes, H., Westermann, S., Boike, J., & Grosse, G. (2024). Atmosphere circulation patterns synchronize pan-Arctic glacier melt and permafrost thaw. *Communications Earth & Environment*, 5, 375.

Schaefer, K., Lantuit, H., Romanovsky, V.E., Schuur, E.A.G. and Witt, R. (2014). The impact of the permafrost carbon feedback on global climate. *Environmental Research Letters*, 9, 085003.

Screen, J. A., Bracegirdle, T. J., & Simmonds, I. (2018). Polar climate change as manifest in atmospheric circulation. *Current Climate Change Reports*, 4, 383–395.

Silva, T., Fettweis, X., Hanna, E., & Huybrechts, P. (2022). The impact of climate oscillations on the surface energy budget over the Greenland Ice Sheet in a changing climate. *The Cryosphere*, 16, 3375–3391.

Strauss J., Schirrmüller L., Grosse G., Fortier D., Hugelius G., Knoblauch C., Romanovsky V.E., Schädel C., Schneider von Deimling T., Schuur E.A.G., Shmelyov D., Ulrich M. snf Veremeeva A.. (2017): Deep Yedoma permafrost: A synthesis of depositional characteristics and carbon vulnerability. *Earth-Science Reviews*, 172: 75-86. <https://doi: 10.1016/j.earscirev.2017.07.007>

Schuur E.A., McGuire A.D., Schädel C., Grosse G., Harden J.W., Hayes D.J., Hugelius G., Koven C.D., Kuhry P., Lawrence D.M. and Natali S.M. (2015) Climate change and the permafrost carbon feedback. *Nature*. Apr;520(7546):171.

Slater, A.G. and D.M. Lawrence (2013). Diagnosing Present and Future Permafrost from Climate Models. *J. Climate*, 26, 5608–5623, <https://doi.org/10.1175/JCLI-D-12-00341.1>

Strauss J., Schirrmüller L., Grosse G., Fortier D., Hugelius G., Knoblauch C., Romanovsky V.E., Schädel C., Schneider von Deimling T., Schuur E.A.G., Shmelyov D., Ulrich M. and Veremeeva A.. (2017). Deep Yedoma permafrost: A synthesis of depositional characteristics and carbon vulnerability. *Earth-Science Reviews*, 172: 75-86. doi: 10.1016/j.earscirev.2017.07.007

Turetsky, M.R., Abbott, B.W., Jones, M.C., Walter Anthony, K., Olefeldt, D., Schuur, E.A.G., Koven, C., McGuire, A.D., Grosse, G., Kuhry, P., Hugelius, G., Lawrence, D.M., Gibson, C., and Sannel, A.B.K. (2019). Permafrost collapse is accelerating carbon release. *Nature*, 569(7754), 32–34. <https://doi.org/10.1038/d41586-019-01313-4>

Vincent, W.F., Lemay, M. and Allard, M. (2017). Arctic permafrost landscapes in transition: towards an integrated Earth system approach. *Arctic Science*, 3(2), 39-64.

Westermann, S., Østby, T., Gisnås, K., Schuler.T. and Etzelmüller, B. (2015) A ground temperature map of the North Atlantic permafrost region based on remote sensing and reanalysis data, *The Cryosphere*, 9, 1303-1319, <https://doi:10.5194/tc-9-1303-2015>.

Williams, J.R. (1965). Groundwater in permafrost regions: An annotated bibliography. U.S. Geological Survey, Professional Paper 696, 83p.

Windirsch, T., Grosse, G., Ulrich, M., Schirrmeyer, L., Fedorov, A. N., Konstantinov, P. Y., Fuchs, M., Jongejans, L. L., Wolter, J., Opel, T., and Strauss, J. (2020). Organic carbon characteristics in ice-rich permafrost in alas and Yedoma deposits, central Yakutia, Siberia, *Biogeosciences*, 17, 3797–3814, <https://doi.org/10.5194/bg-17-3797-2020>

Wouters, B., Gardner, A. S., & Moholdt, G. (2019). Global glacier mass loss during the GRACE satellite mission (2002–2016). *Frontiers in Earth Science*, 7, 96.

van Everdingen R.O. (1985). Unfrozen permafrost and other taliks. Workshop on Permafrost Geophysics, Golden, Colorado, October 1984 (J. Brown, M.C. Metz, P. Hoekstra, Editors). U.S. Army, C.R.R.E.L., Hanover, New Hampshire, Special Report 85-5, pp.101-105

Yamazaki, D., Ikeshima, D., Tawatari, R., Yamaguchi, T., O'Loughlin, F., Neal, J. C., Sampson, C. C., Kanae, S., & Bates, P. D. (2017). A high-accuracy map of global terrain elevations: Accurate Global Terrain Elevation map. *Geophysical Research Letters*, 44(11), 5844–5853. <https://doi.org/10.1002/2017GL072874>

## 6.2 Acronyms

ACOP	Asian Conference on Permafrost
ALT	Active Layer Thickness
Arctic CORDEX	Coordinated Regional Climate Downscaling Experiment
ASSW	Arctic Science Summit Week
AWI	Alfred Wegener Institute Helmholtz Centre for Polar and Marine Research
B.GEOS	b.geos GmbH
CALM	Circumpolar Active Layer Monitoring
CliC	Climate and Cryosphere project
CLM4	Land Community Model Version 4
CLM5	Land Community Model Version 5
CCI	Climate Change Initiative
CMIP-6	The Coupled Model Intercomparison Project
CMUG	Climate Modelling User Group
CRESCENDO	Coordinated Research in Earth Systems and Climate: Experiments, Knowledge, Dissemination and Outreach
CRG	Climate Research Group
ECV	Essential Climate Variable
EO	Earth Observation
ESA	European Space Agency
ESA DUE	ESA Data User Element
FT2T	Freeze-Thaw to Temperature
GAMMA	Gamma Remote Sensing AG
GCOS	Global Climate Observing System
GCW	Global Cryosphere Watch
GTD	Ground Temperature at certain depth
GT	Ground Temperature
GTN-P	Global Terrestrial Network for Permafrost
GTOS	Global Terrestrial Observing System

GUIO	Department of Geosciences University of Oslo
HIRHAM	High Resolution Limited Area Model
HRPC	Hot Spot Regions of Permafrost Change
IASC	International Arctic Science Committee
ILAMB	International Land Model Benchmarking
IPA	International Permafrost Association
IPCC	Intergovernmental Panel on Climate Change
LS3MIP	Land Surface, Snow and Soil Moisture
MAGT	Mean Annual Ground Temperature
NetCDF	Network Common Data Format
NSIDC	National Snow and Ice Data Center
PCN	Permafrost Carbon Network
PE	Permafrost Extent
PERMOS	Swiss Permafrost Monitoring Network
PF	Permafrost
PFR	Permafrost Fraction
PSTG	Polar Space Task Group
PUG	Product User Guide
PVIR	Product Validation and Intercomparison Report
RASM	Regional Arctic System Model
RCOP	Regional Conference on Permafrost
RD	Reference Document
RMSE	Root Mean Square Error
RS	Remote Sensing
SAR	Synthetic Aperture Radar
SCAR	Scientific Committee on Antarctic Research
SU	Department of Physical Geography Stockholm University
TSP	Thermal State of Permafrost
UNIFR	Department of Geosciences University of Fribourg
URD	Users Requirement Document
WCRP	World Climate Research Program
WMO	World Meteorological Organisation
WMO OSCAR	Observing Systems Capability Analysis and Review Tool
WUT	West University of Timisoara